Downscaling Climate Model Outputs for Estimating the Impact of Climate Change on Water Availability over the Baro-Akobo River Basin, Ethiopia

Dissertation

zur

Erlangung des Doktorgrades (Dr. rer. nat.)

der

Mathematisch-Naturwissenschaftlichen Fakultät

der

Rheinischen Friedrich-Wilhelms-Universität Bonn

vorgelegt von

Asfaw Kebede Kassa

aus

Harrar, Ethiopia

Bonn, den 30.04.2013

Angefertigt mit Genehmigung der Mathematisch-Naturwissenschaftlichen Fakultät der
Rheinischen Friedrich-Wilhelms-Universität Bonn

1. Gutachter: Prof. Dr. Bernd Diekkrüger

2. Gutachter: Prof. Dr. Semu Ayalew Moges

Datum der Promotion: 20. September 2013

Erscheinungsjahr: 2013

Acknowledgements

I thank the government of Federal Democratic Republic of Ethiopia via ecbp (engineering capacity building programme) and the German Academic Exchange Service (DAAD) through three years scholarship for my PhD study. I am deeply indebted to my supervisor Prof. Dr. Bernd Diekkrüger, professor at the University of Bonn, Germany, for his unreserved support, guidance and encouragement. His enthusiastic, industrious supervision and scientific guidance have been decisive for timely and successful completion of this thesis. I am highly grateful to my second supervisor Dr. Semu Ayalew Moges, associate professor at Addis Ababa University, Ethiopia, for his valuable contributions, support and encouragement.

I benefited from the support of many people in one way or another and I express my gratitude to Dr. Abebe Fanta, Dr. Tena Alamirew, Dr. Solomon Werku, Dr. Fekadu Beyene, Teshome Seyume, Hamesale Abebe and other staff of Institute of Technology from Haramaya University, Ethiopia. My gratitude also goes to Dr. Tiegist Dejene and Sisay Demeku from University of Bonn for their sincere friendship. I gratefully acknowledge the following organizations for providing data: Ethiopian National Meteorological Services Agency and Ethiopian Ministry of Water and Energy.

Thanks are due to all members of Hydrology Research Group of the University of Bonn for their company, discussions and comments. Special thanks go to Mr. Thomas Jütten for proofreading and Mr. Johannes R. Sörensen for fixing my computer problems. Most importantly, I would like to forward the leading and loving thanks to my helpful wife Rahel Demissie for her never ending concern, support and encouragement. Richo, without your love, support, understanding and patience this achievement would have not been possible. The success belongs to both of us. Special thanks go to my lovely daughter, Hasset Asfaw. They are always the source of my strength, happiness and permanent inspirations. I always grateful to all my family members', whose name is not possible to list here for their great concerns and encouragement,

Above all deep thanks to GOD for everything.

Asfaw Kebede Kassa

Bonn, Germany, 2013

Dedication

To my lovely wife, Rahel Demissie for her charming support and patience

To my parents, my father Kebede Kassa and my mother Azemera Alemu who have always been my sources of inspiration

Table of Contents

Zusammenfassung

Die vorliegende Dissertation untersucht die räumlichen- und zeitlichen Auswirkungen der globalen Erwärmung auf die Wasserressourcen eines der entlegensten Flusseinzugsgebiete Äthiopiens, des Baro-Akobo-Einzugsgebiet. Das Untersuchungsgebiet (76,000 km^2) ist ein wichtiger Oberlieger des weißen Nils im Sudan und gehört zu den landwirtschaftlich produktivsten Regionen Äthiopiens. Derzeit sind vor allem die am Unterlauf des Untersuchungsgebietes gelegenen privaten landwirtschaftlichen Großbetriebe auf die Wasserressourcen des Baro-Akobo-Einzugsgebiets angewiesen. Wissenschaftliche Untersuchungen der Auswirkungen der globalen Erwärmung auf das regionale Klima und die hydrologischen Prozesse des Untersuchungsgebietes fehlten bislang, insbesondere auf der Einzugsgebietsskala. In der vorliegenden Arbeit werden die Ergebnisse großskaliger globaler und regionaler Klimamodelle durch statistisches Downscaling auf meteorologische Variablen der Punktskala in täglicher Auflösung übertragen. Die Ergebnisse zeigen, dass das regionale Klimamodell REMO die im Baro-Akobo-Gebiet gemessenen Temperatur- und Niederschlagswerte reproduziert. Außerdem wurde festgestellt, dass das statistische Downscaling den Trend der Klimamodelle glättet. Die hydrologischen Prozesse des SORE Einzugsgebietes (1711 km^2) - ein Teileinzugsgebiete des Baro-Akobos - sowie der Einfluss der globalen Erwärmung auf das natürliche Wasserdargebot des Gebiets wurden mit verschiedenen Arten von hydrologischen Modellen simuliert. Das prozess-basierte, flächendifferenzierte Einzugsgebietsmodell WASIM-ETH sowie das konzeptuelle hydrologische Modell HBV-Light wurden erfolgreich für den Zeitraum 1990-1997 kalibriert und validiert. Die Leistung der für tägliche Zeitschritte durchgeführten Abflusssimulation der hydrologischen Modelle WASIM-ETH und HBV-Light wird mit Hilfe der Differenz zwischen gemessenen und simulierten Abflüssen bewertet. Bei täglichen Zeitschritten wurde für beide Modelle eine angemessene Modellgüte erreicht (WaSiM-ETH: R^2=0.79, NSE=0.78; HBV-Light: R^2=0.85, NSE=0.84). Für die Simulationen des zukünftigen Abflusses (2011-2050) mit WaSiM-ETH und HBV-Light wurden die Klimadaten des statistischen Downscalings verwendet. Die Simulationsergebnisse beider Modelle zeigen eine Verschiebung der Spitzenabflüsse der Regenzeit (Mai bis Juli), sowie eine Reduktion der Abflüsse im August und September. Allerdings simuliert das HBV-Light Modell im Juni einen um +30% bis +40% erhöhten Abfluss, während WaSiM-ETH eine Abflusserhöhung von +60% für beide Klimamodelle prognostiziert. Daraus folgt, dass die in dieser Arbeit beschriebenen Methoden und Resultate nur als indikative und unterstützende Informationen über die wahrscheinlichen Auswirkungen des Klimawandels im Baro-Akobo-Gebiet verwendet werden können. Das Einsetzen und Abklingen der Regenzeit der Zeitreihe 1972-2000, sowie die Trockenphasen während der Regenzeit wurden mit täglicher Auflösung für das obere Baro-Akobo-Einzugsgebiet untersucht. Die Ergebnisse zeigen, dass die Stabilität des Einsetzens der Regenzeit während der Untersuchungsperiode eine Maximierung des Regenfeldbaus in der Region bei geringem Risiko möglich macht. Zusätzlich wurde der Mann-Kendall Test im oberen Baro-Akobo-Gebiet angewandt, um den statistischen Trend der Trockenphasen zu untersuchen. Die Analyse zeigt, dass es im Baro-Akobo-Einzugsgebiet keinen statistisch signifikanten Trend gibt.

Summary

This work analyses the impact of climate change on the water resources of one of the remote basins of Ethiopia (Baro-Akobo). The study area (76,000 km^2) contributes water to the White Nile in Sudan and it is one of the productive agricultural areas in Ethiopia. Currently large scale private farms are under operation in the lower basin of Baro-Akobo relying on the water resources of the basin. However, a climate change impact assessment in the basin is missing especially at the catchment scale. In this study, large scale global and regional climate model output is downscaled statistically to meteorological variables at the point scale in a daily resolution to assess future variables under climate changes. The results show that the regional model REMO is able to reproduce the precipitation and temperature observed over the basin. We noticed that statistical downscaling smooths out the bias between climate models.

Hydrological models were applied to simulate current behaviour and the impact of climate change on the discharge of the SORE watershed (1711 km^2), a subbasin of the Baro-Akobo river basin. A physically-based distributed hydrological model and a conceptual model were successfully calibrated and validated for recent years (1990-1997). The performance of the two models WaSiM-ETH and HBV-Light to simulate discharge were evaluated by comparing model results with measured discharge of the watershed at a daily time step. The overall performance of both models was quite reasonable at a daily scale (WaSiM-ETH R^2=0.79, NSE=0.78; and HBV-Light R^2=0.85, NSE=0.84). Only small differences in the performance of the two models were observed. Future discharge simulations (2011-2050) were performed using statistically downscaled climate data with both models. Both results show a similar shift of the wet season (May to July) and a reduction of the peak discharge in August and September. However, HBV-Light shows discharge increases in June by 30% to 40% while WaSiM-ETH simulates an increase up to 60% for both climate models. Therefore, methods and results described in this study could be used as indicative and supportive information on the likely impact of climate change in the Baro-Akobo basin.

The onset and the cessation of the rainy season over the period of 1972-2000 and the analysis of the dry spells during the rainy season at a daily scale were analysed for the Upper Baro-Akobo basin. The results show that the stability of the onset dates of the rainy season reveals that rain-fed agricultural activity in the study area is possible at low risk. In addition, the Mann-Kendall test was applied to the Upper Baro-Akobo basin to investigate recent trends of the number and lengths of dry spells. The analyses show that there is currently no significant recent trend across the basin.

List of Figures

List of Table

Chapter 1

1. General Introduction

Our environment has been influenced by human beings for centuries. However, it is only since the beginning of the industrial revolution that the impact of human activities has begun to extend to a global scale (Baede et al., 2001). A statistically significant rise in global mean temperatures during the last century is now detectable (Houghton et al., 1996). Moreover, increased temperatures are not the only consequence of climate change, other effects like rising sea levels, altered precipitation patterns, shifting ecological zones, and alterations in areas that are suitable for farming are some of the changes. Erratic weather, such as tropical storms and extended heat waves are other likely effects of climate change which could cause a higher incidence of death and injury. Thornton and Cramer (2012) reported that in the tropics and subtropics in general, crop yields may decrease by 10 to 20% up to 2050 because of warming and drying, but there are places where yield losses may be much more severe. Agriculture in regions that are currently only marginally productive will probably become even more difficult. It is for these reasons that climate change has become a major topic of interest to the scientific community.

This study will examine the impact of climate change on water resource availability and dry spell analysis at a regional scale. The focus is on the evaluation how climate change would influence the availability of water resources for the Baro-Akobo river basin in western Ethiopia using downscaled GCM and regional climate model outputs. This research analyses the interactions between climate and hydrology that affect water availability and extreme hydrological events.

1.1 Relevance of the study

In countries like Ethiopia, where agriculture serves as a backbone of the economy as well as ensures the wellbeing of the people, the availability of water resources is quite essential. However, unless the available water resources are utilized with a balanced approach of the supply and demand and with a careful consideration of sustainability, satisfying the needs of the future generation will remain under question. The Baro-Akobo basin seems to face such

a problem in the near future. In the basin there is currently a wide expansion of irrigation for the production of food crops and water demands for drinking water supply, fishing, and recreational activities. Moreover the recently expanding large scale commercial farms are the main activities in the area relying on available water resources.

There is a general consensus on the need of proper planning regarding water resources development. For planning sustainable use of water resources, the impact of climate change has to be considered. According to Tadege (2007), Ethiopia is vulnerable to the impacts of climate variability and change; this is due to the low adaptive capacity of the country and the high sensitivity of the socio-economic systems to climate variability and change. Sensitivity and adaptive capacity also vary between sectors and geographic locations, time and social, economic and environmental considerations within a country. Therefore, according to the National Adaptation Program of Action (NAPA) (2007) the current climate variability is already imposing a significant challenge to Ethiopia by affecting food security, water and energy supply, poverty reduction and sustainable development efforts, as well as by causing natural resource degradation and natural disasters. For example the impacts of past droughts such as that of the 1972/73, 1984 and 2002/03 are still fresh in the memories of many Ethiopians. The flood in 2006 caused substantial loss of human life and property in many parts of the country. These threats are likely to be exacerbated by anthropogenic climate change. In this context, planning and implementing climate change adaptation polices, measures and strategies in Ethiopia will be necessary.

According to Tadege (2007) the country has already put in place policies, strategies and programs that enhance the adaptive capacity and reduce the vulnerability to climate variability and change. Regarding the identification of who is vulnerable and to what extent, there was a general consensus that ecologically arid, semi-arid and dry sub-humid parts of the country are most vulnerable to drought. Agriculture is the most vulnerable to climate change, in terms of livelihoods small scale rain-fed subsistence farmers and pastoralists are the most threatened.

The question arises what the future global climate impact in the basin will be. Most of the future climate predictions and studies are on the global and continental scale. In the 4th

IPCC report and other studies, the grid sizes used are greater than 110 km x 110 km in the General Circulation Models (GCM), which could evaluate the continental scale, such as Africa, but it may not be viable to apply it at the regional scale studies, such as Ethiopia in general and the basin in particular. Hence, studies that can narrow this gap are very important.

Future climate change predictions will have substantial importance to be considered in development plans in water resources, agriculture and similar other sectors in Ethiopia to overcome the impacts of intensifying recurrent droughts. Considering the importance of the study area as one of the major agricultural and hydropower potential regions of Ethiopia and one of the major water contributors to the White Nile River, there have been few studies performed at regional scale to fully investigate the future changes of hydrologic regimes, and water resources availability under climate change. Therefore, studies that fill this gap and provide information in supplementing countries policy on adaptive capacity are very important.

1.2 Aims of the research

From the discussions so far the main research issues are derived. The main research questions to be addressed in this study are:

1. *What is the likely trend in temperature and precipitation from the year 2011 till 2050 compared to a baseline period (1970-2000) according to SRES A1B and B1 scenarios?*
2. *How much will the water availability likely change in the future and in what trend, compared to the baseline period?*
3. *How is the recent dry spell trend in the basin?*

Based on the key research questions formulated, the main objective of the research is to evaluate statistically downscaled climate variable outputs, to analyse the impact of climate change on water resources of the basin and to provide supportive information for future water resource management in the area.

The specific objectives of this study are:

- ✓ To evaluate statistically downscaled climate variables from a regional climate model (REMO, 0.5° grid) and a global climate model (CGCM3.1, 3.75° grid) for the Baro-Akobo river basin.
- ✓ To assess future trends in precipitation and temperature compared to a baseline period and to provide first-hand understanding of the direction of climate change in the basin.
- ✓ To assess the performance of two different hydrological models and to quantify the impact of climate change on water resources.
- ✓ To analyse and assess changes in the seasonal variability of rainfall (dry spell).

1.3 Structure of the thesis

The thesis is organized in 8 chapters. This chapter continues with the structural overview of the research. Chapter two describes the study area providing details in climate and hydrology. Climate change impacts in Ethiopia are discussed in chapter three, and the modelling approach (state of the art) is given in chapter four. Application of statistical downscaling in the Baro-Akobo basin is discussed in chapter five. Chapter six presents catchment hydrological response to climate change and a comparative study of physically based-distributed versus conceptual hydrological models. In Chapter seven a dry spell analysis in the highland of the basin is discussed. Finally, general conclusions and perspectives are given in Chapter eight.

1.4 Structural overview

In order to study climate change impacts on water resource availability for the Baro-Akobo basin, physically based-distributed and conceptual hydrological models were run using rainfall and temperature scenarios based on statistically downscaled GCM simulations. An overview of the datasets and the procedures used for subsequent impact studies is given in the flowchart (Figure 1). Relevant data on climate and hydrometeorology was provided by MoWE (Ministry of Water and Energy) and NMA (National Meteorological Agency). Results

of the statistically downscaled GCMs and regional model data were compared with baseline data to see the models performance for the study area. Then an analysis on water balance and seasonal variability of rainfall was conducted using hydrological models and statistical analysis respectively.

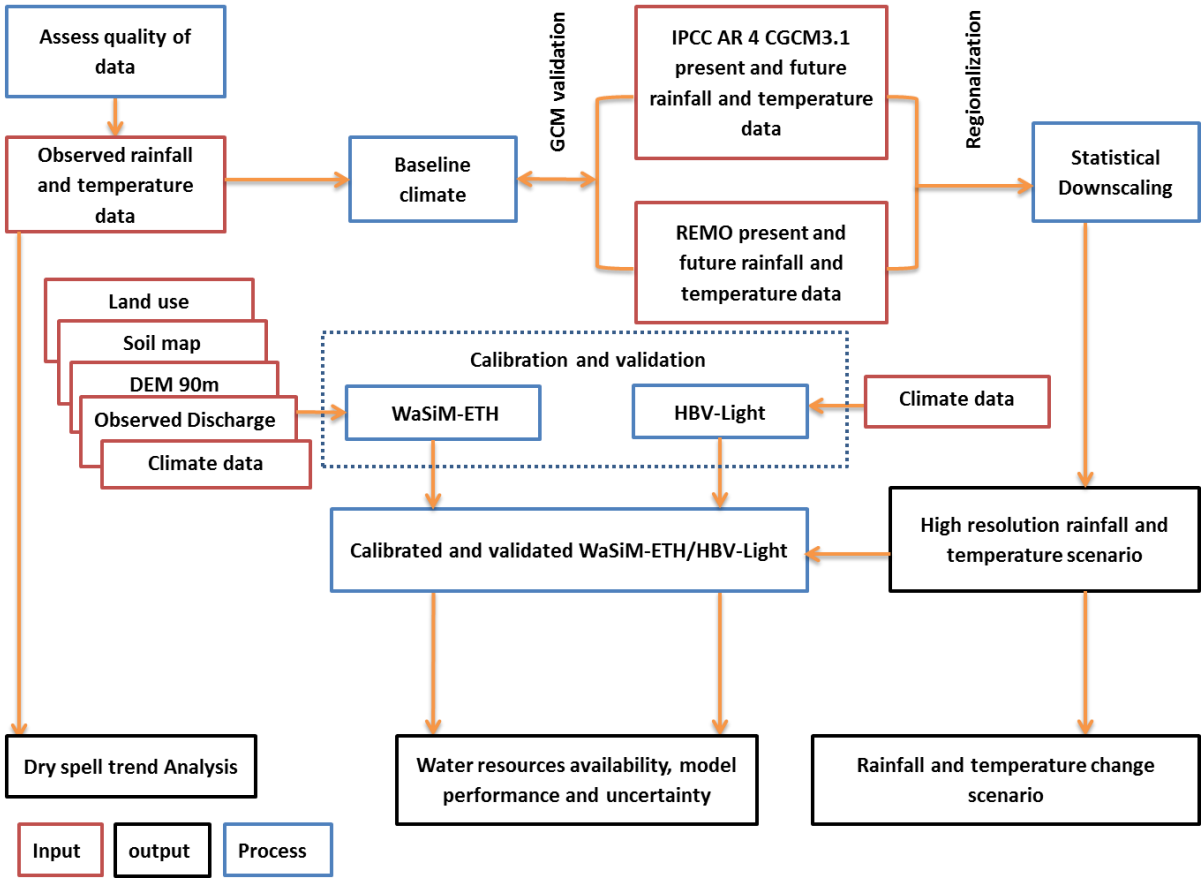

Figure 1: An overview of the general approaches of this study.

Chapter 2

2. Research area description

2.1 Background

Ethiopia has a total area of 1.13 million km^2 and had a total population of 83 million in 2011 (McCornick et al., 2003; UNFPA, 2011). Agriculture is the leading sector in the countries' economy, 47.68 % of the total GDP, as compared to 14.28 % from industry and 38.03 % from services (World Bank 2011).There is a tremendous diversity of climatic, biophysical and socio-economic settings in the country. The climate ranges from equatorial rainforest type in the south and southwest characterized by high rainfall and humidity to afro-alpine type on the peaks of the Semien mountains (Abbay and central Tekeze basin) and Bale mountains (west of Wabi Shebele basin) and desert like conditions of the Northeast, East and Southeast lowlands (Figure 2). Elevations vary from the Afar depression (Denakil basin) (Figure 2) in the northeast, which is 110 meters below sea level (m.b.s.l), to the top of Ras Dashen Mountain in the north (central Tekeze basin), which is 4,620 meters above sea level (m.a.s.l) (McCornick et al., 2003). Within these elevation ranges there are high mountains, deep gorges, river valleys and lowland plains.

Rainfall pattern of the country show that the mean annual rainfall varies from more than 2500 mm in highland to less than 60 mm in lowland (McCornick et al., 2003). Denakil basin has the highest mean annual temperature in the country 45°C from April to September. The lowest mean annual temperature in a very few highland parts of Abbay, Tekeze and Wabi Shebele basins is observed to be around 0°C or lower from October to December.

The diversity also extends to socio-economic conditions. Economic activities in the country ranges from booming industrialization and modern agriculture in and around Metropolitans such as Addis Ababa, Bahir Dar, Mekele and Adama to traditional cultivators and nomadic pastoralists in the rural area. The distribution of social and economic infrastructure and amenities is also likewise very variable with some parts of the country relatively well served and others barely reached (MoWR, 2002).

The Ethiopian highlands contribute to three major river systems, the Nile, Awash and Omo. The northern and central highlands drain westward into Ethiopia's largest river system, the

Abbay (Blue Nile), and the Tekeze River, a tributary of the main Nile, and the Baro-Akobo River, a tributary of the White Nile (Figure 2). The eastern highlands drain into the Awash River, which never reaches the sea, but is ultimately absorbed into a succession of lakes and marshes near the Djibouti border. In the south, the Omo-Gibe River drains into Lake Turkana, and a number of streams flow into the other Rift Valley lakes. In the southeast, the mountains of Arsi, Bale, and Sidamo drain towards Somalia and the Indian Ocean, but only the Genale Dawa or Juba River permanently flows into the Indian Ocean (Figure 2). Apart from the larger rivers, there are few perennial streams below 1,000 meters (McCornick et al., 2003). The country's many rivers have the potential to generate 45,000 megawatt (MW) of electric power, however so far able to generate a little over 2,000 MW (MoW 2011). Currently 450MW Gibe III at Omo-Gibe, 6000MW Grand Renaissance dam at (Abbay) Blue Nile is under construction (MoFED, 2012).

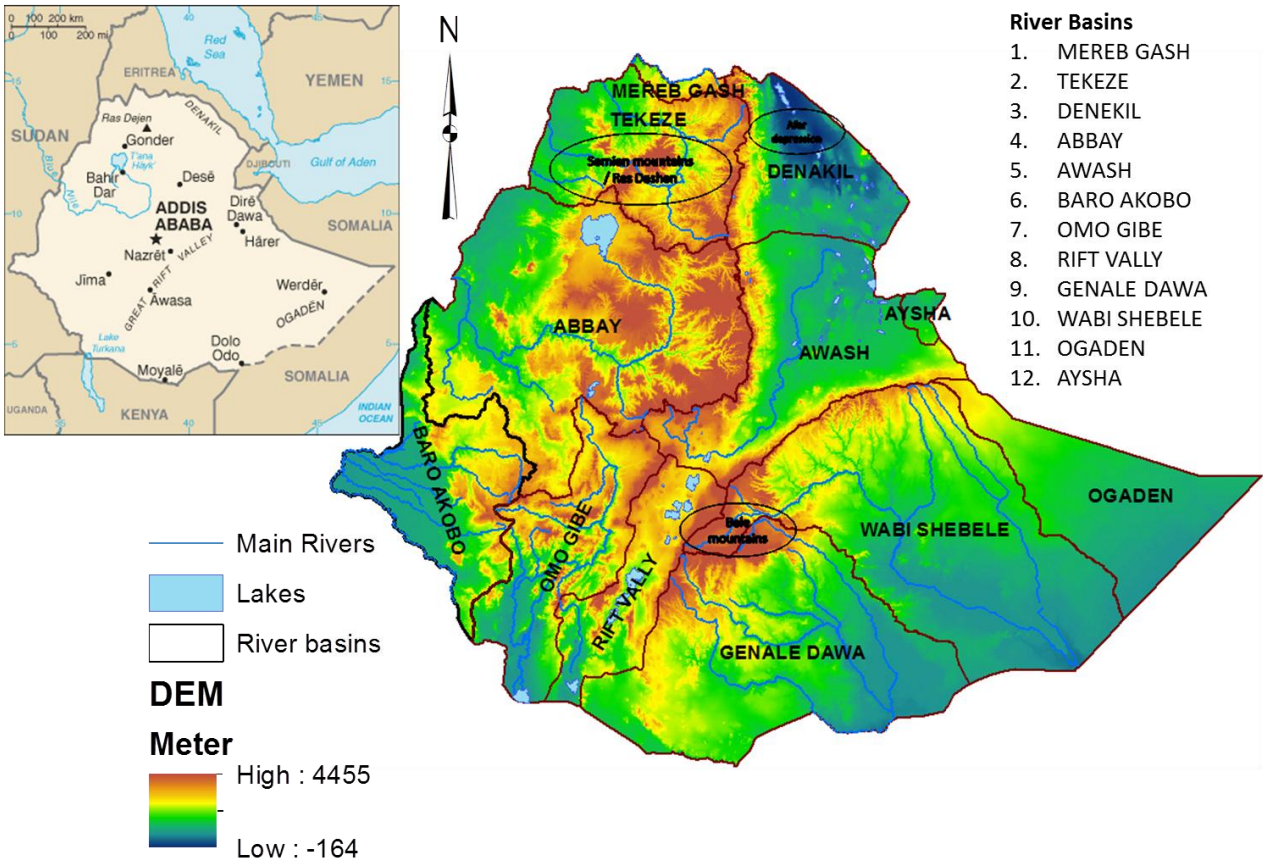

Figure 2: Location map of Ethiopia and 12 major river basins (adapted from MoWR).

This study focuses on the Baro-Akobo Basin (Figure 3) which is one of the 12 major river basins in the country. It drains from the western highlands of Ethiopia and flows westward to the Sudanese border to join the White Nile. The basin is located in the southwest of the country, between latitudes 5°31` and 10°54` North, and longitudes 33° and 36°17´ East and

covers an area of about 76,000 km^2. It is bordered by the South Sudan in the west and southwest, Sudan in the northwest and the Abbay and Omo-Gibe Basins in the east. The eastern part of the basin consists of the hilly upland areas of a plateau (Figure 3). The basin is characterized by mountainous in the altitude ranges of below 500 to over 3000 m.a.s.l with 50% of the area falling in the altitude of below 1000 m.a.s.l and 42% in between 1000 and 2000 m.a.s.l. The eastern two-third of the basin area lies between 1000 to 2400 m.a.s.l and the plain is gently sloping towards 400 to 500 m.a.s.l in the west.

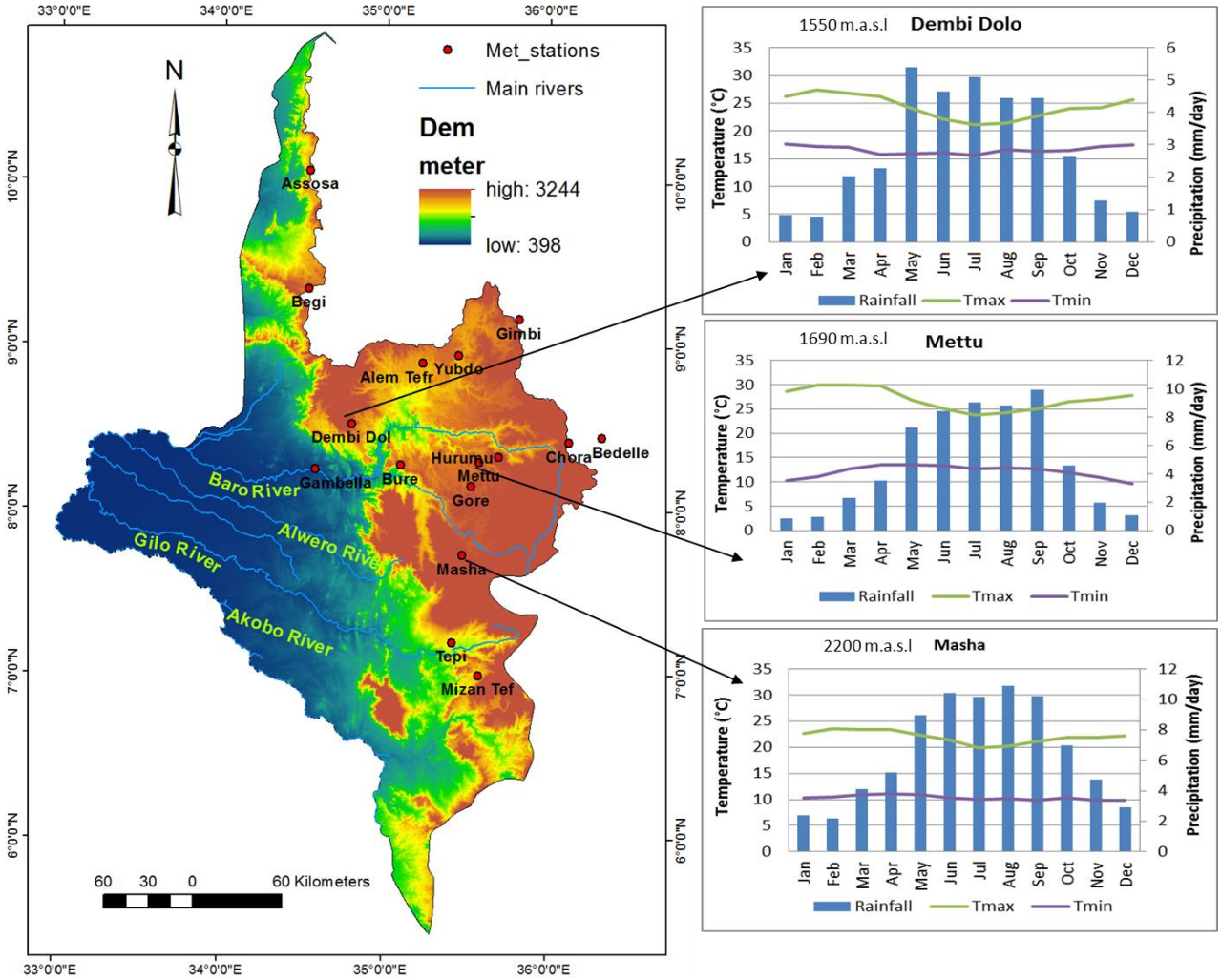

Figure 3: Digital elevation model of the Baro Akobo basin, main rivers, meteorological stations and observed monthly mean rainfall, maximum and minimum temperatures for three stations.

2.2 Climate

The mean temperature range in the area is about 27.5°C below 500m on the flood plain to about 17.5°C at 2,500m in the highland. The range in mean maximum temperature is 35 to 24°C and in mean minimum temperature from 20 to 10°C. Temperature peaks during

February and March on the flood plain but high values extend into April in the highlands. Below about 700m elevation mean maximum temperature values exceed 38°C for two to three months. In contrast to the low land, the area above about 2,000m is markedly cooler, with mean maximum temperature in the hottest period not exceeding 28°C and generally being in the range 21-26°C.

The precipitation within the Baro-Akobo is formed under the influence of the south-eastern monsoons from the Indian Ocean. Like in other parts of the country, the precipitation is strongly influenced by altitude (Khor, 2006). The annual rainfall is in the range of 900mm to 1500mm in areas with an altitude range between 400m and 500m, and in the range of 1900mm to 2400mm in areas with an elevation of 500m to 2000m.

2.3 Hydrology

The major rivers within the Baro-Akobo basin are Baro, Alwero, Gilo and the Akobo (Figure 3 and 4). These rivers originate in the eastern part of the highlands, flow westward to Gambela plain. The mean annual runoff of the basin is estimated to be about 23 km^3 at Gambela (MoWR 1997). The river discharge increases through May to September and decreases from December through to April. Groundwater is reported to occur in rocks throughout the entire basin and to move generally westwards. Water yields vary from 1 to 18 l/s for boreholes and springs and 0.1 to 1 l/s for wells (MoWR, 2011). The abundance of water combined with the relief of the basin provides favourable conditions for hydropower in this basin. The gross hydroelectric potential in the Baro-Akobo basin is estimated to be 13,765 MW/year (Awulachew et al., 2007). Nevertheless, getting information on existing and up-to-date water resources development in the basin is challenging.

2.4 Land Use and Cropping

The basin is shared by four regional states, Gambela, Oromia, SNNPS (Southern Nation Nationalities People State) and Benishangul-Gumaz (Figure 4). Baro-Akobo basin is the second next to Genale-Dawa from all basins in Ethiopia regarding irrigation potential. According to MoWR (1997) twenty-two large scale potential irrigation sites in Baro-Akobo basin are identified with an irrigable area of 1,019,523 hectares (Awulachew et al., 2007).

Currently large scale private farms are established in the lower basin of Baro-Akobo cultivating rice, oilseeds, palm oil and sugarcane like Saudi stars Plc and Karuturi Global Ltd., except the Alwero dam build in 1992 there was no major water resources development taken place before these new large scale private commercial farms.

The highland part of the basin (above 1800m) is characterized by a high density of farmers like in the other parts of Ethiopia. Nearly all farmers in the basin practice mixed farming with rotation of crops dominated by cereals. The proportion is somewhat greater in Keficho Shekich, Assosa and the lower basin and less in West Welega (see Figure 4). In the two largest zones, Illu-Aba- Borra and West Welega, maize is the most popular cereal but in Assosa and the lower basin, sorghum displaces maize, perhaps because of its greater reliability under drought conditions. Teff, the source of the staple food of the highland people, is particularly important in Illu-Aba-Borra, but much less so in other zones (MoWR 1997).

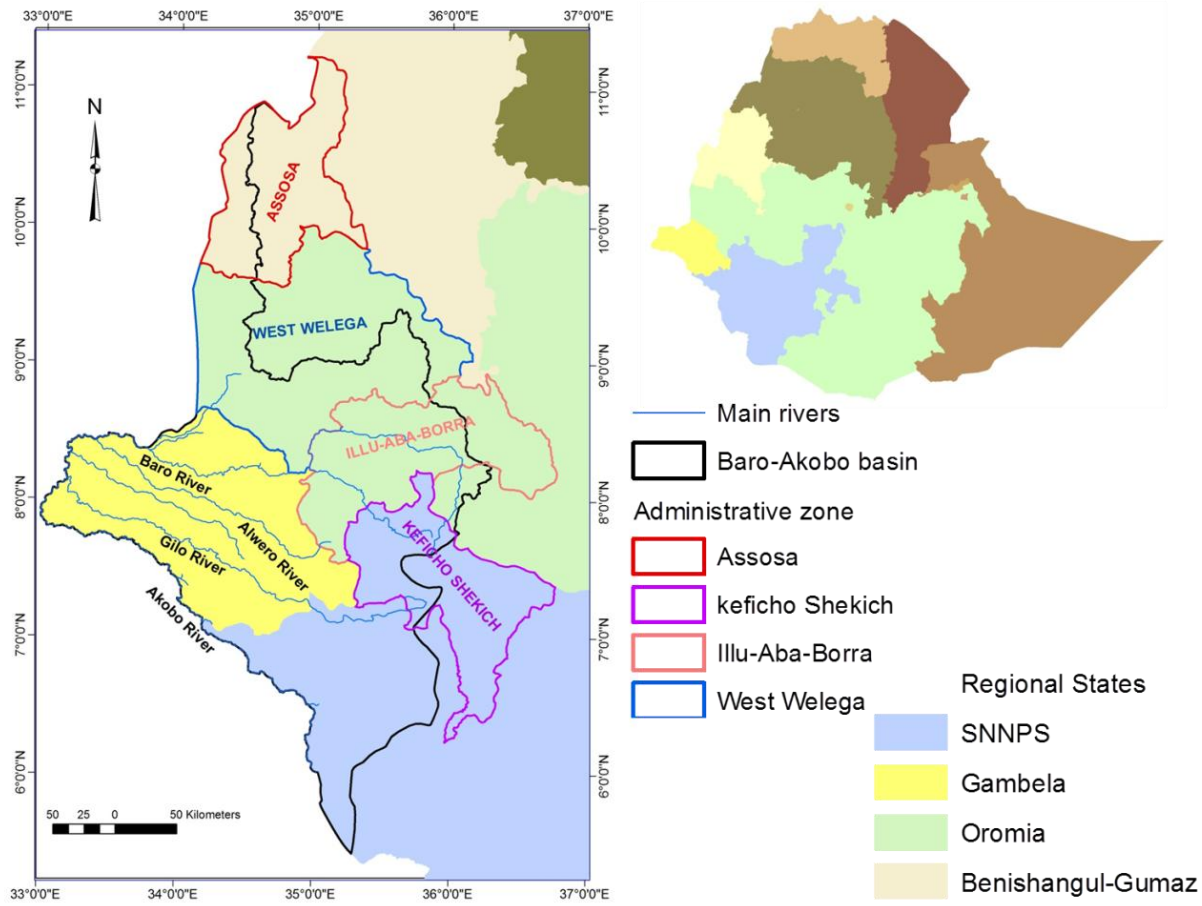

Figure 4: Baro Akobo basin and administrative zones sharing the basin.

The other important crop is coffee, which occupies more than a quarter of the areas in West Welega, somewhat less in Illu-Aba-Borra and very little or nil in other zones. This crop is the only cash crop of importance in the area at present. There are tea, coffee and cotton plantations farms in the area.

Chapter 3

3. Climate change impact studies on water resources of Ethiopia

Ethiopia relies on low-productivity rain fed agriculture for a majority of its national income. The reliance on agriculture is even more acute in rural areas, where small farmers reportedly accounted for over 90% of agricultural output (Cheung et al., 2008). Given such a heavy dependence on rainfall, it is likely that climate extremes such as droughts or floods can pose significant health and economic threats to the entire nation. IPCC findings indicate that developing countries such as Ethiopia and the other countries in East Africa will be more vulnerable to climate change, mainly Ethiopia because of its low economic, climatic and geographic settings it would be more affected. Arid and semi-arid part of the country is highly prone to drought and desertification and the livelihood depends on available rainfall. Abdo et al. (2009) reported that the country has a fragile highland ecosystem that is currently under stress due to still increasing population pressure. Therefore, there is a need to quantify and assess the future scenarios of climate change and its impact on water resources of the country in general and the basin in particular, because the country's future development relies on this resource.

Literature shows that some climate change impact studies on hydrology have been conducted in Ethiopia. Among these studies Sayed (2004) has shown that the change in rainfall over the Blue Nile basin would be between +2 and +11% for 2030, while rainfall over the White Nile basin would increase between 1 and 10% for the same year. Elsahmay et al. (2009) run the Nile Forecasting Model with bias corrected precipitation and temperatures from 17 GCMs for 2081-2098 periods to assess effects of climate change on stream flow of the Blue Nile. The conclusion of Elsahmay et al. (2009) was that the uncertainty in future precipitation change makes the future stream flow of the Blue Nile at Diem very uncertain. Taye et al. (2011) also investigated the potential impact of climate change on the hydrological extremes of the Lake Tana catchment, Blue Nile – Ethiopia. They stated that unclear trend is observed for the catchment for mean volumes and high/low flows for the 2050s using 17 GCMs. From the IPCC Fourth Assessment Report (IPCC, 2007) and the country report of Ethiopia (Tadege, 2007) there is a general consensus on the rise of the temperature. Di Baldassarre et al. (2011) reported that while there is generally no significant change detected in the annual rainfall in most of the Nile sub-basins, there appears to be

decreasing seasonality in some key watersheds of the upper Nile in Ethiopia such as the southern Blue Nile and Baro-Akobo. Conway (2005) showed that climate variability of the Ethiopian Highlands is primarily due to rainfall fluctuations. Kim et al. (2008) conducted research on climate change impacts on hydrology and water resources of the upper Blue Nile river basin, Ethiopia. The result suggested that the climate in most of the upper Blue Nile river basin is likely to become wetter and warmer in the 2050s (2040-2069) and droughts are likely to become less frequent throughout the entire basin.

Therefore, there are large uncertainties in predicting climate change impacts on the countries water resources and this leads to unreliable development of water resources plans in the future. By nature, the future is uncertain and this is partly handled via emission scenarios that capture different visions of how the world will develop in the future in terms of population, technology and energy use. Even though much research has been done in continental or global scale studies related to climate change, the magnitude and type of impact at the regional-catchment scale is not investigated in many parts of the world that also includes Ethiopia. In addition to this, the climate change studies in water resources of Ethiopia has largely focussed on existing information over Blue Nile and not much research has been seen from South western part of the country (Baro Akobo basin). Investigating climate change at local level gives an opportunity to define the degree of vulnerability of local water resources and plan appropriate adaptation measures that must be taken ahead of time. Moreover this will give enough room to consider possible future risks in all phases of water resource development projects at the local scale.

Extreme hydrological events have negatively affecting Ethiopia's past economic development by affecting crop production through drought and flooding. The future projections also show a likely variability of precipitation, which translates as fluctuating rainfall, reduces the availability of a stable water supply and increases the risk of floods. You and Ringler (2010) reported that in Ethiopia, climate change is expected to intensify the already high hydrological variability and frequency of extreme events, and drought and flood may have a significant negative effect on the development of the agriculture sector and the economy as a whole. Therefore, projection of climate change impact on water resources of the country should not be neglected on the future development plan.

Chapter 4

4. Modelling Approach

4.1 Downscaling

The behaviour of the climate system, its components and their interactions, can be simulated and studied using global climate models (GCM). They are designed mainly for studying climate processes and natural climate variability and for projecting the response of the climate to human-induced forcing (Baede et al., 2001). Global Climate Models (GCMs) are a class of computer-driven models for weather forecasting, understanding climate and projecting climate change. Since global or regional climate models are still relatively coarse they cannot explicitly capture the fine-scale structure that characterizes climatic variables at local scale which is needed for impact assessment studies. The spatial resolution gap on what climate modellers are currently able to provide and what impact assessors require can be bridged through the application of "downscaling" techniques, thus downscaling is required for climate impact studies at local scale.

The two downscaling approaches that are being used currently are dynamic downscaling and statistical downscaling. In the dynamic downscaling approach, a Regional Climate Model (RCM) is nested into a GCM (e.g. Xu, 1999; Fowler et al., 2007). The RCM is essentially a numerical model in which GCMs are used to fix boundary conditions. The major drawback of RCM, which restricts its use in climate impact studies, is its complicated design and high computational cost (Anandhi et al., 2008). In addition to these limitations they are usually still too coarse especially in mountainous areas. However, the statistical downscaling involves less computational cost for developing quantitative relationships between large-scale atmospheric variables (predictors) and local surface variables (predictands) (e.g. Wilby et al., 2007; Dibike et al., 2006; Fowler et al., 2007). There are three types of statistical downscaling methods namely, weather classification, weather generators and transfer functions. The most common statistical downscaling approaches are based on transfer functions, which model direct relationships between predictors and predictands (Anandhi et al., 2008; Dibike et al., 2006). In this study precipitation and temperature from IPCC 4AR, CGCM3.1 models and REMO (Developed at Max-Plank Institute for Meteorology based on

ECHAM4 boundary condition, Paeth et al.,2005) were used for downscaling climate variables to station scales.

We applied the Statistical Downscaling Model (SDSM) version 4.2 for downscaling CGCM3.1 and REMO outputs to station scales suitable for hydrological modelling. It is a decision support tool used to assess local climate change impacts using a statistical downscaling technique (Figure 5). The tool facilitates the rapid development of multiple, low–cost, single–site scenarios of daily surface weather variables under current and future climate forcing (Palmer et al., 2004; Wilby and Dawson, 2007). A number of studies show that SDSM yields reliable estimates of extreme temperatures, seasonal precipitation totals, and areal and inter-site precipitation behaviour (Wilby and Dawson, 2012). The software manages additional tasks of data quality control and transformation, predictor variable pre–screening, automatic model calibration, basic diagnostic testing, statistical analysis and graphing of climate data. The downscaling process is shown in Figure 5. Data used are 1972-2000 for current or base period and 2011-2050 for future scenario. And the future changes determined as deltas (for temperature) and as percentage (for precipitation) from the base period values.

The SDSM model performs the task of statistically downscaling daily weather series using seven discrete steps as shown in the simplified model structure (Figure 5). The following steps were taken from Wilby and Dawson (2007) that describes the procedures in SDSM.

(i) *Quality control and data transformation* which mainly focuses on identification of gross data errors, specification of missing data codes and outliers prior to model calibration,

(ii) *Screening of predictor variables* aims to identify empirical relationships between gridded predictors (such as mean see level pressure) and single site predictands (such as station rainfall),

(iii) *Model calibration* steps takes a user-specified predictand along with a set of predictor variables, and computes the parameters of multiple regression equations via an optimization algorithm (either dual simplex or ordinary least squares),

(iv) *Weather generation* (using observed predictors) steps generates ensembles of synthetic daily weather series given observed atmospheric predictor variables,

(v) *Statistical analysis* steps provides means of interrogating both downscaled scenarios and observed climate data with the summery statistics and frequency analysis,

(vi) G*raphical analysis* steps provides option for analysing the result graphically,

(vii) *Scenario generation* is the final step which allows to produces ensembles of synthetic daily future weather series given atmospheric predictor variables supplied by a climatic model.

Further detail information can be found from Wilby and Dawson (2007).

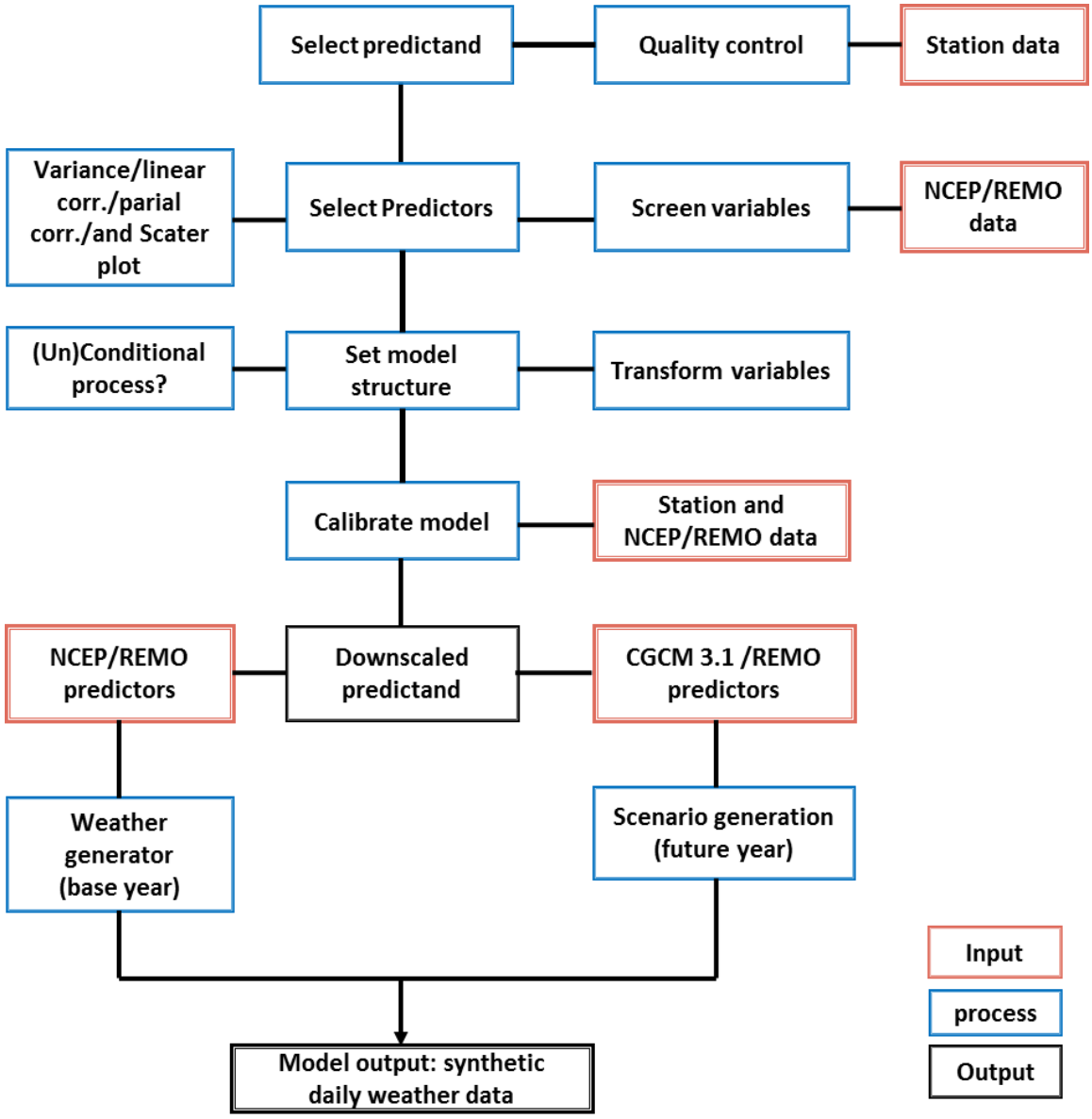

Figure 5: SDSM Version 4.2.2 a hybrid of stochastic weather generator and regression-based climate scenario generation (adapted from Wilby and Dawson 2007).

4.2 Hydrological models

4.2.1 Hydrological models and their applications in Ethiopia/Nile

As briefly explained in many publications (e.g. Beven 2001; Singh and Frevert, 2002a, b.; Duan et al., 2003; and Wagener et al., 2004) a model is a simplified representation of a real world system and consists of a set of simultaneous equations or a logical set of operations contained within a computer program. Models have parameters which are numerical measures of a property or characteristic that is constant under specified conditions. According to Beven (2001) a lumped model is one in which the parameters, inputs and outputs are spatially averaged and take a single value for the entire catchment. Wagener et al. (2004) explained that a distributed model is one in which parameters, inputs and outputs vary spatially and a semi distributed model may adopt a lumped representation for individual sub catchments. A model is deterministic (Beven, 2001 ; Wagener et al., 2004) if a set of input values will always produce exactly the same output values and stochastic if, because of random components, a set of input values need not produce the same output values. Singh and Woolhiser (2002) as well as Singh and Frevert (2006) point out, that improving the fundamental understanding of existing hydrological systems and assessing the impact of climate change on water resources are among the different aims of hydrological modelling.

In recent years, scientific communities have made efforts to analyse the projected impact of climate change on water resources of Ethiopia and or the Nile using different hydrological models. More recently Taye et al. (2011) used two lumped conceptual hydrological models namely VHM and NAM in two sources of the Nile River at the Lake Tana catchment in Ethiopia and Nyando River, and reported that the models performed better in Lake Tana in simulating the hydrological regimes than for Nyando. Setegn et al. (2009) investigated the performance and application of the Soil Water assessment Tool (SWAT) model for prediction of stream flow in Lake Tana Basin in Ethiopia, and reported that there is good agreement between the measured and simulated flows. Moreover Elshamy et al. (2009) and Soliman et al. (2009) applied the Nile forecasting system (NFS) hydrological model for the Blue Nile in Ethiopia, which is a real-time distributed hydro-meteorological forecast system designed for forecasting the Nile flows. Yimer et al. (2009) also used the HEC-HMS

hydrological model on the Upper Blue Nile in Ethiopia to investigate climate change impact, and reported that the model performance is reasonably good in simulating flows. Abdo et al. (2009) found that HBV rainfall-runoff model performs well in simulating the base flow, the rising and recessing limb of the hydrograph in Gilgel Abay catchment in Lake Tana basin, Ethiopia. Zeray et al. (2006) used SWAT to study climate change impacts in a Great East African Rift Valley Lake of Ethiopia, Lake Ziway and the report indicated that the model performs well. The physically based distributed Precipitation Runoff Modelling System (PRMS) was also used to investigate the response of catchments in central Ethiopia to climate and land use change (Legesse et al., 2003) and reported that the model provided relatively good fits between measured and simulated discharge. Nevertheless, there is neither a clear recommendation as to the application of a specific set of hydrological models nor such types of models were tested extensively in Ethiopia widely. As a result, modelling some of the remote basins like Baro-Akobo required starting from scratch. In this study we opted to use two sets of distinct hydrological models, one physically based and the other lumped conceptual models, to test and apply the models to study the impact of climate change in the water resources of Baro-Akobo basin.

4.2.2 Model descriptions

Hydrological impacts of climate change are usually analysed by using conceptual and/or physically based hydrological models. In this study a physically based distributed model, namely WaSiM-ETH (the Runoff Water balance Simulation Model ETH) and one of the many versions of a conceptual hydrological model, HBV-Light have been applied. The following section gives brief descriptions of the models.

A. WaSim-ETH

The hydrological catchment model WaSiM-ETH was initially developed by Schulla (1997). As described in Schulla and Jasper, (2007) it is a spatially distributed, process and grid based hydrological catchment model (Figure 6). Despite focusing on the spatial variability of atmospheric boundary conditions, WaSiM-ETH represents all relevant hydrological processes. Version 7.9.11 of the model developed in 2007 (Schulla and Jasper, 2007), which base on Richards-equation to represent the soil water flow is applied in this study.

The model hydrological processes and modules used in this study are as follows:

(i) The *potential evapotranspiration* was calculated using the Penman-Monteith (1975) approach (Equation 1), and the *actual evapotranspiration* was estimated depending on soil moisture availability.

(ii) *Infiltration rates* were simulated based on the approach of Peschke (1977) and Green and Ampt (1911), and vertical processes in the unsaturated zone were modelled using the Richards equation (1931).

(iii) *Interflow* of each modelled raster cell was simulated as a function of slope length and slope inclination, saturated water conductivity, drainable porosity and the amount of drainable water stored in the saturated zone and directly added to the natural drainage channel using the concept of storage approach and comparing the maximum and actual rate (Japser et al., 2004). Groundwater flow can be simulated using a conceptual linear storage or a 2-dimensional (2d) model. Due to the unavailability of groundwater data, the conceptual method was used in this study.

(iv) *Discharge routing* was based on a kinematic wave approach that considered the translation-retention approach using hydraulic parameters for channels (Wagner et al., 2009).

Potential evapotranspiration

The approach after PENMAN-MONTEITH (Equation 1) is used for potential evapotranspiration estimation. While climate data are required in at least daily time steps, monthly values for a minimum bulk-surface resistance for each land use type are used. A more detailed description of the model can be found in Schulla and Jasper (2007).

$$\lambda E = \frac{3.6 \times \left(\frac{\Delta}{\gamma p}\right) \times (R_N - G) + \frac{p c_p}{\Upsilon_p r_a} \times (e_s - e) \times t_i}{\frac{\Delta}{\Upsilon_p} + 1 + \frac{r_s}{r_a}} \qquad \ldots 1$$

Where: λ= Latent heat of vaporizations (kJ/kg); λ= (2500.8-2.372 T); T=temperature (^{o}C); E=Latent heat flux (kg/m^{2}); Δ= Tangent of the saturated vapour pressure curve (hPa/K^{-1}); R_N=

net radiation, conversion from Wh/m^2 to KJ/m^2 by factor 3.6 (Wh/m^2); G= soil heat flux (Wh/m^2); p= density of dry air (kg/m^3);c_p= specific heat capacity of dry air at constant pressure, cp=1.005 KJ/(kg*k); e_s= saturation vapour pressure at temperature T (hPa); e= actual vapour pressure (hPa); t_i= number of seconds within a time step; Y_p=psychometric constant (hPa/K); r_s= bulk-surface resistance (s/m); r_a= bulk-aerodynamic resistance (s/m).

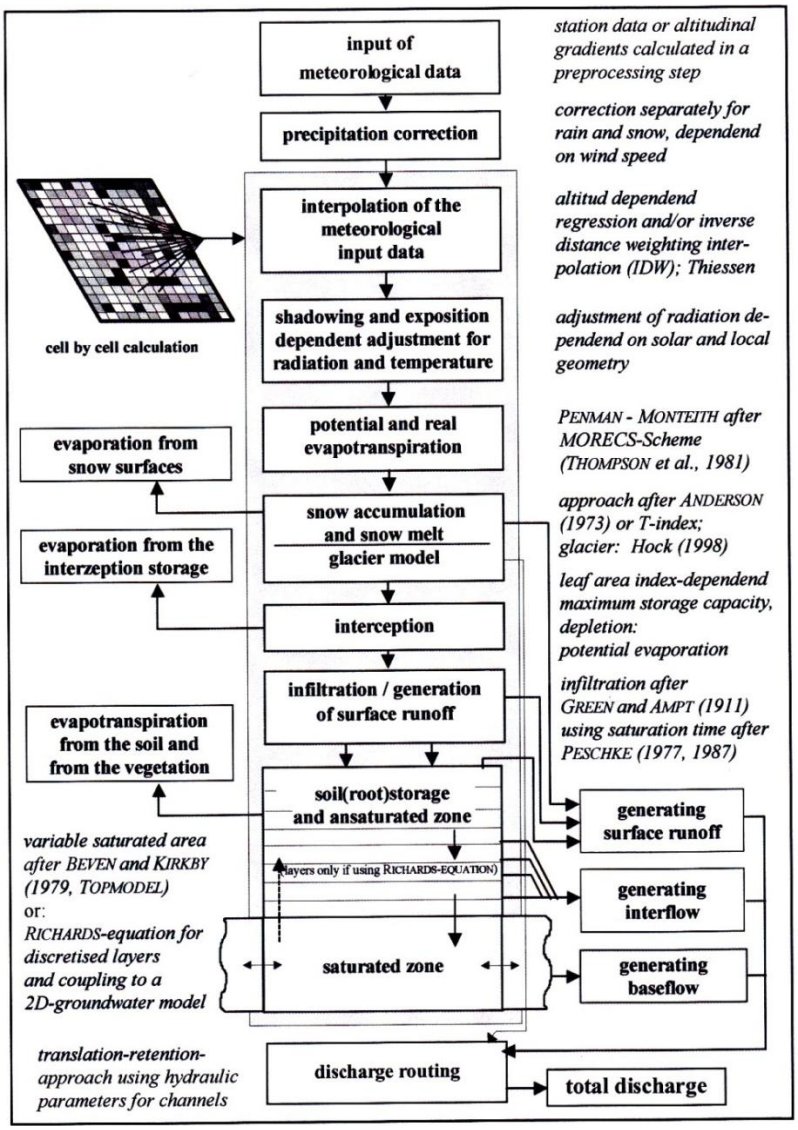

Figure 6: Model structure of WaSiM-ETH (Schulla and Jasper, 2007).

B. HBV-Light

One of the many versions of the HBV (Hydrologiska Byråns Vattenbalansavdelning) model is the HBV-Light version 3.0 (Seibert, 2005), which is a conceptual model that simulates daily

discharge using daily rainfall, temperature and potential evapotranspiration as input (Figure 7). The model has four routines for discharge simulation:

(i) The "*snow routine*" was ignored in this study due to absence of snow in the study area.

(ii) The "*soil routine*" is a process where rainfall goes to the root zone and to groundwater as recharge depending on the relation between field capacity (FC[mm]) and moisture content in the root zone (SM[mm]) (Equation. 2), and actual evaporation is estimated depending on soil moisture availability using the relation between SM and FC (Equation. 3).

(iii) The "*response routine*" is for computing runoff from upper (SUZ[mm]) and lower (SLZ[mm]) groundwater boxes as the sum of two or three linear outflow equations depending on a threshold parameter, UZL[mm] (Equation. 4).

(iv) The "*routing routine*" is used to transform runoff to simulated runoff [mm/day] (Equations. 5 and 6) using a triangular weighting function defined by the parameter MAXBAS (Seibert, 2005).

$$\frac{recharge}{P(t)} = \left(\frac{SM(t)}{FC}\right)^{BETA} \quad .....2$$

$$E_{act} = E_{pot}\ min\left(\frac{SM(t)}{FC.LP}, 1\right) ..... 3$$

$$Q_{GW}(t) = K_2 SLZ + K_1 SUZ + K_0 \max(SUZ - UZL, 0) \quad .....4$$

$$Q_{sim}(t) = \sum_{i=1}^{MAXBAS} c(i)\, Q_{GW}(t - i + 1) \quad .....5$$

$$where\ c(i) = \int_{i=1}^{i} \frac{2}{MAXBAS} - \left|u - \frac{MAXBAS}{2}\right| \frac{4}{MAXBAS^2} du \quad .....6$$

where **P (t)** is the precipitation at time t, **FC** is the field capacity, **BETA** is a parameter that determines the relative contribution to runoff from rain or snow melt, $\mathbf{E_{act}}$ is the actual evapotranspiration, $\mathbf{E_{pot}}$ is the potential evapotranspiration, **LP** is the soil moisture value above which $\mathbf{ET_{act}}$ reaches $\mathbf{ET_{pot}}$, $\mathbf{Q_{GW}}$ is the groundwater recharge, $\mathbf{Q_{sim}}$ is the simulated runoff, and $\mathbf{K_i}$ is the recession constant. A more detailed description of the model can be found in Seibert (2005).

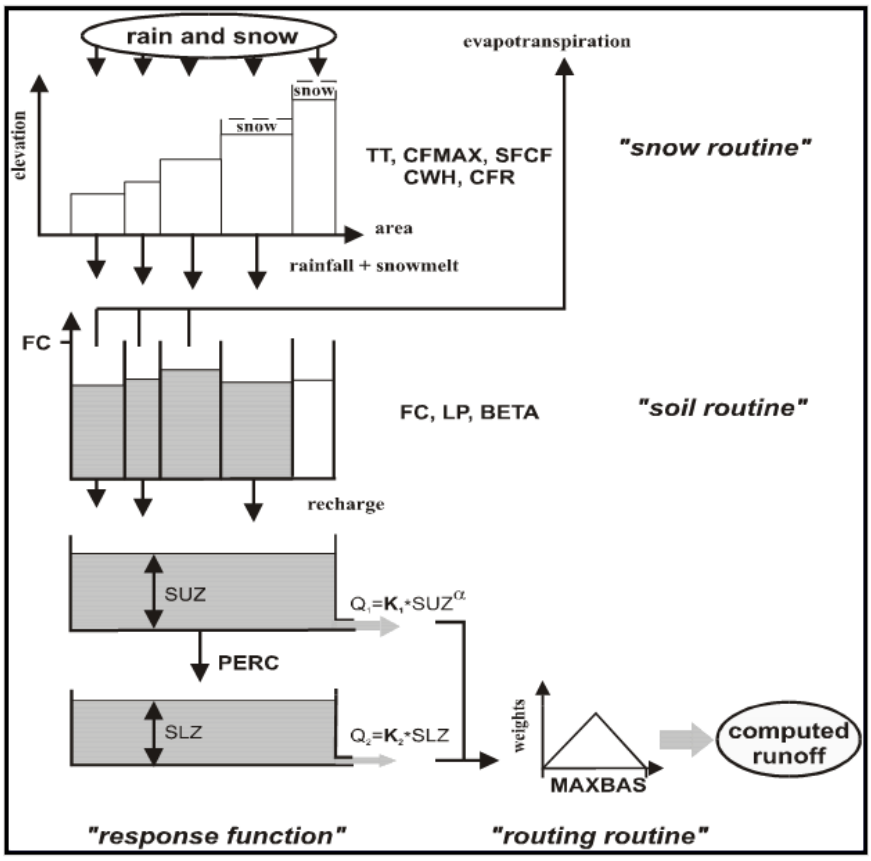

Figure 7: General structure of the HBV model (Seibert, 2005).

4.2.3 Model performance criteria

In order to assess the performance of the models, three criteria were used. These are: coefficient of determination (R^2) (Equation 7), Nash-Sutcliffe efficiency (NSE) (Equation 8) and Explained variance (EV) (Equation 9). For this purpose observed runoff at Sore-Mettu gauging station were incorporated into the modelling process.

$$R^2 = \frac{(\sum(Q_{obs} - \bar{Q}_{obs})(Q_{sim} - \bar{Q}_{sim}))^2}{\sum(Q_{obs} - \bar{Q}_{obs})^2 \ \sum(Q_{sim} - \bar{Q}_{sim})^2} \quad \ldots\ldots 7$$

The coefficient of determination (R^2) expressed as the squared ratio between the covariance and the multiplied standard deviations of the observed and predicted values (Krause et al., 2005). A model may result good R^2 even if it is over or underestimate the simulation, therefore it has to be supported by other efficiency criteria like Nash and Sutcliffe efficiency (NSE, 1970). Another performance criterion used is the explained variance (EV). EV is

calculated as one minus the ratio of residual variance under the modelling and residual variance under the null model (Gelman and Pardoe, 2006). It is able to eliminate the impact of systematic shifts of the data (e.g. systematically to large or to small modelled data, even if they are right in time) (Schulla and Japser, 2000). A comparison between the EV and the R^2 may show these effects. If the explained variance EV is larger than the corresponding R^2, then it is highly probable that there are systematic errors in the modelled data.

$$NSE = 1 - \frac{\sum_{i=1}^{n}(Q_{obs} - Q_{sim})^2}{\sum_{i=1}^{n}(Q_{obs} - \bar{Q}_{obs})^2} \quad \ldots . 8$$

$$EV = 1 - \frac{\sum(Q_{sim} - Q_{obs})^2 - \frac{1}{n}(\sum(Q_{sim} - Q_{obs}))^2}{\sum(Q_{obs})^2 - \frac{1}{n}(\sum Q_{obs})^2} \ldots . 9$$

Where: Q_{obs}= observed runoff; Q_{sim}=simulated runoff; $\bar{Q}_{obs}$, $\bar{Q}_{sim}$= mean observed and simulated runoff; n= number of time steps used for EV calculation

Additional criteria used to compare the performance of the models are the overall agreement between the predicted and measured runoff discharges (Equation 10), and runoff volume errors (Meselhe and Habib, 2004). The absolute volume error were estimated and used to quantify the performance accuracy of both models during simulation periods.

$$V_e = \frac{|V_p - V_r|}{V_r} \times 100 \quad \ldots\ldots 10$$

Where: V_e is the runoff volume error (%), V_r is the observed runoff volume (km^3), and V_p is the predicted runoff volume (km^3).

Chapter 5

5. An assessment of temperature and precipitation change projections using a regional and a global climate model for the Baro-Akobo Basin, Nile Basin, Ethiopia[1]

Abstract

In this study, large-scale atmospheric output variables from CGCM3.1 global circulation model and the regional model REMO are downscaled statistically to meteorological variables at the point scale in a daily resolution to assess future climatic variables under climate changes. The area of study is Baro-Akobo river basin in Ethiopia, which contributes to the White Nile in Sudan. The minimum and maximum temperature and precipitation variables were selected, and future time scenarios of these variables were projected based on climate scenarios of A1B and B1 for a period of 2011 to 2050.Both REMO and CGCM3.1 outputs capture the observed 20th century trends of temperature and precipitation change over the basin. However, the result of downscaled precipitation reveals that precipitation does not verify a systematic increase or decrease in all future time horizons for both A1B and B1 scenarios unlike that of maximum temperature. For REMO A1B and B1 scenarios similar trend +1.3°C changes for maximum temperature are expected, and rainfall increases as much as 24% for the 2011 to 2050 period. For the CGCM3.1 model +2.55°C changes in maximum temperature and 23% increase in rainfall is likely

KEY WORDS*: Climate Change; Statistical Downscaling; REMO; CGCM*

5.1 Introduction

Climate change impact studies associated with global warming as a result of Green House Gases (GHG) has been given ample attention worldwide in the recent decades because of perceived impact on global, regional as well as local socio-economic, livelihood and natural resources. According to the Intergovernmental Panel on Climate Change (IPCC) 4th assessment report (Solomon et al., 2007) global average surface temperature would likely rise between 2°C to 4.5°C by 2100 with the doubling of atmospheric carbon dioxide (CO_2). For the continent of Africa (Solomon et al., 2007), the warming during this century would

[1] Most of this chapter is published as: Kebede, A., Diekkrüger, B., Moges, S.A. (2013): An Assessment of Temperature and Precipitation Change Projections using a Regional and a Global Climate Model for the Baro-Akobo Basin, Nile Basin, Ethiopia. J Earth Sci Climate Change 4: 133. doi:10.4172/2157-7617.1000133.

very likely be larger than the global average (3°C). With respect to precipitation, the results are different for different regions; the report also indicates that an increase in mean annual rainfall in East Africa is likely. The minimum temperature over Ethiopia show an increase of about 0.37°C per decade, which indicates the signal of warming over the period of the analysis 1957-2005 (Di Baldassarre et al., 2011) Previous studies in Nile basin provide different indication regarding long term rainfall trends; Elsahmay et al. (2009) reported future precipitation change in the Blue Nile is uncertain in their assessment of climate change on stream flow of the Blue Nile for 2081-2098 period using 17 GCMs. Wing et al. (2008) showed that there are no significant changes or trends in annual rainfall at the national or watershed level in Ethiopia; Taye et al. (2011) reported impact of climate change on rainfall trend is unclear for the Lake Tana catchment (Blue Nile part) while for Nyando River (White Nile part) rainfall shows increasing trend under two future SRES emission scenarios A1B and B1 for 2050s. Beyene et al. (2010) showed that the Nile River is expected to experience an increase in stream flow early in the study period (2010-2039), due to generally increased precipitation; it is expected to decline during mid (2040-2069) and late (2070-2099) century as a result of both precipitation declines and increased evaporative demand. Furthermore, Conway (2005), Elsahmay et al. (2009), Yimer et al. (2009) also reported about uncertainty of the direction and magnitude of future changes in rainfall whilst temperature are expected to increase. Therefore previous studies show that many parts of the Nile are sensitive to climate change and it has a prospective impact on the water resources in the area. However, the climatic regions of the Nile are variable and dividing the basin into different regions and sub-basin will be a convincing and proficient approach when studying impacts of climate change (Taye et al., 2011).

Generally, climate change scenarios are coarse in resolution and may not be directly applied to local scale studies to understand the likely impact of the climate change. This study mainly focuses on the impact of climate change on the hydrology of a river basin scale at local scale application. It is widely accepted that Atmospheric-Ocean General Circulation Models (GCMs) are the best physically based means for predicting future climate (Bardossy, 2000). Despite the fact that the impact of climate change scenarios forecasted at a global scale, their coarse spatial resolution may not be used directly for studies at a small watershed scale. Dibike et al. (2008) reported a clear need for high resolution scenarios at a

spatial scale much finer than that provided by a global or even some regional climate models. Consequently, as Yimer et al. (2009) described, downscaling techniques emerged as a means to relate the scale mismatch between the GCMs and the small scales required at watershed level. The main downscaling approaches frequently used in development of higher resolution climate scenarios are dynamical and statistical downscaling (Yimer et al., 2009; Dibike et al., 2008; Dibike et al., 2005). Dynamical downscaling generates regional or local scale climate scenario data by developing and using Regional Climate Models (RCMs) with the coarse GCM data used as boundary conditions. Statistical Down-Scaling Method (SDSM) on the other hand involves developing quantitative relationships between large scale atmospheric variables, the predictors, and local surface variables, the predictands.

The focus of this chapter is to provide first-hand understanding of the direction of climate change in one of the remote basins of Ethiopia (Baro-Akobo basin) where there is little previous research work on likely impact of climate change. The basin is one of a productive agricultural area and covers a higher percentage of natural forest than the rest of the country. The objective of the study is assessing temperature and rainfall change projection from CGCM3.1 and REMO using downscaling techniques within the Baro-Akobo basin for a period of 2011-2050.

Approaches for Climate Downscaling

This section briefly summaries the various downscaling approaches available in the literature. Although the GCMs' ability to reproduce the current climate has increased, direct outputs from GCM simulations are inadequate for assessing hydrological impacts of climate change at regional and local scales (Xu et al., 2005). Indeed, many hydrological impact assessments need station/point scale climate variables; therefore there is a clear need for reliable high resolution scenarios at station scale finer than that of GCMs performed through downscaling. Two downscaling approaches that are commonly used for climate scenario development are dynamical downscaling and statistical downscaling.

In the dynamical downscaling approach a Regional Climate Model (RCM) is nestled into a GCM were GCMs are used to fix boundary conditions. The major disadvantage of dynamical downscaling in climate impact study is its high computational and technical demands at the

outset (Wilby and Dawson 2012). Statistical Downscaling (SD) involves developing quantitative relationships between large-scale atmospheric variables and local-scale surface variables, since SD is derived from the historical observed data, it provide site specific information as recommended in many climate change impact studies (Dibike et al., 2008, and Anandhi et al., 2008).

The most common SD approaches are namely; Statistical Down-Scaling Model (SDSM), Long Ashton Research Station Weather Generator (LARS-WG) and Artificial Neural Network (ANN). SDSM is a hybrid of a stochastic weather generator and multiple regression based method (Wilby et al., 2002). During downscaling with SDSM a multiple linear regression model is developed between a few selected large-scale predictor variables and local scale predictands such as precipitation and temperature (Dibike et al., 2008 and Wilby et al., 2004). As Yimer et al. (2009) described Predictor is input data used in SDSM, typically a large scale variable describing the circulation regime over a region, it is also known as "independent variable", or simply as the "input variable". The predictand is the output data, typically the small-scale variable representing temperature or precipitation at a weather/climate station.

SDSM can be used to provide local information, which could be used in many climate change impact assessment. It is computationally inexpensive and thus can be easily applied to the output of different GCM experiments (Wilby and Dawson, 2007). According to Wilby and Wigley (2000) in SD the following assumptions are made in order to use such type of downscaling methods for assessing climate change (i) appropriate relationships can be developed between large scale and small scale grid predictor variables; (ii) these observed empirical relationships are valid also under climate change conditions; and (iii) the predictors variables and their change are well characterised by GCMs. If these assumptions hold, it is then possible to produce climate scenarios of regional and small scale with finer resolution and more reliable than raw GCMs from future climate change data produced by GCMs

In LARS-WG, for precipitation downscaling, observed daily local station precipitation of each month are analysed using a number of years of historical data to obtain statistical characteristics such as number of dry days, wet days and mean daily precipitation in each

month of a year. This information is used to develop semi-empirical distributions for the lengths of wet and dry day series and daily precipitation amount, the precipitation value is generated from the semi-empirical precipitation distribution. On the other hand ANN is a non-linear regression type in which a relationship is developed between a few selected large-scale atmospheric predictors and basin scale meteorological predictands (Khan et al., 2006).

Compared with dynamic downscaling, SD methods have the following advantages (Xu et al., 2005): (i) based on standard and accepted statistical procedures, (ii) computationally inexpensive, (iii) may be flexibly crafted for specific purpose, (iv) able to directly incorporate the observational record of the region. Wilby and Dawson (2012) reports a number of studies show that SDSM yields reliable estimates of extreme temperatures, seasonal precipitation totals, areal and inter site precipitation behaviour. Thus we applied the program SDSM 4.2 (Wilby et al., 2004) as described in chapter 4 section 4.1 for this study to downscale the outputs of REMO and CGCM for Baro-Akobo basin. There is little study on climate change in Baro-Akobo basin and this study may form one of the first understandings of the direction of climate change.

The organization of this chapter is as follows; the next section continues with description on scenarios used for downscaling approaches. Study area and data used in this study are described in section 5.2. In section 5.3 ‘methodology’ methods used in the analysis presented, results are shown and discussed in section 5.4 ‘Results and discussion’ while conclusion and some remarks are given in section 5.5 entitled ‘conclusion’.

Scenarios used

The IPCC developed scenarios that have been widely used in the analysis of possible climate change and options to mitigate, among these A1B and B1 scenarios were used in this study. A1B scenario belongs to A1 family that describes a future world of very rapid economic growth and rapid introduction of new and more efficient technologies. A1B group is distinguished by balanced across all sources of energy not relaying on one particular source, on the assumption that similar improvement rates apply to all energy supply and end use technologies. Whereas the B1, scenario describes rapid change in economic structures

towards a service and information economy, with reductions in material intensity and the introduction of clean and resource-efficient technologies (Solomon et al., 2007).

REMO: The regional climate model REMO is a hydrostatic, three-dimensional atmospheric model that has been developed in the context of the Baltic Sea Experiment (BALTEX) at the Max-Planck-Institute for Meteorology in Hamburg[2]. It is based on the Europamodel (EM), the former numerical weather prediction model of the German Weather Service (DWD) and is described in Jacob (2001). Additionally, the physical parameterization package of the general circulation model ECHAM4 has been implemented. Physical parameterizations are taken from ECHAM4 and adjusted to the scale of REMO (Paeth, 2005). Further detailed information on the REMO development and model characteristics can be found at http://www.remo-rcm.de/REMO-Model-Characteristics.1268+M54a708de802.0.html

In the present version, the model is run at 0.5° horizontal resolution with 20 terrain-following vertical levels. The model domain covers the entire tropical and northern parts of Africa from 30°W to 60°E and from 15°S to 45°N (Paeth and Thamm, 2007). The model considers land use change for both A1B and B1 scenarios and also it has ensemble runs for A1B without land use change. The REMO model which covers the area of interest (5 to 11° N and 33 to 37°E) with land use change was used in this study. The basin is covered by 50 REMO raster nodes (Figure 9). Among these are 17 REMO nodes near climate/meteorological stations used for downscaling. The predictor variables used for downscaling REMO are precipitation, maximum and minimum temperature, radiation and relative humidity data of REMO grid cells surrounding each meteorological station.

CGCM3.1: CGCM3.1 is the third version of Canadian Coupled Global Climate Models (CGCM3.1) and shares many basic features with the second generation model as described in McFarlane et al. (2005) and Scinocca et al. (2008). Further detailed information on CGCM3.1 development and model characteristics can be found at (http://www.ec.gc.ca/ccmac-cccma/default.asp?lang=En&n=89039701-1). Predictor data files or SDSM inputs from CGCM3.1 and NCEP (National Centre for Environmental Prediction) were extracted from the Data Access Integration (DAI) website

[2] http://www.remo-rcm.de/

(http://loki.ouranos.ca/DAI/gcm-e.html); which is an online climate and environmental data distribution tool. The predictor variables for CGCM3.1 (Third generation of the Canadian Coupled Global Climate Model) were provided on a grid box by grid box basis of size correspond and to the value over the centre of the cell defined an area of a 3.75° longitude and 3.75° latitude. The NCEP/NCAR (National Centre for Atmospheric Research) reanalysis products have been interpolated onto the CGCM3 grid, and made available for the calibration procedure of SDSM over the base period (1961-2001). The study area Baro-Akobo basin lies in four CGCM grid nodes [9.28° Lat 33.75°Lon, 5.57° Lat 33.75°Lon, 9.28° Lat 37.5° Lon and 5.57° Lat 37.5° Lon] (Figure 9), from these grid nodes 25 large scale atmospheric variables[3] were extracted and used as potential inputs to SDSM.

5.2 Study area and data used in this study

Baro-Akobo basin as described in chapter 2 section 2.1 lies in the southwest of Ethiopia between latitudes of 5° 31` and 10° 54` N, and longitudes of 33° 0` and 36° 17` E. This chapter discuss the study covers the basin with elevation ranges 1230 to 2200 m.a.s.l (Figure 3 and 10). In the study area, there is high variability in temperature with large differences between the daily maximum and minimum temperatures. Figure 10 shows that large temperature differences can be observed by the catchment topographic settings where temperature decreased with increase in altitude.

Climate station data (Predictands)

Data used in the study are daily rainfall, maximum and minimum temperature collected and archived by the Ethiopian National Meteorological Agency (NMA) from 12 stations in and around the Baro-Akobo river basin, from 1972 to 2000 in general. The choice was forced by data extent and the sparse station network in the basin. The number of meteorological stations and extent of data used in downscaling experiment are depicted in Table 1.

[3]Source: http://loki.ouranos.ca/DAI/CGCM3_predictors-e.html, (accessed on June 10,2011)

Table 1 Meteorological stations and data periods used in the study area.

Station	Elevation (m)	Lat (degree)	Lon (degree)	Precipitation (mm)	Maximum Temperature(^{0}C)	Minimum Temperature(^{0}C)
Tepi	1230	7.20	35.42	1981-2000	1981-2000	1981-2000
Mezan Teferi	1400	7.00	35.58	1987-2000	1982-1991	1982-1991
Dembi Dollo	1550	8.53	34.80	1979-2000	1979-2000	1979-2000
Yubdo	1560	8.95	35.45	1976-2000	1976-2000	1976-2000
Mettu	1690	8.30	35.58	1976-2000	1976-2000	1976-2000
Bure	1700	8.28	35.10	1976-2000	1976-2000	1976-2000
Begi	1722	9.35	34.53	1979-2000	1978-2000	1978-2000
Hurumu	1800	8.33	35.70	1973-2000	-	-
Chora	1930	8.42	36.13	1975-2000	-	-
Gimbi	1970	9.17	35.80	1978-2000	1979-1993	1979-1993
Gore	2024	8.15	35.53	1972-2000	1972-2000	1972-2000
Masha	2200	7.73	35.48	1975-2000	1980-1999	1980-1999

In Ethiopia, as shown in the Figure 8, the pattern and character of rainfall varies in different parts of the country. There are some regions which experience three seasons (tri-modal type, region A) with two rainfall peaks (where one peak is more prominent than the other), while some regions have four seasons with two distinct rainfall peaks (bi-modal type, region C). There are still some regions, which have two seasons with a single rainfall peak (mono-modal type, region B). The Area under region B is where the Baro-Akobo basin lies and is characterized by a single rainfall peak during a year, with two distinct seasons, one being wet (rainy season) locally called “Kiremt” and the other dry called “Bega”.

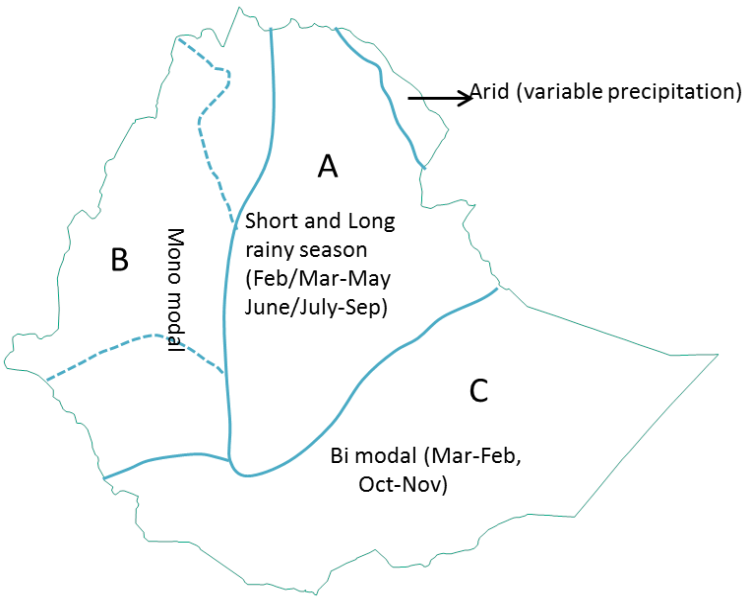

Figure 8: Rainfall regimes over Ethiopia (NMSA, 1996).

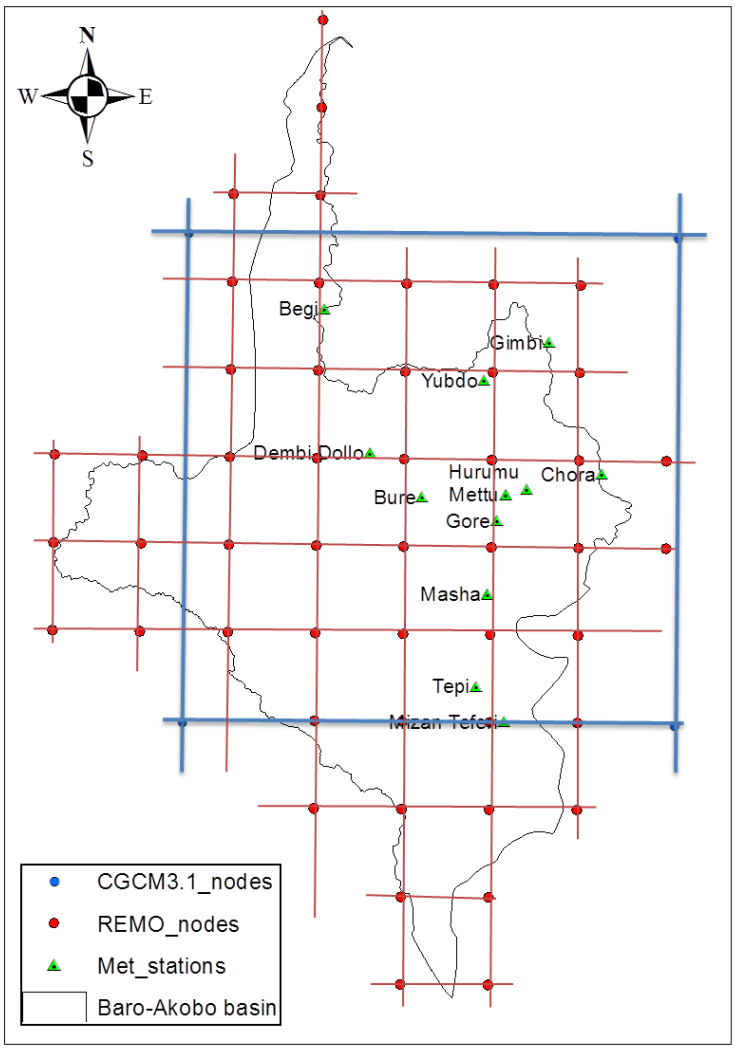

Figure 9: Grids of REMO and CGCM3.1 selected for study area. (Station elevation range: 1230 to 2200 m.a.s.l)

Mean monthly rainfall pattern shows that the south-western and western part of the country in region B is under the wet season during February/March to October/November and April/May to October/ November respectively. Therefore, stations Tepi, Mezan Teferi and Masha belong to the Bega (December, January and Feberuary) and Kiremt (March to October) seasons and are named as southern part of the basin here after. Whereas stations Gore, Bure, Yubdo, Dembi Dollo, Gimbi, Mettu, Begi and Assosa are in Bega season (November, December, January and February) and will be in Kiremt season (May to October) and named as Northern part of the basin here after for the purpose of looking at seasonal climate change in the area.

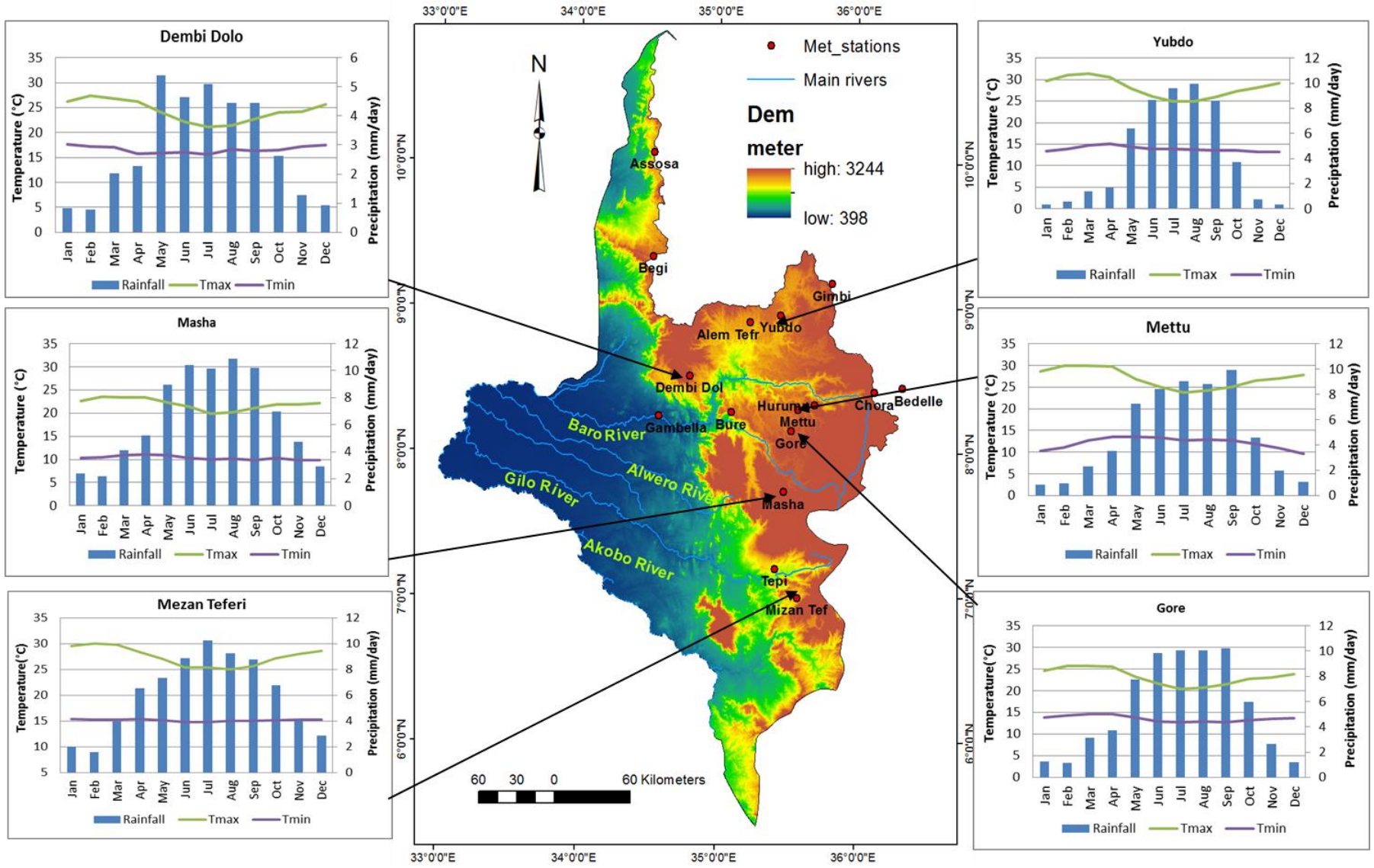

Figure 10: Baro Akobo Basin Map, distribution of meteorological stations used in the study area and observed monthly mean rainfall, Tmax, and Tmin of some stations.

5.3 Methodology

Downscaling

,,,

SDSM 4.2 statistical downscaling model was supplied on behalf of the Environment Agency of England and Wales. It is a decision support tool used to asses local climate change impacts using a SD technique. The software manages additional tasks of data quality control and transformation, predictor variable pre-screening, automatic model calibration, basic diagnostic testing, statistical analysis and graphing of climate data (see section 4.1). SDSM (Wilby et al., 2002) is best described as a hybrid of stochastic weather generator and regression-based methods. Through downscaling using SDSM, multiple regression models were developed between selected large-scale predictor variables (NCEP/NCAR), (REMO) and local scale predictands. The parameters of the regression equation are estimated using an ordinary Least Squares algorithm. Precipitation is modelled as a conditional process in which the local precipitation amount is correlated with the occurrence of wet days. As the distribution of precipitation is skewed, a forth root transformation is applied to the original series to convert it to the normal distribution, and then used in the regression analysis. Minimum and maximum temperatures are modelled as unconditional process, where a direct link is assumed between the large scale predictors and local scale predictand. Additionally, stochastic techniques are used to artificially inflate the variance of the downscaled daily time series to better accord with observations.

One of the challenging stages in SD is the choice of appropriate predictor variable(s), this is due to the fact that downscaling is highly sensitive to the choice of predictor variables, and also decision on predictor variables determines the character of the downscaled climate scenario. Beside this the explanatory power of individual predictor variables varies spatially and temporally (Wilby and Dawson 2007). Screening of the most appropriate predictor variables was carried out through the percentage of explained variance analysis, linear correlation analysis, partial correlation analysis, and scatter plots between predictor and predictand variables. SDSM normally calibrated by a linear regression based on NCEP/NCAR reanalysis data and station data then later applied to GCM data. For this study, large-scale NCEP/NCAR predictor variables representing the current climate condition were used for analysis subsequently applied to CGCM3.1. Table 2 shows the selected predictor variables

from NCEP/NCAR for each meteorological station in the downscaling procedure. Whereas for downscaling REMO, SDSM calibrated using precipitation, maximum temperature, minimum temperature, wind, radiation, and relative humidity data of each stations served as predictands, while the surrounding grid cells of REMO for the same variable of each climate model served as predictor variables.

Ensemble Simulation

The advantage of using SD is the possibility of generating statistical ensembles. An ensemble is a large (possible infinite) number of copies of a system, considered all at once, each of which represents a possible state that the real system might be in at some specified time (Araujo and New 2006). Depending on the total number of simulations conducted, ensemble forecast analyses range from simply averaging forecasts and evaluating their variability using bounding boxes to much more sophisticated approaches analysing the probabilities of forecasts (Rößler et al., 2012). For this study 20 statistical ensembles were generated using the model and used to examine the precipitation and temperature change in Baro-Akobo basin. SDSM have the capacity to generate up to 100 ensembles and can be used to research the uncertainty analysis of climate scenario. Due to the computational capacity of the hydrological models subsequently to be used after downscaling and storage required we were forced to restrict the number of ensembles to 20 for each climate models (REMO and CGCM3.1) and each scenario A1B and B1.

Calibration and Validation

Model calibration was done based on the selected predictor variables that were derived from the REMO and NCEP/NCAR data set. Calibration in this case aims to find the coefficients of the multiple regression equation parameters that relate the climatic variables derived from REMO, NCEP/NCAR and local scale variables. SDSM has the possibility of finding annual, seasonal and monthly regression functions to downscale the meteorological variables. For this study the temporal resolution of the downscaling model was specified as monthly for the entire stations because the correlation between the data produced by the meteorological stations and the grid cell prediction was found to be good for the purpose.

Table 2 Predictors selected for model calibration at different station.

Station	Predictand	Predictors*					
Tepi	Temperature max	Ncepp_thaf	Nceptempaf				
	Temperature min	Ncepp_vaf	Ncepp_zaf	Ncepp850af	Nceps850af		
	Rainfall	Ncepp8zhaf	Nceps850af				
Mezan	Temperature max	Ncepp_thaf	Ncepp8_uaf	Ncepp8thaf	Nceptempaf		
Teferi	Temperature min	Ncepp_vaf	Ncepp500af	Nceps850af	Nceptempaf		
	Rainfall	Ncepp_zaf	Ncepp5thaf	Ncepp8zhaf			
Dembi	Temperature max	Ncepp_thaf	Ncepp5_zaf	Nceptempaf			
Dollo	Temperature min	Ncepp8_faf	Ncepp850af				
	Rainfall	Ncepp8_uaf	Nceptempaf				
Yubdo	Temperature max	Ncepp_thaf	Ncepp5_zaf	Ncepp8thaf	Nceptempaf		
	Temperature min	Ncepp_vaf	Ncepp500af	Nceps850af	Nceptempaf		
	Rainfall	Ncepp_zaf	Ncepp5thaf	Ncepp8zhaf	Nceps850af		
Mettu	Temperature max	Ncepp5_zaf	Ncepp8thaf	Ncepp8zhaf	Nceptempaf		
	Temperature min	Ncepp_thaf	Ncepp5_zaf	Ncepp8thaf	Nceptempaf		
	Rainfall	Ncepmslpaf	Ncepp5thaf	Nceps850af			
Bure	Temperature max	Ncepp_zaf	Ncepp_thaf	Ncepp5thaf	Ncepp8thaf	Nceptempaf	
	Temperature min	Ncepp_uaf	Ncepp5thaf	Nceptempaf			
	Rainfall	Ncepp_thaf	Ncepp5thaf	Ncepshumaf			
Begi	Temperature max	Ncepp_thaf	Ncepp5_zaf	Nceptempaf			
	Temperature min	Ncepp_vaf	Ncepp500af				
	Rainfall	Ncepp_zaf	Ncepp5_zaf				
Hurmu	Temperature max						
	Temperature min						
	Rainfall	Ncrpp8zhaf	Nceptempaf				
Chora	Temperature max	Ncepp_thaf	Nceptempaf				
	Temperature min	Ncepp8_faf	Nceps850af	Nceptempaf			
	Rainfall	Ncepp_zaf	Ncepp_zhaf				
Gimbi	Temperature max	Ncepp_thaf	Ncepp8thaf	Nceptempaf			
	Temperature min	Ncepp_vaf	Ncepp_thaf	Nceptempaf			
	Rainfall	Ncepp_faf	Ncepp8zhaf				
Gore	Temperature max	Ncepp_faf	Ncepp_thaf	Ncepp_zhaf	Ncepp5thaf	Ncepp8thaf	Nceptempaf
	Temperature min	Ncepp5thaf	Ncepp8thaf	Nceptempaf			
	Rainfall	Ncepp_zaf	Ncepp_zhaf	Nceps500af			
Masha	Temperature max	Ncepp_faf	Ncepp5_vaf	Ncepp8thaf	Nceptempaf		
	Temperature min	Ncepp_zaf	Ncepp5_uaf	Ncepp8_vaf	Nceptempaf		
	Rainfall	Ncepp8zhaf	Nceps850af				

Description of each predictor variables indicated in Table 2*

Predictors	Description	Predictors	Description
ncepp_faf.dat	10_WS	Ncepp5zhaf.dat	5_Di
ncepp_vaf.dat	10_MWC	Ncepp8_faf.dat	8_WD
ncepp_zaf.dat	10_Vor	Ncepp8_uaf.dat	8_ZWD
ncepp_thaf.dat	10_WD	Ncepp8_vaf.dat	8_MWC
ncepp_zhaf.dat	10_Di	Ncepp850af.dat	8_Gp
Ncepp5_zaf.dat	5_WD	Ncepp8thaf.dat	8_WD
Ncepp5_uaf.dat	5_ZWC	Ncepp8zhaf.dat	8_Di
Ncepp5_vaf.dat	5_MWC	Nceps500af.dat	5_SH
Ncepp5_zaf.dat	5_Vor	Nceps850af.dat	8_SH
Ncepp500af.dat	5_Gp	Ncepshumaf.dat	10_SH
Ncepp5thaf.dat	5_WD	Nceptempaf.dat	Temperature @ 2m

Where: WS= wind speed; MWC= Meridional wind component; Vor= vorticity; WD= wind direction; Di= divergence; ZWC= zonal wind component; Gp= Geopotential; SH= Specific humidity; 10_= 1000hpa; 8_=850hpa; 5_= 500hpa

Model setup parameters like event threshold, bias correction and variance inflation were adjusted during calibration to obtain best statistical agreement between the observed and simulated climate variables. During the calibration of precipitation: daily and monthly mean,

variance, QQ-plot, PDF plot, dry and wet-spell lengths were used as performance criteria. The stochastic component of SDSM allows for performing 100 ensembles in the validation process. In this study 20 ensembles are performed, and the average of the twenty independent stochastic GCM ensembles was taken for analysis. The model developers Wilby et al. (2002) suggested that, as the target here is only to see the general trend of the climate change in the future; it is adequate to consider the average of the ensembles. They also added that to preserve inter-variable relationships, the ensemble mean should be used.

Climate Change Scenario

The base line data for the base period were from 12 stations in and around the Baro-Akobo basin within the range of 29 to 14 years period from 1972-2000 and 1987-2000 respectively. Accordingly REMO and CGCM3.1 was downscaled for two emission scenarios (A1B and B1 for REMO and A1B for CGCM3.1) this is because NCEP/NCAR has no predictor variables for the B1 scenario. The first 18 (1972-1989) to 8 (1987-1994) years of data were considered for calibrating SDSM while the remaining 11 to 6 years (1990-2000) to (1995-2000) respectively, were used for validation. Beside graphical fit, the statistical analyses like mean absolute error (MAE) and standard deviation (STD) were used to compare downscaled data and base period observation. The performance of the model during the calibration and validation period and the climate change scenario results are explained in the following section.

5.4 Results and Discussion

For all stations, downscaled base-line daily temperature data shows good agreement with observation for both calibration and validation periods. In case of daily precipitation even though there were little variations in individual months the performances of the model overall shows a good agreement between the observed and calibrated for almost all months of the year. Figures 11-13 shows the performance of the models during calibration/downscaled period and the original REMO/ CGCM3.1 data before downscaling. As depicted in the figures (Figures 11-13) despite the discrepancy in the values, the skill of both models in capturing the seasonal pattern of both the temperature and rainfall makes the models a good choice for the region. It is also important to recognize the improvement in the outputs of the statistical downscaling can also attributed to the good skill of the

REMO/CGCM3.1 model in the region. Unlike temperature, precipitation is a conditional process that depends on other physical intermediate processes like occurrence of humidity, cloud cover, and /or wet-days and the accuracy of downscaling precipitation is less consistent as anticipated mainly due to the obvious complex physical processes and intermediate processes that may not be captured by statistical downscaling.

Generally, results of downscaling for both climate model reveals that all stations considered in this study show good agreement with the observed data. To examine the performance of the climate models, observed and downscaled values of the base period were averaged to mean annual rainfall, and rainy days were calculated (Table 3). The result shows mean annual rainfall and rainy days partly captured by both models REMO and CGCM3 (Table 3).

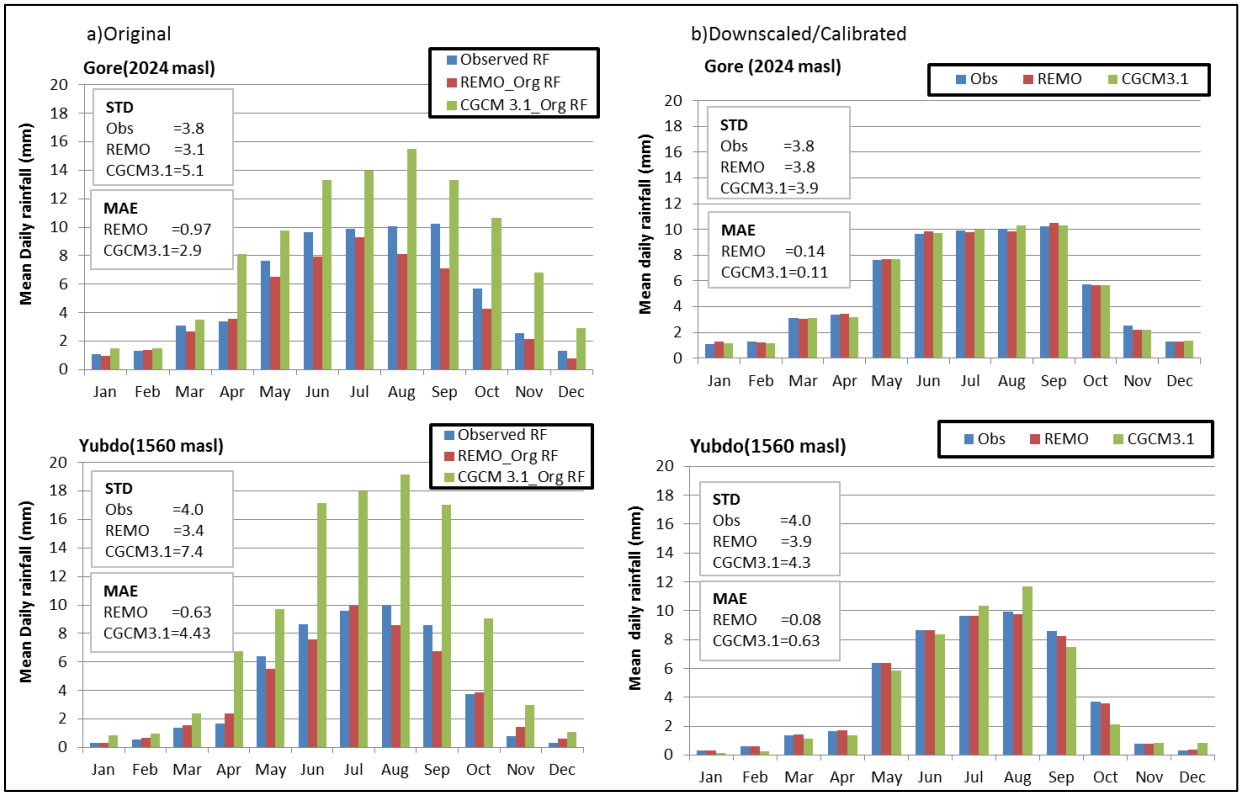

Figure 11: Current climate (1972-2000); precipitation (a) original (REMO and CGCM3.1 not downscaled) and (b) downscale using SDSM for Gore and Yubdo stations. (Abbreviations: Org=original, Obs=observed, RF=rainfall, STD=standard deviation, MAE=mean absolute error)

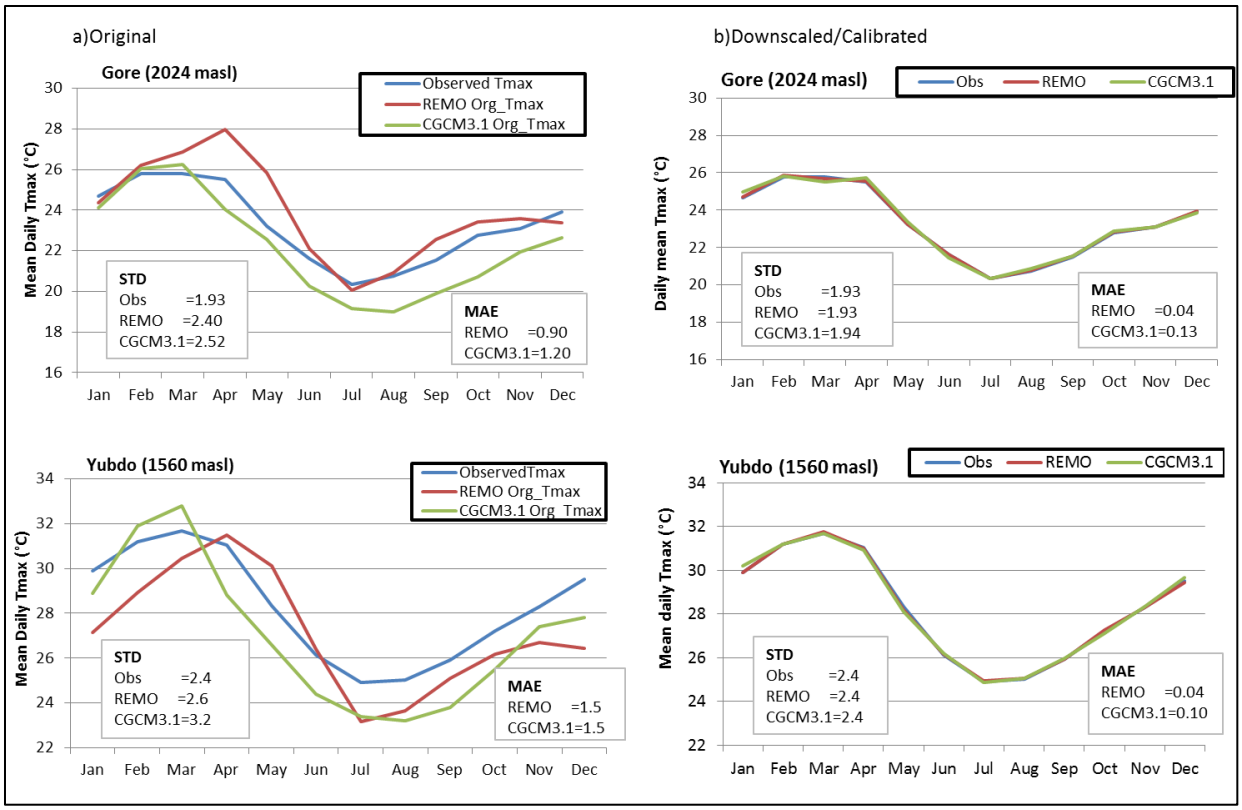

Figure 12: Current climate (1972-2000); maximum temperature (a) original (REMO and CGCM3.1 not downscaled) and (b) downscaled using SDSM for Gore and Yubdo stations.

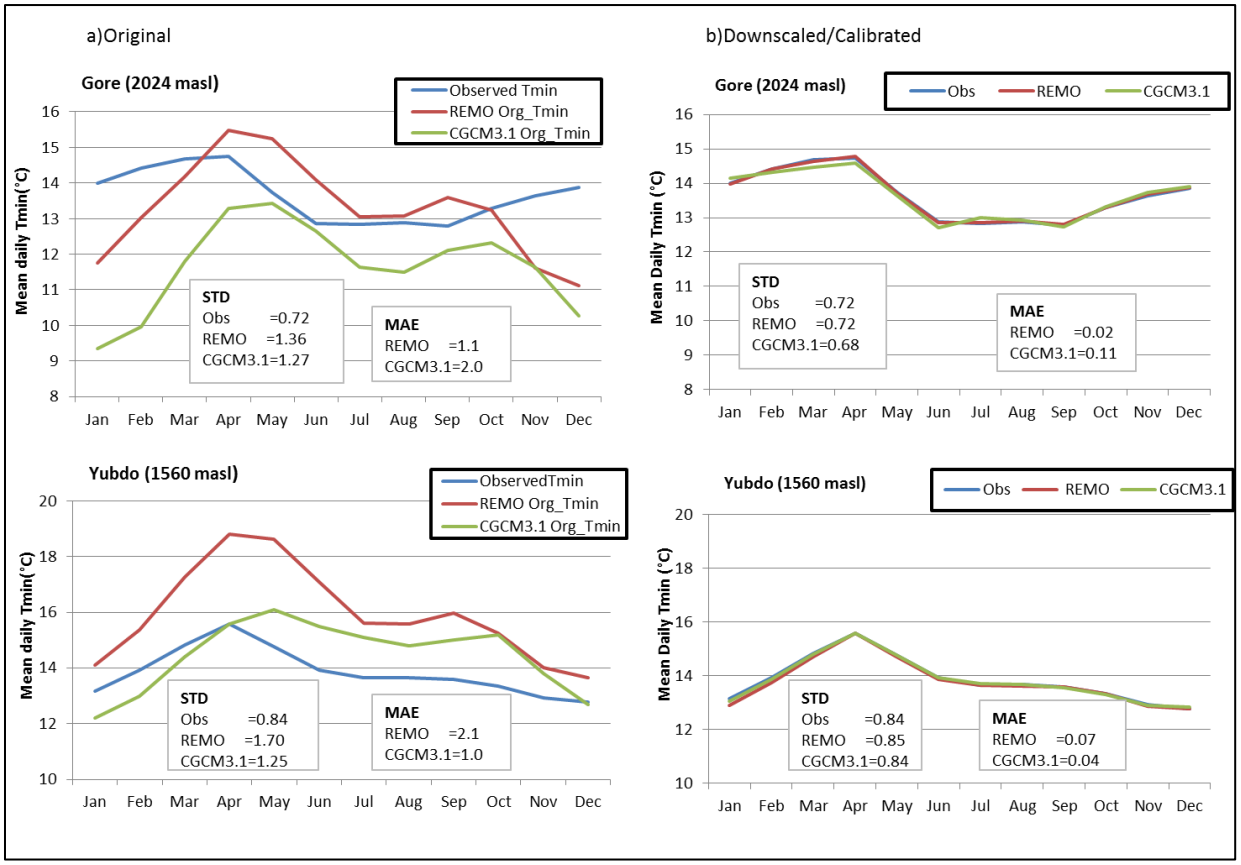

Figure 13: Current climate (1972-2000); minimum temperature (a) original (REMO and CGCM3.1 not downscaled) and (b) downscaled using SDSM for Gore and Yubdo stations.

Table 3 Comparison of base period (observed and downscaled) annual rainfall and rainy days values for station Gore, Bure, Chora and Yubdo.

Stations (altitude)	Original Observation / Model run	Mean Annual (mm)	Rainy days (days/year)
Gore (2024 masl)	Observation	2035	170
	REMO	2033	176
	CGCM3.1 A1B	2012	179
Bure (1700 masl)	Observation	1283	153
	REMO	1213	154
	CGCM3.1 A1B	1393	144
Chora (1930 masl)	Observation	1648	135
	REMO	1690	138
	CGCM3.1 A1B	1992	181
Yubdo (1560 masl)	Observation	1474	120
	REMO	1538	145
	CGCM3.1 A1B	1631	128

Downscaling Future Scenario

After calibrating the model, the empirical relationships created between the large scale predictor and local scale variables were applied to downscale the future climate change scenario. Twenty ensembles of synthetic daily time series for the period of 40 years (2011-2050) were generated for A1B and B1 SRES emission scenarios. The period 2011-2050 aggregated to 20 years for future trend comparison from base year for REMO and CGCM3.1. The following section shows projected change of rainfall, maximum and minimum temperature annually and seasonally for stations considered in the study area.

I. Maximum Temperature

As depicted in Figure 14, it can be seen that generally increasing annual trend is likely for maximum temperature in all stations except Gore for both A1B and B1 scenario of REMO. Statistically downscaled REMO results show that there might be a general incremental trend of maximum temperature for A1B and B1 scenario for the period of 2011-2030 and 2031-2050 in the range of +0.1°C to +1.23°C and +0.1°C to +1.3°C respectively. However, stations Masha, Bure and Mettu show almost no change. It is also noted that the projected change appears to show generally increasing trend with decreasing altitude in the basin (Figure 14 and 15). In case of CGCM3.1 A1B scenario, generally increasing annual trend is expected for the period of 2011-2030 and 2031-2050 in the range of +0.2°C to +2.52°C and +0.1°C to

+2.55°C respectively. However, the decreasing annual trend Bure, Begi, Gimbi and Tepi stations may be associated to the problem of downscaling from Global models. We don't think the results are correct, however, the basin wide temperature increase is evident even with this mode. Therefore, the A1B scenario of REMO and CGCM3.1 agrees for most stations with the direction of maximum temperature change.

Other studies in Ethiopia and the Nile basin in particular using CGCM show similar pattern to this work. Hulme et al. (2001) found mean temperatures for CGCM1 B1 scenario increasing to 0.8°C in 2020s and 1.2°C in 2050s in Ethiopia. McSweeney et al. (2010) also shows an increase in mean temperatures in Ethiopia by 0.9°C to 1.6°C for 2030s and 1.7°C to 2.9°C for 2060s A1B scenario, and 0.5°C to 1.1°C by 2030s and 1.1°C to 1.8°C for 2060s for B1 scenario. Elshamy et al. (2009) also reported an average increase in temperature over Nile basin is 2°C to 4.3° C by year 2050 from 7 different CGMs. Conway (2005) also indicates that, with respect to the future climate in the Nile basin, there is high confidence that the temperature will increase. Nevertheless, this work focuses only on the catchment level and uses REMO higher solution regional model with 0.5° Lat/ Lon in addition to CGCM which were not tested in the region, further application of SDSM was the first time in the basin.

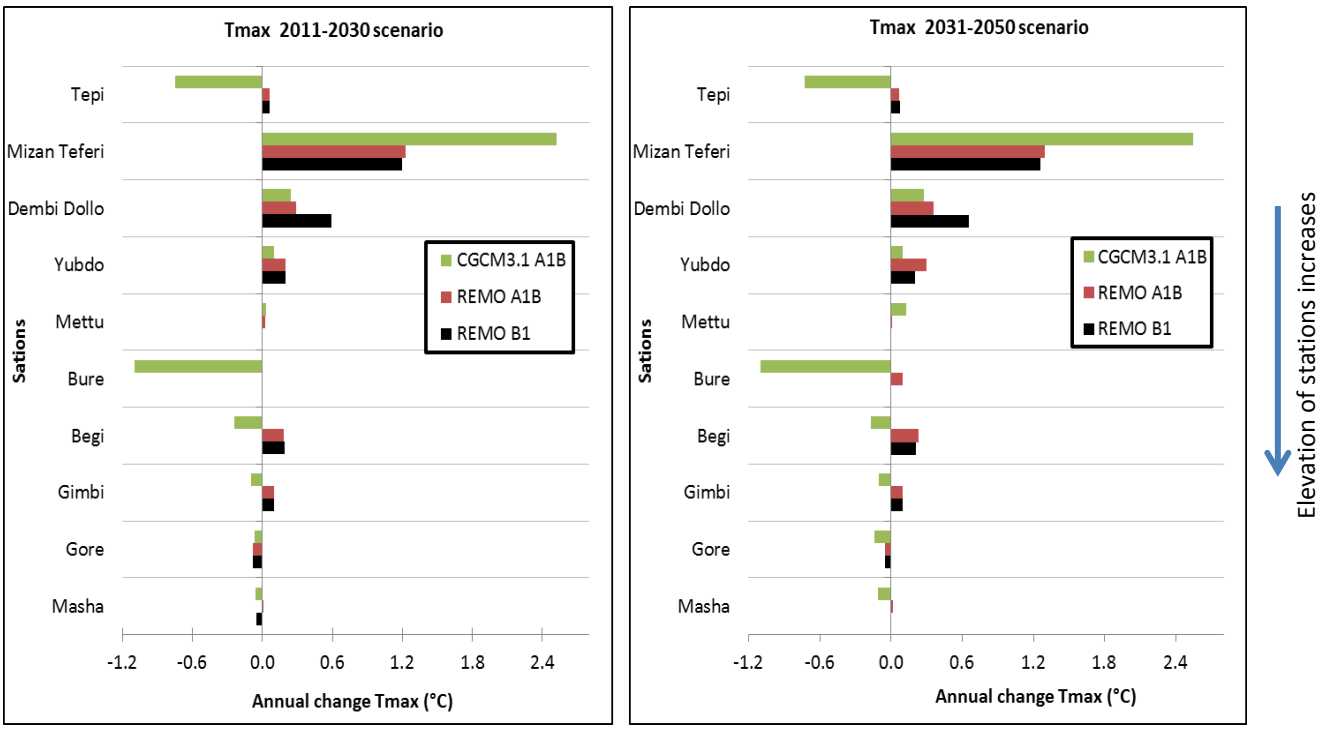

Figure 14: Projected change in **annual maximum temperature** (Delta value) from base period. Stations are ordered by increasing elevation.

Elevation is linearly regressed and correlated with annual maximum temperature and the relationship is shown in Figure 15. In almost all cases, the actual values are confined within one standard deviation of the regression line. Elevation is negatively and highly significantly correlated (R^2=0.78) for maximum temperature. This implies that elevation has a dominant role in the modification of the annual minimum and maximum temperature fields. After

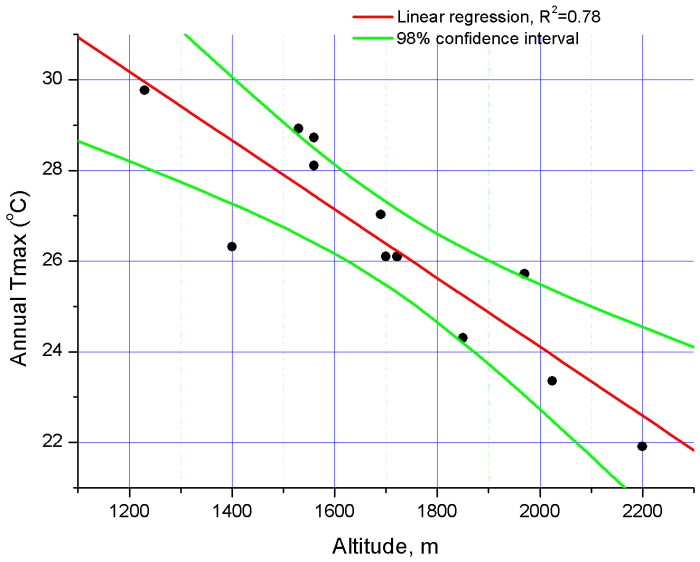

Figure 15: Relationship between observed maximum temperature and elevation.

multiple linear regression we also found that there is higher negative correlation (R^2=0.91) between altitude, latitude and annual maximum temperature, and this implies that altitude and latitude has a dominant role in the modification of annual temperature, and this relation is used to create a raster map (Figure 16) which shows temperature changes over the basin based on a 90 meter DEM. From the analysis it was possible to see temperature changes across the basin spatially. Figure 16 shows higher temperature changes likely in the lowland (western basin) and minimum change in highland (East basin).

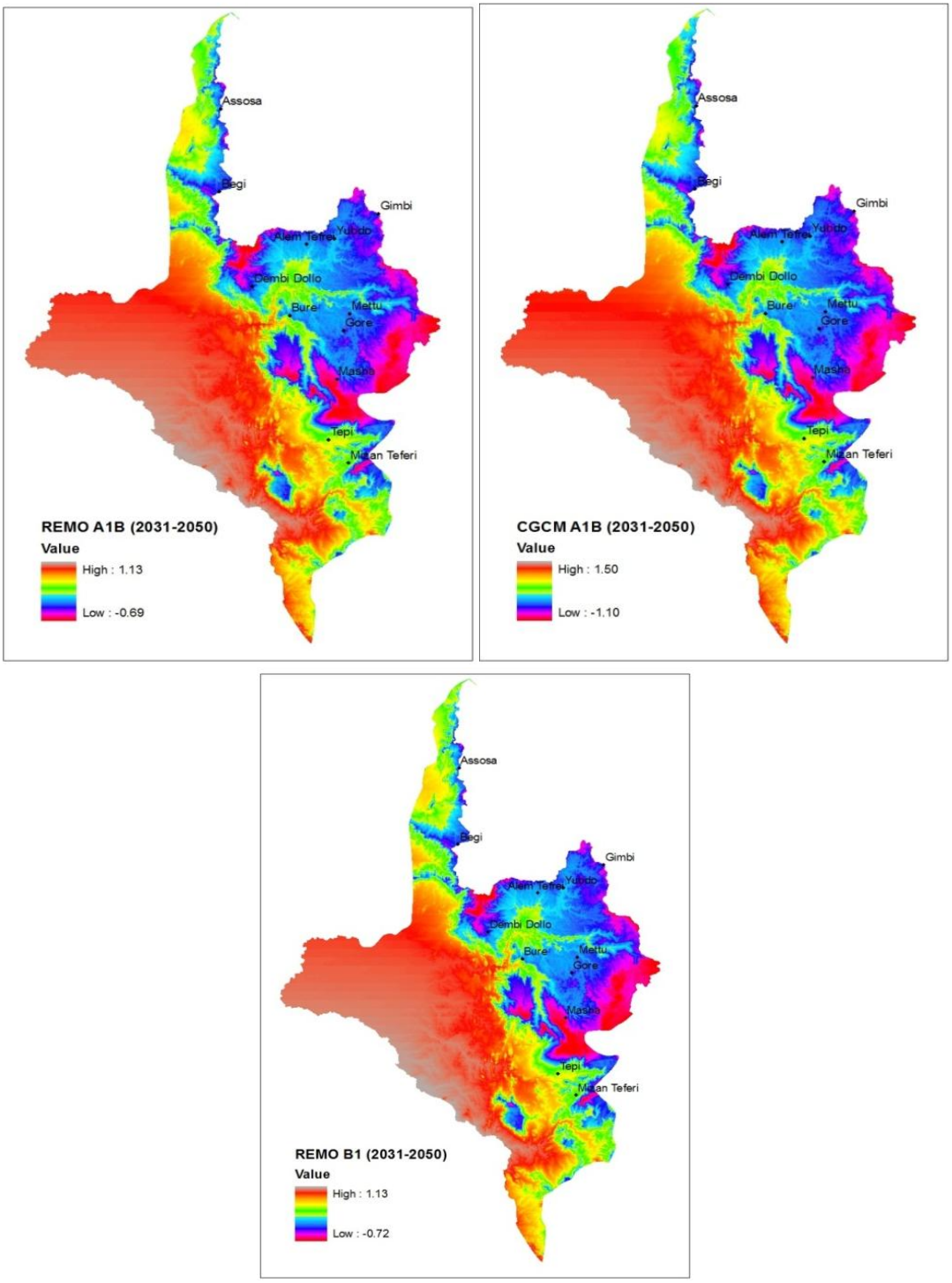

Figure 16: **Spatial change in annual maximum temperature** 2031-2050 (with respect to 1972-2000) for REMO and CGCM3.1.

II. Minimum Temperature

As regards to minimum temperature the future scenario does not show similar trends across the basin. Decreasing annual trend is likely for minimum temperature in all stations except Mettu, Mezan Teferi, Gore and Bure with the range of -1.89°C to -0.1°C for both REMO A1B

and B1 scenario, Whereas Stations Mettu, Mezan Teferi, Gore and Bure projected to +0.1°C to +0.82°C for REMO in the time horizon, here the projection shows that minimum temperatures have increased slightly faster than maximum temperatures for these four stations. Even though variability is observed among the stations for CGCM3.1 A1B,generally increasing annual trend is expected in the range of +0.06°C to +1.55°C for all stations except Dembi Dollo and Tepi which shows decreasing trend like REMO as shown in Figure 17.

Furthermore to elaborate the influence of elevation on average annual temperature within the upper Baro-Akobo river basin, a regression analysis was done. The outputs of the regression analysis are depicted in Figure 18. The figure shows a linear relationship plot between mean minimum temperature and elevation. The actual values in this plot are contained within one standard deviation of the regression line. The middle line (red) is the regression line; the two external lines (green) are lines of the 98% confidence interval. To quantify the relationship between the annual minimum temperature and the elevation, a regression analysis is performed. The analysis shows that the linear relationships between these two physical quantities are negative and significant (R^2=0.40).

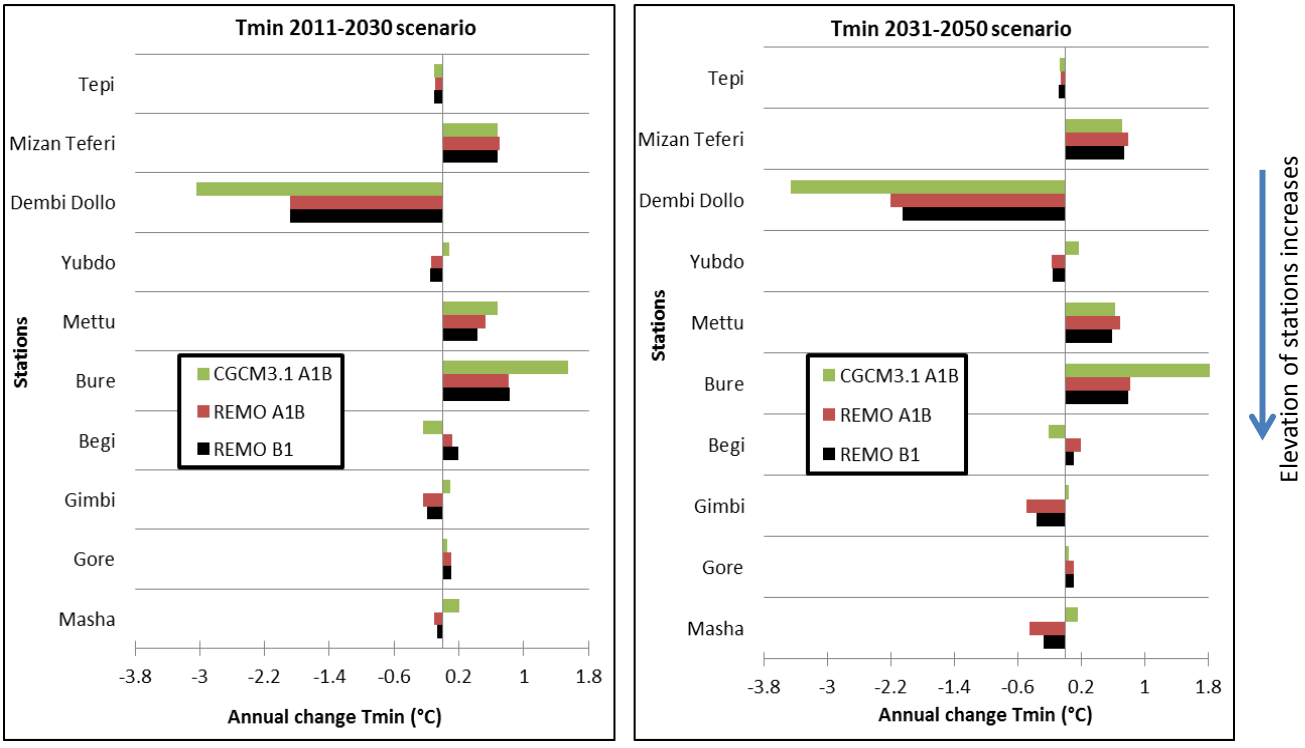

Figure 17: Projected change in **annual minimum temperature** (Delta value) from base period, stations are ordered by increasing elevation.

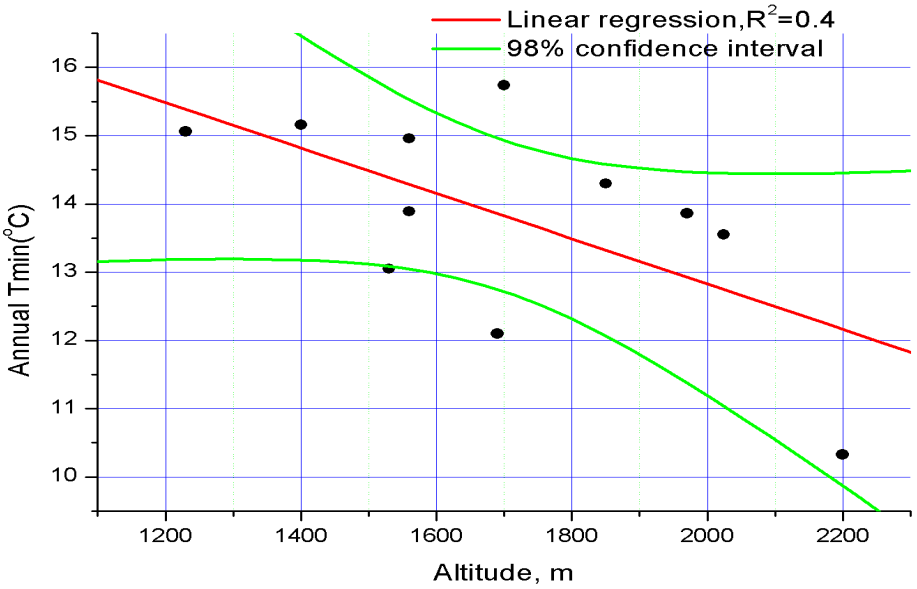

Figure 18: Relationship between observed minimum temperature and elevation.

III. Precipitation

In case of annual rainfall trend as shown in Figure 19, it is general likely to have a change of -2% to +21% from the base period for both A1B and B1 scenario of REMO. However, the A1B scenario of CGCM3.1 projected -25% to +22% changes annually over the study area in the time horizon. Yet, each station perceives a different trend. From the REMO model 10 stations show increasing annual rainfall for A1B and B1 scenario within the range of +1% to +22%and +0.5% to +21% respectively. However, stations like Bure and Mettu show a decreasing trend for both scenarios of REMO. Regarding CGCM3.1 annual rainfall is expected to have an increasing trend in the range of +0.3% to +25% for nine stations in the basin and a decreasing trend for stations like Begi and Yubdo.

Looking of the precipitation change scenario at seasonal or monthly level has great practical importance, because in the basin activities like agriculture and water supply depend on rainfall. The basin has only one rainy season “Kiremt” begins mid of May and ends mid of October (MJJASO) for the northern part of the basin, whereas for the southern part of the basin it starts in March and ends mid of October (MAMJJASO). Kiremt’s precipitation change did not manifest a systematic increase or decrease for both REMO (A1B and B1) and CGCM3.1 (A1B) scenario. About -3% kiremt precipitation changes are expected for stations Bure, Dembi Dollo and Mettu for both REMO A1B and B1 scenario in all time horizons (Figure

20). Generally REMO shows Kiremt precipitation change in the range -22% to +25% and -21% to +13% for both A1B and B1 scenario respectively in 2011- 2050, except stations Tepi and Chora which show a +48% change. As indicated in Figure 20, CGCM3.1 A1B scenario projected Kiremt rainfall likely to change by -37% to +44% for the study area in 2011- 2050. Generally both models (REMO and CGCM3.1) shows a similar direction of change for rainy seasons in the time period (2011-2050), nevertheless higher differences are found for stations Bure, Begi and Yubdo between REMO A1B and CGCM3.1 A1B (Figure 20).

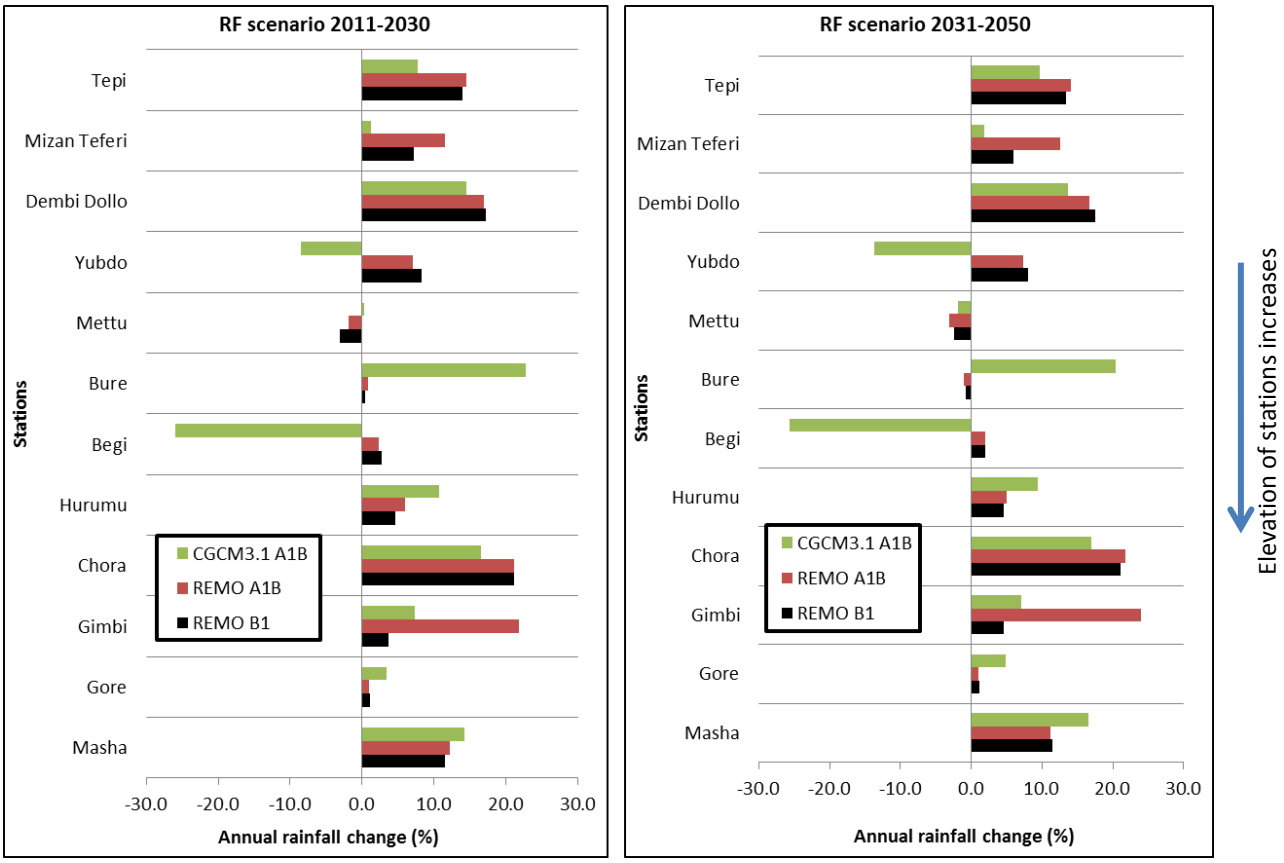

Figure 19: Projected percentage change in **annual rainfall** from base period for A1B and B1 scenario, REMO and CGCM 3.1, stations are ordered by increasing elevation.

Monthly rainfall also shows a similar trend to that of annual or rainy season precipitation which lack systematic trend. There is variability within the stations in the monthly rainfall but this variation in the annual rainfall is less because it considers the precipitation change in the dry season also which has no significance since the driest months contribute to less than 1% of the annual rainfall in the study area. Therefore, it is wise to see the change in the time horizon at a monthly or seasonal time scale.

Different studies in the Nile basin and the country in general figure out that future rainfall change does not verify systematic decreasing or increasing (Elshamy et al., 2009; Conway 2005; Yimer et al., 2009). This study also confirms overall annual future rainfall trend in the basin is increasing and consistent with IPCC 4 projection. However, the models (REMO and CGCM3.1) agreed on direction of change except some stations regardless of the magnitude. Conway (2005) pointed out that there are large inter-model differences of rainfall change over Ethiopia. Humle et al. (2001) also found that mean annual rainfall in Ethiopia for the 2050s is expected to change in between the range of -10% to 25% considering 7 GCM models. Figure 21 shows annual trends of percentage rainfall changes (2011-2050) considering 20 runs of uncertainty ensembles for A1B scenarios of REMO and CGCM3.1.

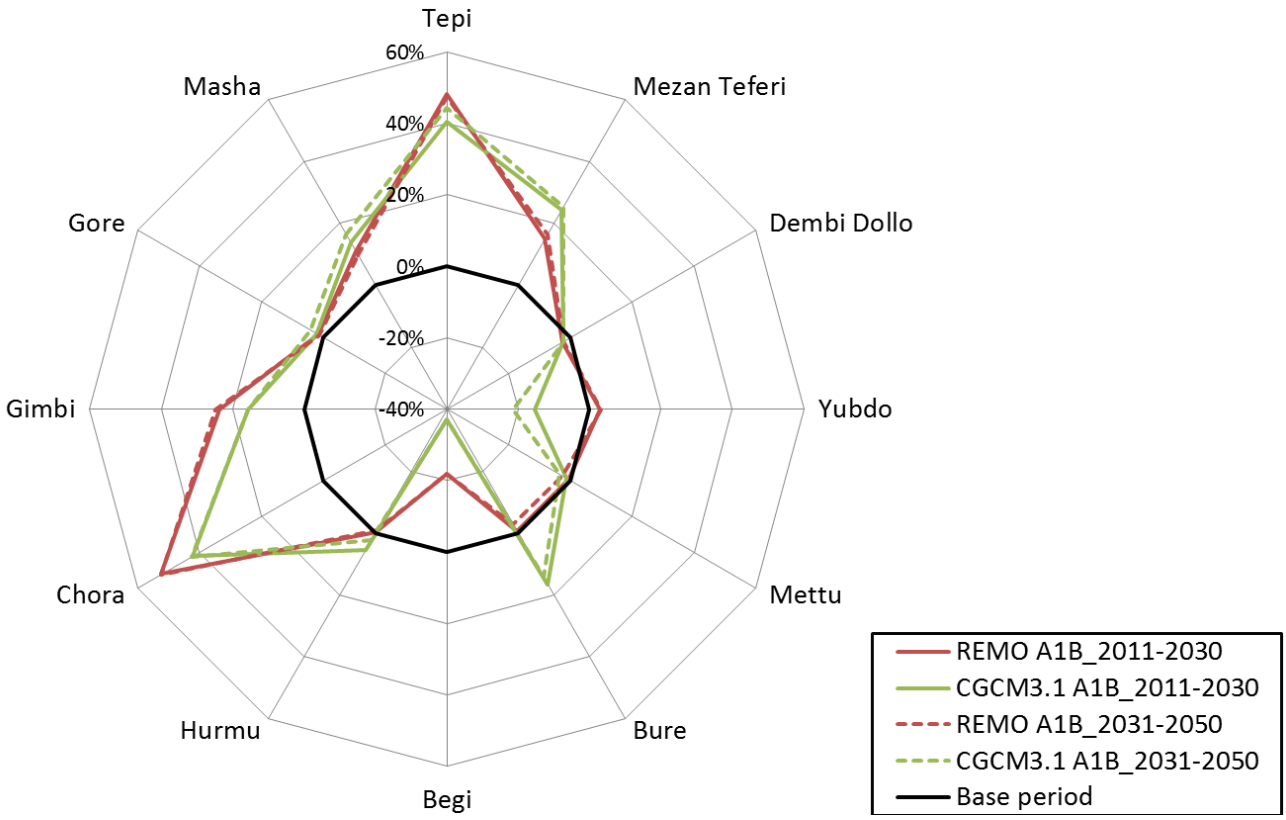

Figure 20: Projected **rainy season precipitation** (2011-2050) percentage change from the baseline period (1972-2000). Stations elevation increases clockwise (Tepi 1230 m.a.s.l., Masha 2200 m.a.s.l).

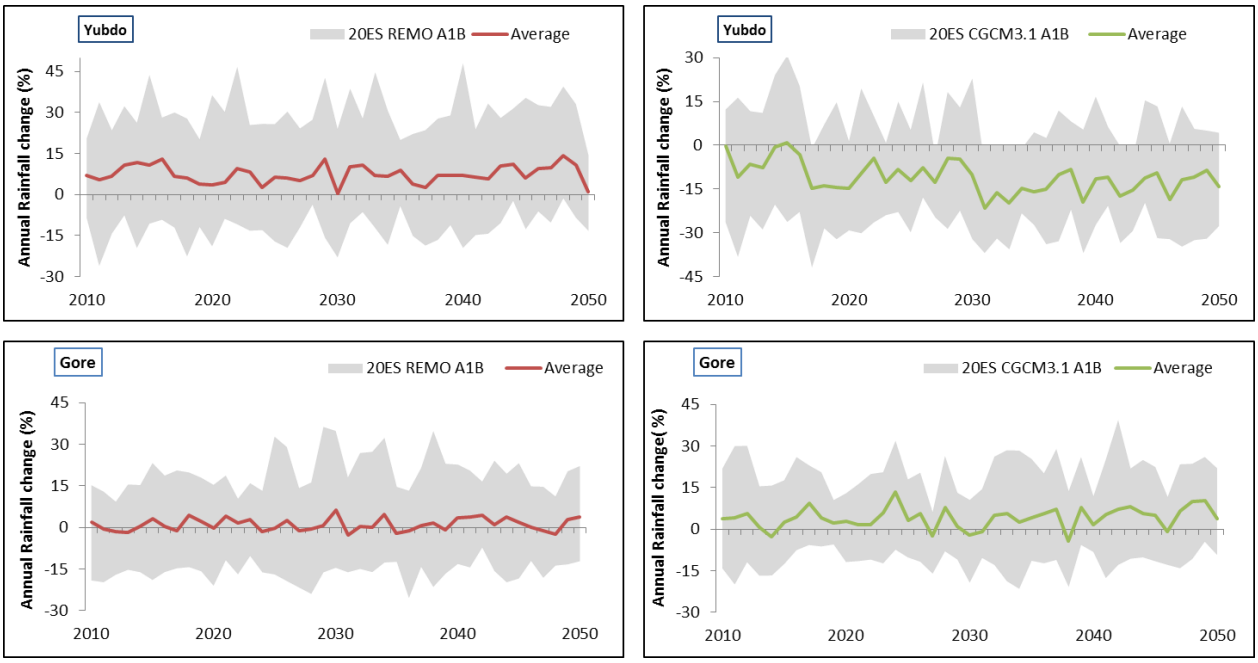

Figure 21: Projected (2011-2050) percentage change of **annual rainfall** and uncertainty of the climate models (REMO A1B and CGCM3.1 A1B) for station Yubdo and Gore (20ES=20 Ensemble runs).

5.5 Conclusion

This study analysed the output of regional (REMO) and global (CGCM3.1) climate change simulation. Downscaled precipitation and temperature were assessed over the Baro-Akobo basin for baseline climatology (1972-2000) and for the 2011-2050 aggregated in 20 years period. It appears that REMO is able to reproduce the precipitation and temperature observed over the basin. In this study maximum effort was made to assess rainfall and temperature change projections, and our main conclusions can be summarized as follows:

- Output shows SDSM smooth out the bias of REMO and CGCM3.1 during downscaling, and we found that SDSM can be used as a tool for downscaling for this region.
- Both model (REMO and CGCM3.1) projections show relatively good agreement on the direction of annual rainfall change regardless of magnitude at station scale over the basin.
- Both models indicate an increasing trend in annual maximum temperature for most of the stations with noticeable seasonal variations. The change was found to be higher in drier months (Bega) and lower in rainy season (Kiremt).
- Important finding of this study is that temperature change is inversely correlated with altitude.

- Rainfall changes show considerable uncertainty over the basin during rainy season (-20% to +50%).
- In general, SDSM approximate the observed climate data corresponding to the base period reasonably well, however the analysis of the downscaled future climate data from REMO and CGCM3.1 does not lead to identical conclusions.

Studies show that different GCMs have different projections and subject to uncertainty with respect to the many modelling issues involved. Therefore further studies in the basin have to be done considering additional climate models and exploring the relationships between climate and land use change in the basin, especially as it related to the new huge commercial farm projects. The methods described in this paper could be used to provide an indication to the likely impact of climate change in Baro-Akobo basin.

Chapter 6

6. Comparative study of a physically based distributed hydrological models versus a conceptual hydrological model for assessment of climate change response in the Upper Nile, Baro-Akobo Basin: A Case study of Sore Watershed, Ethiopia[4]

Abstract

This chapter presents a comparative study of two distinctively different hydrological models for simulating future discharge response in climate change scenarios. The largely undisturbed Sore watershed (1117 km²), Ethiopia, was used as a case study. Two climate model outputs were used in the study. The outputs of the REMO (Regional Model) and CGCM3.1 (Global Climate Model) were used as inputs for hydrological models after statistical downscaling. Data from the REMO A1B and B1 and CGCM3.1 A1B scenarios were selected to represent future conditions. The models used in this study, the physically based distributed hydrological model WaSiM-ETH and the conceptual model HBV-Light, were applied to simulate the flow conditions for a reference period (1990-1997) and a future period (2011-2050).

The results confirm that the uncertainty caused by using different climate models is larger than the uncertainty caused by using different hydrological models. In both hydrological models, the future peak discharge decreases in the future climate change scenarios regardless of the type of climate model and emission scenario considered. Whereas peak discharge was shifted from August/September for the reference period to June in the future with CGCM 3.1, the discharge was generally shifted to one month earlier for both climate models. For low-flow conditions, the HBV-Light model always computed slightly higher values than the WaSiM-ETH model. This study demonstrates that both the hydrological and climate models were consistent concerning the overall direction of change, regardless of magnitude.

Keywords: Climate change impact; hydrological models; Baro-Akobo, climate scenario; model comparison

6.1 Introduction

Several studies have attempted to evaluate the impacts of climate change on the highlands of Ethiopia (e.g. Taye et al., 2011; Beyene et al., 2010; Elsahmay et al.; 2009, Melesse et al.,

[4] Submitted for publication: Kebede, A., Diekkrüger, B., Moges, S.A. (2013): Comparative study of a physically based distributed hydrological model versus a conceptual hydrological model for assessment of climate change response in the Upper Nile, Baro-Akobo Basin: A Case study of the Sore Watershed, Ethiopia. Submitted to Journal of River Basin Management.

2009; Conway, 2005). Most of these studies have concerned the Blue Nile Basin and focused on the sensitivity of discharge to temperature and precipitation change (e.g., Abdo et al., 2009; Sayed, 2004; Conway and Hulme, 1996). Abdo et al. (2009) demonstrated that the runoff volume in the rainy season of the Lake Tana basin in Ethiopia is sensitive to climate change and indicated that significant changes and variations in the seasonal and monthly flows are to be expected. For the Blue Nile, similar results have been reported (e.g., Conway and Hulme, 1996; Sayed, 2004). Hulme et al. (2001) conducted an extensive study of climate change in Africa between 1900 and 2100 using observed and Global Climate Model (GCM) results for special report on emission scenarios (SRES) (IPCC, 2000). In Ethiopia, the expected change in annual rainfall varied between -10 and +25% by the year 2050, depending on the model and the emission scenario. Even with an increase in rainfall, river runoff might decrease due to an expected increase in the evaporation demand caused by a temperature rise. Based on the results of Raper and Cubasch (1996), it is expected that the change in the rainfall in the Blue Nile will be 2 to 11% by the year 2030, and in the White Nile, there will be a 1 to 10% increase by the same year, whereas the range of flow change in Lake Nasser is 14 to 32%. Therefore, there are large uncertainties in predicting climatic change over the Nile basin and impacts on discharge in addition to the uncertainties of the GCMs. In addition, these studies did not use model ensemble predictions, which provide a means of forecasting robust simulations for weather and climate prediction uncertainties. Despite the fact that the impact of climate change is commonly projected at the continental, country or basin scale, the magnitude and types of impact at mesoscale catchments has not been investigated in the Baro-Akobo basin thus far. No comparative study of models using ensemble simulation had been performed for the Sore watershed of the Baro-Akobo basin, even though conceptual and physically based models have been applied to the highlands of Ethiopia (e.g., Taye et al., 2011; Abdo et al., 2009; Elsahmay et al., 2009; Kim et al., 2008, Sayed, 2004). Therefore, physically based and conceptual models using ensemble simulation were applied in this study to investigate the effects of discharge change caused by model type or climate change impacts.

Future climate change predictions will have substantial importance in development plans for water resources, agriculture and similar other sectors in Ethiopia to overcome the impacts of intensifying recurrent droughts. Despite the importance of the study area as one of the

major agricultural and hydropower potential regions of Ethiopia and one of the major water contributors to the Nile River, there have been no studies performed at the regional scale to fully investigate the future changes of hydrologic regimes, drought, and water resource availability under climate change. Therefore, studies that fill this gap and aid in supplementing national policy on adaptive capacity are of outmost importance.

Despite the uncertainties, GCMs are the best tools to estimate future global climate changes resulting from the continuous increase of greenhouse gas concentrations (Busuioc et al., 2001; Dibike and Coulibaly, 2005; Abdo et al., 2009). However, due to their coarse spatial resolution, the outputs from these models cannot be used directly for impact studies. Because hydrological models deal with sub-catchment scales, the large spatial scale of GCMs has to be downscaled to the catchment scale. Therefore, in this chapter, results of statistically downscaled scenarios of the CGCM3.1 and regional model REMO as discussed in chapter 5 were used.

Models suitable for scenario analyses must be validated for current climate conditions in advance. Therefore, hydrological models are set up for the current climate before defining the expected future changes. In a second step, the models are applied to climate change scenario conditions. In this study, the physically based and distributed hydrological catchment model WaSiM-ETH (Schulla, 1997) and the conceptual model HBV-Light (Seibert, 2005) were calibrated and validated for the Sore watershed in the Baro-Akobo basin, Ethiopia. Next, the hydrological models were applied to downscaled CGCM3.1 A1B, REMO A1B and B1 scenarios.

In this chapter, we examined the comparative uncertainty in discharge modelling of physically based distributed and conceptual models under climate change. The aim of the analysis was to compare the performances and possible uncertainty in predicting the hydrological response of the catchment to climate change using two different hydrological model structures. In addition, the applicability of WaSiM-ETH and HBV-Light to the Baro-Akobo basin using daily climate data for the base period (1990-1997) and future scenarios (2011-2050) was verified. Two scenarios of the regional model REMO and one scenario of the CGCM3.1 are used

6.2 Materials and Methods

6.2.1 Climate data

Downscaling

Although the ability of GCMs to reproduce the current climate has increased, direct outputs from GCM simulations are inadequate for assessing the hydrological impacts of climate change at regional and local scales (Xu et al., 2005). Indeed, many hydrological impact assessments require station/point-scale climate variables. Therefore, there is a clear need for reliable high-resolution scenarios at station scales finer than GCMs via downscaling. The downscaling approaches used in this study were discussed in chapter 5 section 5.1 and 5.3. Further details on downscaling approaches and methods used for this study were also explained in chapter 4 section 4.1 and Kebede et al. (2013). The regional model REMO (A1B and B1 scenarios) and Canadian Coupled Global Climate Model (CGCM3.1, A1B scenario) for the years 2011 to 2050 was the two climate model used in this study after downscaling as explained in chapter 5 section 5.1.

Ensemble forecasting

Ensemble forecasting provides a means of producing a robust climate prediction simulation. This technique is currently in use at the European Centre for Medium-Range Weather Forecasts, the United State National Centre for Environmental Prediction, and the Meteorological Service of Canada (Palmer et al., 2005). Rößler et al. (2012) explained that depending on the total number of simulations conducted, ensemble forecast analyses range from simply averaging forecasts that can have their variability evaluated using bounding boxes to much more sophisticated approaches for analysing the probabilities of forecasts. Ensemble modelling has been widely used in climate change studies to assess regional climate variations (Collins, 2007). For this study, 20 statistical ensembles were generated using the SDSM 4.2 and used as inputs for the WaSiM-ETH and HBV-Light models to compare the performance and uncertainties of the two models and the catchment hydrological response to climate change. Due to the computational capacity of the hydrological models and storage required especially for WaSim-ETH, the number of ensembles was limited to 20 for each climate model (REMO and CGCM3.1) and each scenario (A1B and B1).

6.2.2 Hydrological Modelling

Generally, the available watershed models range from simple lumped conceptual to complex physically based distributed models (Beven, 2001). A lumped conceptual model (Yu, 2002; Beven, 2001) is applied for the simulation of various hydrological processes and treats the catchment as a single unit. The parameters used in such models represent the spatially averaged characteristics of the hydrological system. As Yu (2002) pointed out, conceptual models often are preferred because of their computational efficiency and simplified parameterisation. In contrast, physically based models (Meselhe and Habib, 2004; Wagener et al., 2004) are based on a spatial discretisation using grids, hill slopes or some type of hydrologic response unit. Therefore, physically based models have the advantage of simulating complex hydrological systems and utilising distributed field hydrological data, but they are more complex to set up and have more rigorous data requirements (Meselhe and Habib, 2004).

Due to the type of hydrological models used, climate change impact studies on water resource systems using different hydrological models may display variation in terms of the direction and magnitude. Taye et al. (2011) use lumped conceptual models for the analysis of the catchment of Lake Tana, Blue Nile, Ethiopia and found that the models performed better in simulating the historical flows, but the projected impact results are highly uncertain due to GCM uncertainty. Surfleet et al. (2012) also illustrated that the interpretation of climate change projection requires estimates of uncertainties associated with the modelling approach. The uncertainties in climate scenario quantification may be better quantified using different models and studying the consistency of the results. In this study, we adapted two distinct models: physically based and conceptual based hydrological models, namely the WaSiM-ETH (Water Balance Simulation Model ETH) (Schulla, 1997) and HBV-Light models (Seibert, 2005), respectively. The theoretical background of the two models were discussed in chapter 4 section 4.2.2, the following section gives brief description on the two models applications and their data inputs used for each model.

WaSiM-ETH model*:* it is a spatially distributed, process and grid-based hydrological catchment model (Figure 6). Different studies are available in which WaSiM-ETH has been applied to determine the impact of climate change on hydrology (e.g., Jasper et al., 2004;

Rößler and Löffler, 2010; Rößler, 2011; Gurtz et al., 2003; Verbunt et al., 2003; Jasper et al., 2004; Leemhuis, 2005; Jung, 2006; Wagner et al., 2009; Bormann and Elfer, 2010). Bormann and Elfer (2010) reported that the model is a suitable tool for the simulation of the hydrological behaviour of lowland catchments. Habte et al. (2007) indicated that the model satisfactorily simulates the hydrological behaviours for all sub-basin catchments of the Blue Nile basin in Ethiopia. The model was also applied successfully in the sub-humid catchment of West Africa, the Volta Basin (Wagner et al., 2009; Kasei, 2010), for both historical analysis and for scenario quantification.

The WaSiM-ETH requires meteorological data, such as temperature, precipitation, relative humidity, wind speed, and solar radiation, as well as spatial data, including elevation, vegetation, and soil properties. The vertical and horizontal water fluxes are calculated for each raster cell for user-defined temporal time steps and spatial scales.

HBV-Light model*:* is a conceptual model that simulates daily discharge using daily rainfall, temperature and potential evapotranspiration as input (Figure 7). HBV models have been applied to a wide range of applications, including climate change, analysis of extreme floods, and analysis of the effects of land-use change (e.g. Abdo et al., 2009; Leander and Buishand, 2007; Dibike and Coulibaly, 2005; Booij, 2005).

In this study, both models were applied to compare model performance and uncertainty in predicting the hydrological response of the catchment to climate change. In general, the structure of the experimental design using these models in the study of the hydrological impact of climate change is described in Figure 22.

Model Performance criteria*:* To assess the performance of the models, three criteria were used: coefficient of determination (R^2), Nash-Sutcliffe efficiency (NSE), and explained variance (EV), in addition for comparing the overall agreement between the predicted and measured runoff discharges, runoff volume errors were used as explained in chapter 4 sections 4.2.3.

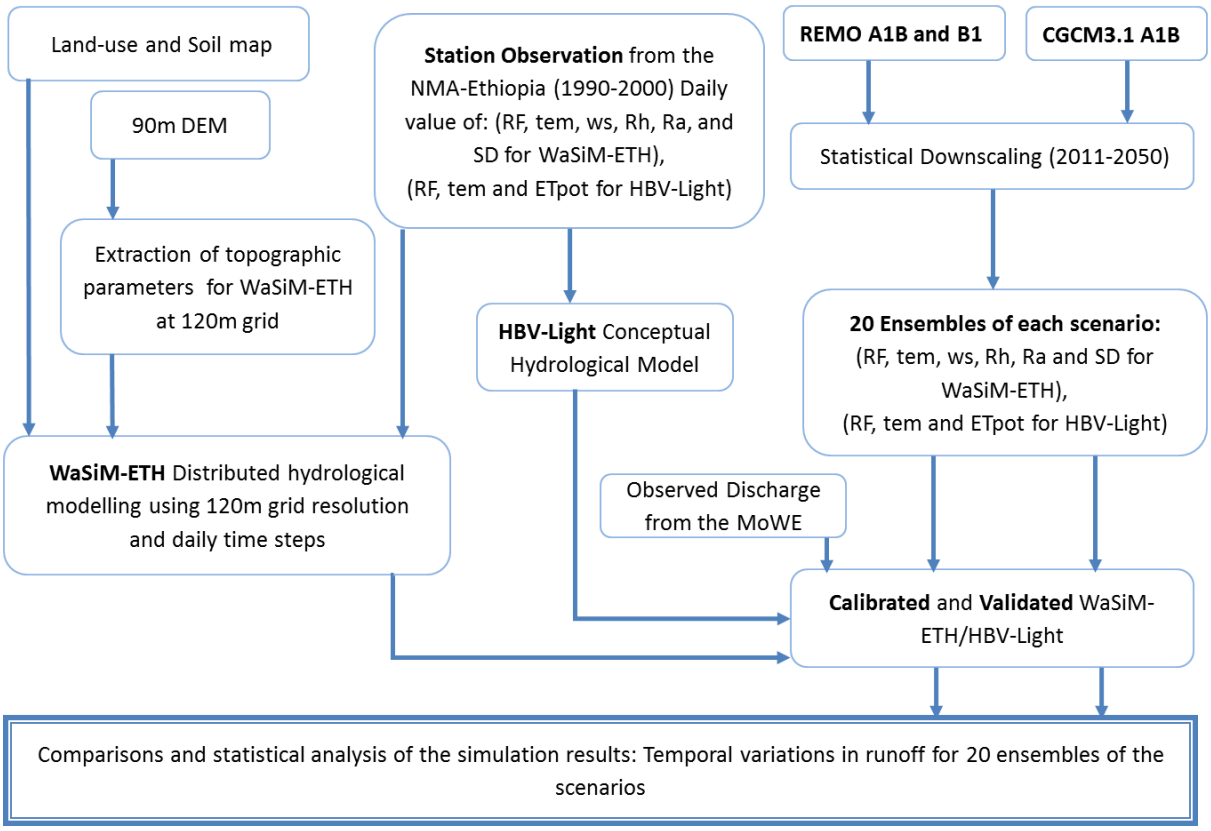

Figure 22: Structure of experimental design using WaSiM-ETH/HBV-Light for this study. Abbreviation: RF=rainfall, tem=temperature, ws= wind speed, Rh=relative humidity, Ra=radiation, SD=Sunshine Duration.

6.2.3 Study Area

The study area selected for this research was the Sore watershed, which has an area of 1,711 km^2 and is located in the highland region of the Baro-Akobo basin, Ethiopia. At 8^{o}21' and 7^o 49' latitude and 35^{o}31' and 35^o 57' longitude, as extracted from a shuttle radar topographic mission (SRTM) digital elevation model (DEM), the elevation of the Sore watershed varies from 2661 to 1547 m.a.s.l, and the highest elevation ranges are located east and south. The elevation decreases towards the north and north-west (Figure 23). The annual rainfall ranges between 1804 and 2020 mm. The monthly maximum temperature is between 24°C and 28°C, and the monthly minimum temperature is between 12°C and 14°C (Figure 24). The major river within the catchment is the Sore River and its tributaries. The river, which arises in the southern part of the catchment, flows to the north and joins the Baro River. Flow data recorded near the town of Mettu were used for this study.

The WaSiM-ETH was set up using elevation data (a DEM), soil data and land cover data as shown in Table 4. The DEM of the study area with a resolution of 90 m by 90 m was obtained from the SRTM data. This DEM was used for delineation of the watershed, hydrological simulation and extraction of physiographic WaSiM-ETH parameters such as river network, sub-basins, slope, aspect, flow times, river depth, river width and channel parameters. Table 4 summarises the data sources used for both hydrological models.

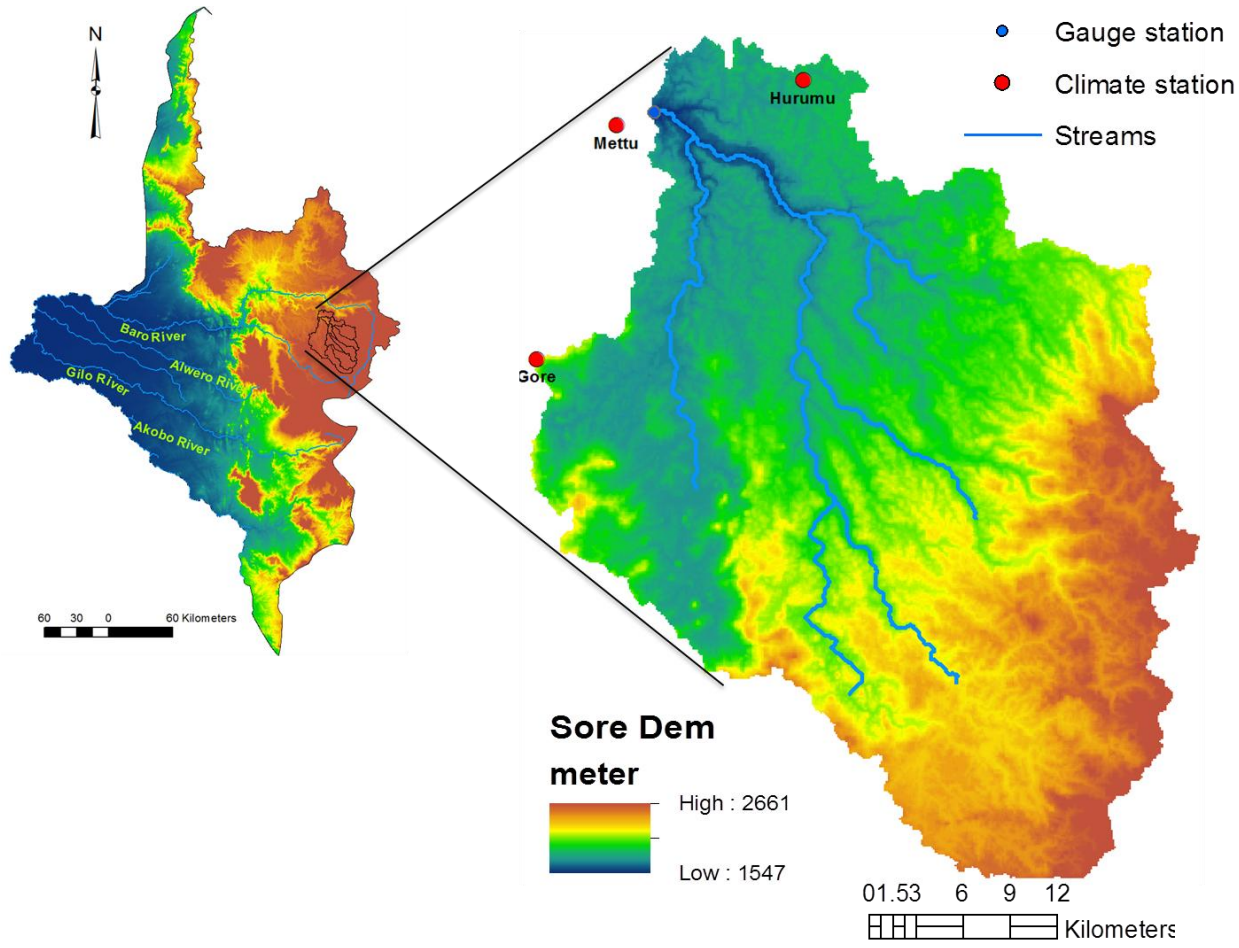

Figure 23: Location map of the studied **SORE watershed (1,711km^2)**, DEM, climate and gauging station.

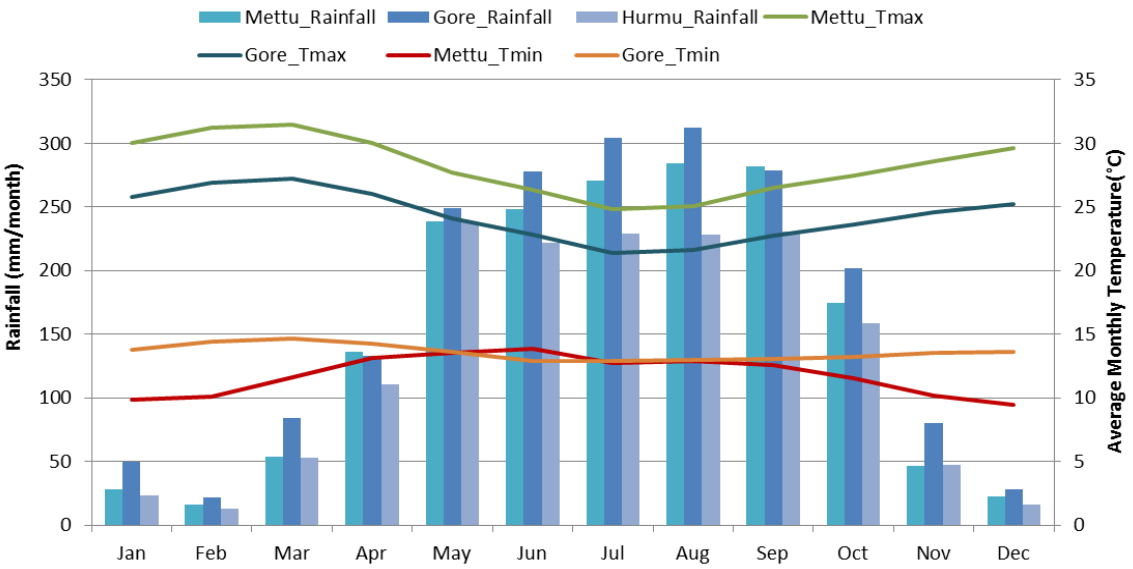

Figure 24: Monthly rainfall, maximum and minimum temperature of Mettu, Gore and Hurumu stations in the SORE watershed.

The observed precipitation from three stations (Gore, Mettu and Hurmu) and the temperature data from two stations (Gore and Mettu) were used for calibration and validation of the HBV-Light model. The same stations were used for the calibration and validation of the WaSiM-ETH model, but relative humidity, wind speed, radiation and sunshine duration at the Gore station were also used.

Table 4 Data sources for the HBV-Light and WaSiM-ETH simulation.

	Type	Resolution/Time Period	Processing	Source
DEM	Digital Elevation Model	90 m	-	SRTM
SOIL	Soil Properties	-	Soil profiles	MoWE (Ministry of Water and Energy), and FAO
	Soil map	1:250,000	extract	MoWE
Land cover	Land cover map	300m/2005	extract	FAO-UN
Climate	Rainfall,	Daily, 3 stations 1990-1997	Gap filling	NMA (National Meteorology Agency)
	temperature,	Daily, 3 stations 1990-1997	Gap filling	NMA
	solar radiation, wind speed, and relative humidity	Daily, Gore station 1990-1997		NMA
Discharge	Discharge	Daily 1990-1997		MoWE

Table 4 summarises the data used, the resolution and their sources. Both models ran at a daily scale, and the WaSiM-ETH was run with a spatial resolution of 120 m X 120 m. The soils database describes the surface and upper subsurface of a watershed and is required to determine a water budget for the soil profile and daily runoff. The WaSiM-ETH model requires physical soil properties, as described in Table 5. The major data used for estimating

the soil parameters were mainly from the MoWE and FAO soil database. The dominant soils in the watershed are Eutric Nitisols (70%), according to FAO/MoWE soil classification. Humic Cambisols also account for 29% of the soils, and the rest of the watershed consists of Orthic Acrisols and Eutric Cambisols.

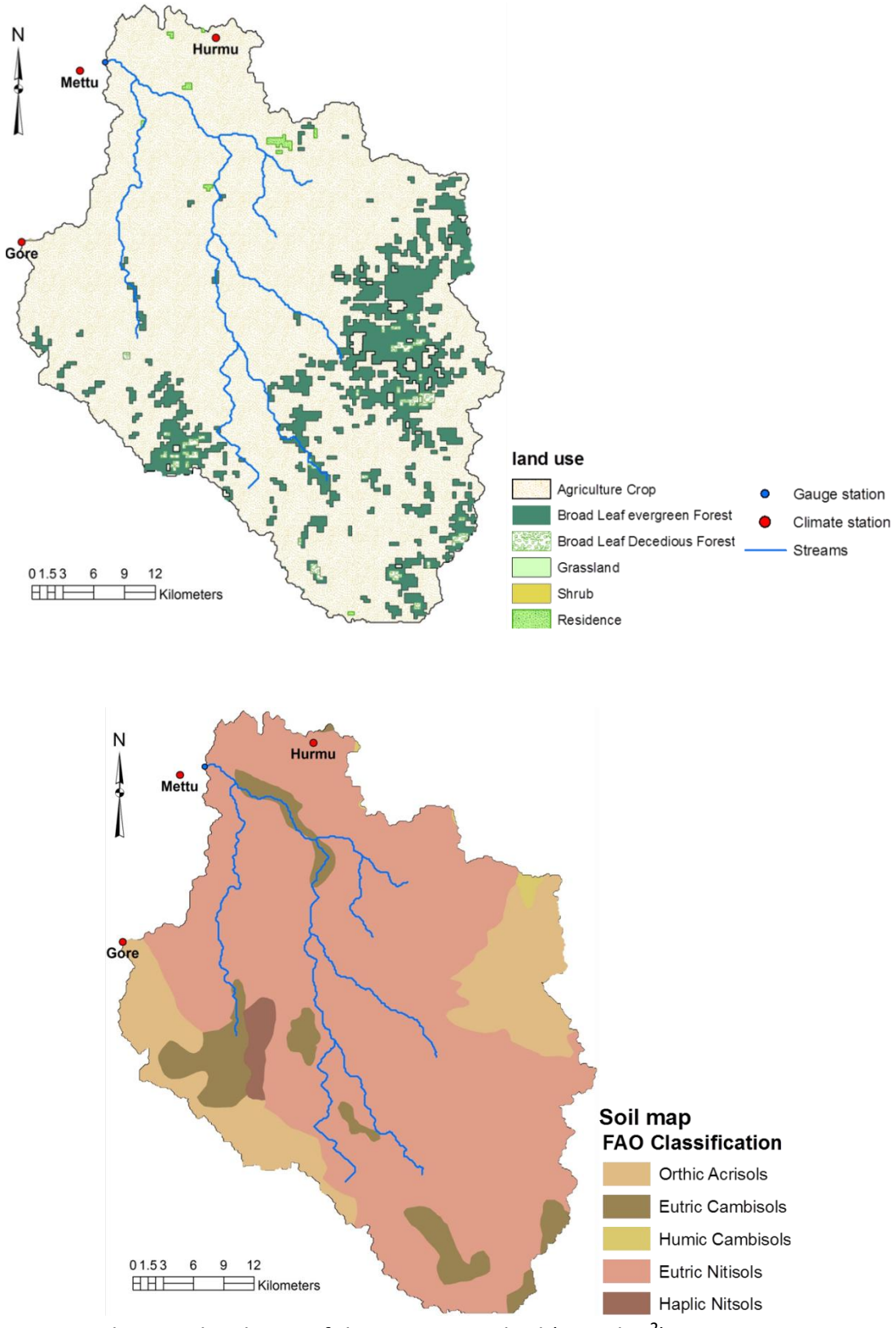

Figure 25: Land use and Soil map of the Sore watershed (1,711km^2).

Table 5 Soil parameters used for WaSiM-ETH.

Parameters	Description	Method
Ksat	Saturated hydraulic conductivity (m/s)	Estimated using Brakensiek et al. (1984) method
θ_{sat}	Saturated water content (vol. %)	Estimated using van Genuchten (1980) method
θ_{res}	Residual water content (vol. %)	Estimated using van Genuchten (1980) method
α	Van Genuchten parameter (1/m)	Estimated using van Genuchten (1980) method
n	Van Genuchten parameter (-)	Estimated using Rawls and Brakensiek (1985)

Land cover affects water runoff and ET in a watershed. A land cover map of Ethiopia with a resolution of 300 meters was the available map of the study area. The map was a FAO Land cover of Ethiopia - Shape file format, and the map represented, in raster or vector form, the year 2005. From this data source, the land cover map of the study area (Figure 26) was extracted. According to the map, the dominant land use of the watershed is agricultural crops (more than 85%), whereas the remaining portions are residential areas and dispersed forest, mainly in the south-western and eastern part of the catchment. The forest is dominated by broad leaf evergreen type vegetation.

6.3 Result and Discussion

6.3.1 Model calibration and validation

As one of the aims of this chapter was to investigate the performance of the two distinct hydrological model types for the assessment of the impact of climate change, both models were calibrated (1994-1997) and validated (1990-1992) on daily, weekly and monthly temporal resolutions. Simulation of stream flow corresponding to future climate change scenarios based on downscaled future climate data input was conducted for both hydrological models for the time period from 2011 to 2050. The simulations were at daily time steps of 20 ensembles for each scenario for both hydrological models. The calibration was performed for total discharge as a composition of surface runoff, base flow, and interflow as estimated at the routed gauged station to obtain the goodness-of-fit statistics and a fairly good graphical fit. The main calibration parameters for both models are shown in Table 6 and Table 7.

Table 6 Main calibration parameters of WaSiM-ETH.

ID	Unit	Description
K_D	[h]	Storage coefficient for surface runoff
K_H	[h]	Storage coefficient for interflow
dr	[m^{-1}]	Drainage density for interflow
Krec	[-]	Recession constant for saturated hydraulic conductivity with depth
rs_evaporation	[s/m]	Soil surface resistance (for evaporation only)
rsc	[s/m]	Leaf surface resistance

The land-use parts of the WaSiM-ETH have five parameters that do not vary during the year (e.g. root density distribution, interception capacity of leaves, and hydraulic head for beginning dryness stress), and the default values were adopted (see WaSiM-ETH manual, Schulla and Jasper, 2007). The other vegetation parameters, like such as albedo, leaf area index, aerodynamic roughness length, interception surface resistance, vegetation covered fraction, and root depth, are variable in the year and were taken from the literature. However, parameters such as **rs_evaporation** (soil surface resistance for evaporation only) and **rsc** (leaf surface resistance) were calibrated manually. The other parameters in the soil water dynamics of the WaSiM-ETH are **K_D** and **K_H** (Table 6), which control the surface runoff and interflow storages effects in the Richards equation. The calculation of interflow, which is one of the components of total simulated discharge, depends on saturated hydraulic conductivity (Ksat), river density, hydraulic gradient, and soil layer thickness. The parameter Ksat was estimated using Brakensiek (1984) methods from soil data, but river density, considered with the scaling parameter **dr,** was optimised by manual calibration. The **Krec** is a parameter in the soil model that governs the saturated hydraulic conductivity with depth and that in turn has an effect on interflow. This parameter was also calibrated manually. The remaining parameters per soil mapping unit, such as the van Genuchten values, were calculated from available soil data. The parameters K_{rec}, dr, K_D and K_H were found to be very sensitive (Kasei, 2010; Schulla and Jasper, 2007; Cullmann et al., 2006).

Table 7 Main calibration parameters of HBV-Light.

ID		Unit	Description
	FC	[mm]	Maximum soil moisture storage
Soil Moisture Routine :	**BETA**	[-]	Parameter that determines the relative contribution to runoff from rain or snow melt
	LP	[-]	Soil moisture value above which ETR reaches ETP
Routing Routine:	**MAXBAS**	[day]	Triangular weighing function
Response Routine :	**K_i**	[1/day]	Storage coefficient
	UZL	[mm]	Threshold parameter
	PERC	[mm/day]	Defines max percolation rate from the upper to the lower ground box

Table 7 summarises the main parameters calibrated manually to obtain the optimum values in the HBV-Light model. The model has 14 parameters to be calibrated. In this study, the snow routine was not used due to the absence of snow in the area. From the soil moisture routine, **FC** was used to determine the amount of water that goes to the root zone and groundwater as recharge and parameters, **BETA** determines the relative contribution to runoff from rain (Equation 2), and **LP** is a parameter used to determine the relation between actual and potential evaporation (Equation 3). The response routine works with 3 parameters. **PERC** controls the maximum percolation rate from the upper to the lower groundwater zone. **UZL** is a parameter used to compute runoff from the groundwater zone as the sum of linear outflow equations using storage coefficient (**K_i**) depending on whether the upper groundwater zone is above a threshold parameter UZL (Equation 4). Lastly, the routing routine has one parameter, **MAXBAS,** which is used to transform runoff to simulated runoff using a triangular weighting function (Equations 5 and 6).

The resulting hydrographs using optimised parameters are portrayed in Figures 26 to 29. Visual inspection of the hydrographs indicates that the models were good at simulating the hydrographs at the daily, weekly and monthly scales. Regarding the goodness-of-fit statistics shown in Figures 26 and 27, **NSE**, **EV**, and **R^2**, as described in section 4.2.3, were calculated from simulated discharge values and the available observed runoff for the simulation time period. Both models performed well and with good fit. In addition, the models were validated using independent data, which indicated good statistics, as shown in Figures 28 and 29. As shown in Table 8, the simulated water balance for the Sore watershed using the WaSiM-ETH reveals the interflow component of the water balance takes a higher fraction of simulated discharge. Generally, both models managed to simulate the peak and low flows very well and can reasonably be used for hydrologic impact studies in the catchment.

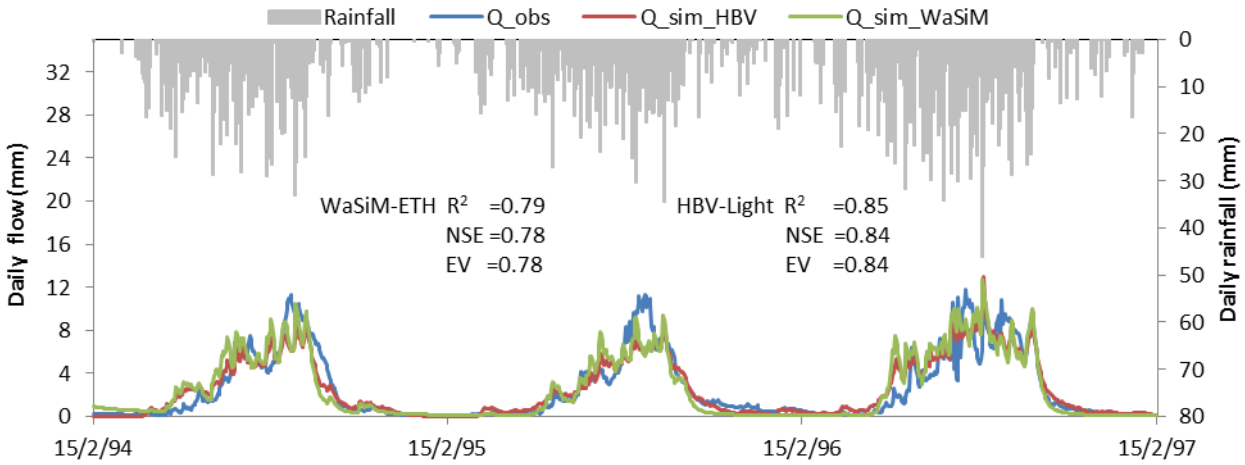

Figure 26: Daily calibration results and model performances for the Sore watershed from Feb 1994 to Feb 1997 for the WaSiM-ETH and HBV-Light models.

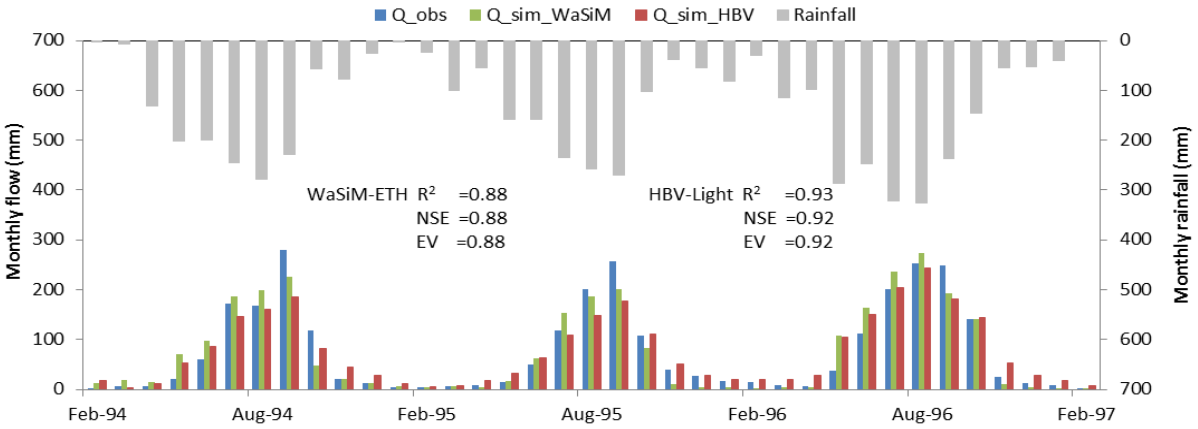

Figure 27: Monthly calibration results and model performances for the Sore watershed from Feb 1994 to Feb 1997 for the WaSiM-ETH and HBV-Light models.

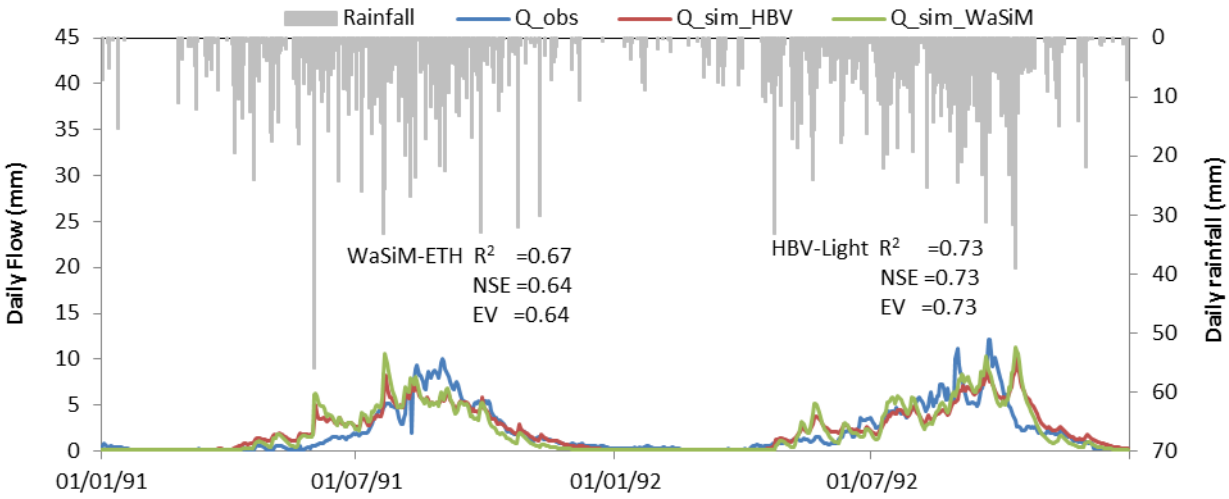

Figure 28: Daily validation results for the Sore watershed from Jan 1991 to Dec 1992 for the WaSiM-ETH and HBV-Light models.

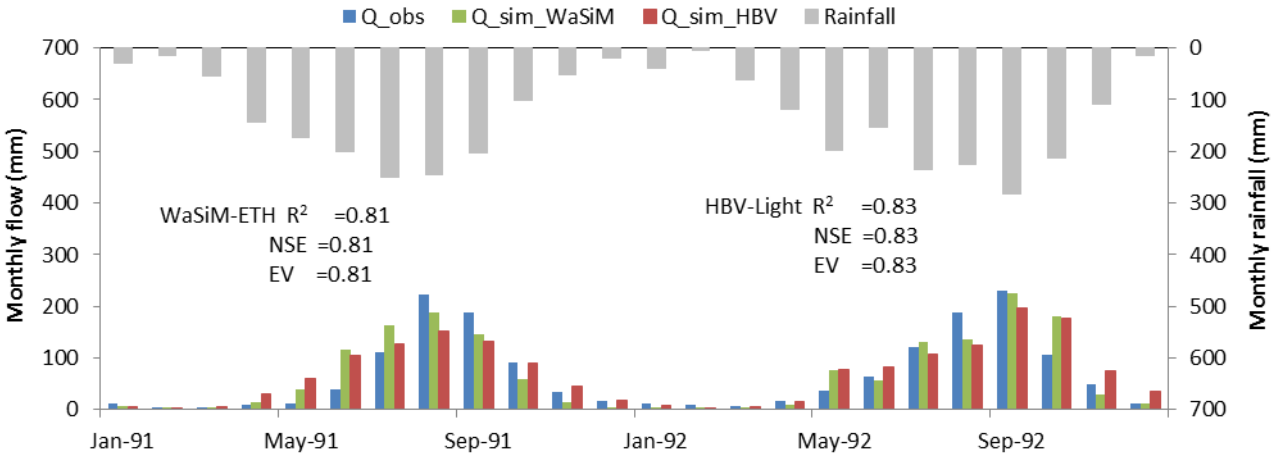

Figure 29: Monthly validation results for the Sore watershed from Jan 1991 to Dec 1992 for the WaSiM-ETH and HBV-Light models.

Table 8: Summary of the simulated water balance (in mm) for the Sore watershed (1711 km^2) for the calibration and validation periods (WaSiM-ETH).

year	Rainfall (mm)	Q_T-Sim (mm)	Surface RO (mm)	Inter flow (mm)	Base flow (mm)	ETP (mm)	ETR (mm)	Soil water content change(mm)	Q_T-obs (mm)	Balance error (Qs-Qo) (mm)
					Calibration					
1994	1453	910	47	848	15	1098	554	-10	868	42
1995	1454	741	40	691	10	1459	671	45	838	-97
1996	1993	1142	76	1059	8	1430	792	59	1075	68
					Validation					
1991	1491	758	44	704	10	1496	680	54	738	20
1992	1655	859	48	804	8	1489	705	91	846	13

Q_T-Sim=simulated total discharge, RO=run off, ETP=Potential Evapotranspiration, ETR=Actual Evapotranspiration, Q_T-obs= Observed total discharge, Q_s-Q_o= simulated-observed discharge

HBV-Light and WaSiM-ETH Performance validation

The performance evaluation criteria used were the overall agreement between the observed and predicted hydrographs and the models' ability to predict the time and magnitude of peak discharges and runoff volume (Meselhe and Habib, 2004). The results indicated that the WaSiM-ETH model captured the peak discharge (Figures 26 and 30) better than the HBV-Light model. Table 9 compares the performance of both models estimated using Equation 10 (section 4.2.3). The overall performance of both models was quite reasonable for predicted runoff volume (Table 9). Figure 30 also compares the measured mean monthly discharge [mm/month] over the calibration period with the WaSiM-ETH and HBV-Light model results,

and the coefficient of determination of the resulting regression function indicates an acceptable model performance. The analysis indicates that there was not a large difference in performance between the two models.

Table 9 Summary of model performance (Annual total volume error during calibration and validation).

			WaSiM-ETH		HBV-Light	
	year	*Q_Obs (km^3)	*Q_Sim (km^3)	% Vol. Error	Q_Sim (km^3)	% Vol. Error
Calibration	1994	1.48	1.56	+4.9	1.43	-3.7
	1995	1.43	1.27	-11.6	1.30	-9.0
	1996	1.84	1.95	+6.3	1.99	+8.4
Validation	1991	1.26	1.30	+2.7	1.33	+5.3
	1992	1.45	1.47	+1.6	1.49	+3.1

*Q_Obs=observed discharge, *Q_Sim=simulated discharge

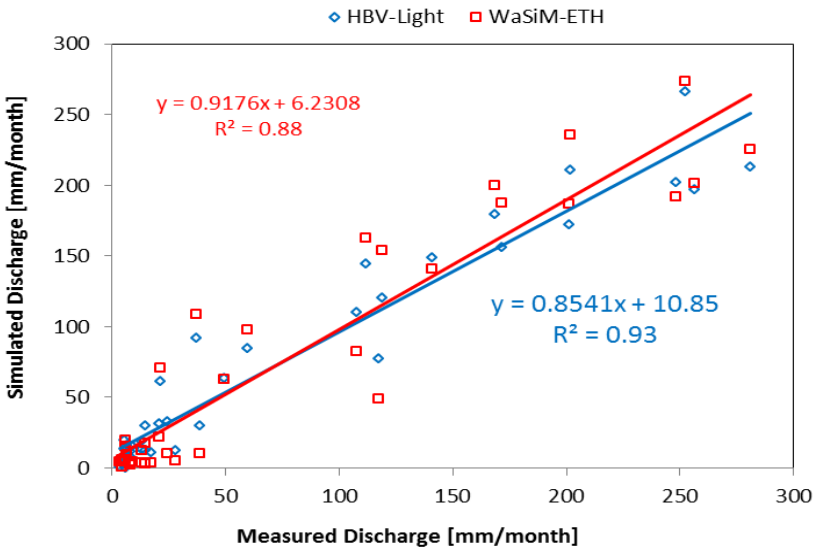

Figure 30: Correlation plots of WaSim-ETH (red line) and HBV-Light (Blue line) for the whole period.

Therefore, the two hydrological models can be used for scenario quantification using the downscaled model outputs of precipitation, temperature, and evapotranspiration from the REMO and the CGCM3.1 models for the A1B and B1 scenarios. However, we learnt that on the basis of model performances, these two hydrological models perform similarly for the study area. Therefore, for flow simulation, less complex calibration and simple models are preferred.

6.3.2 *Model results comparison and catchment hydrological response to climate change*

For comparison of the model performance under climate change scenarios, 20 climatic data ensembles for each of the REMO A1B and B1 and CGCM3.1 A1B scenarios were developed. The purpose was to identify the response behaviour as well as detect any change in the future direction of climate change in the Baro-Akobo basin (based on the Sore watershed). The impacts of climate change on total discharge were analysed by comparing the future wet season and monthly mean simulations of the models for two periods of 20 years each. Moreover, the annual mean total discharge, rainfall and potential and actual evapotranspiration were compared per decade. The simulation results are depicted in Figures 31 to 34 and Table 10.

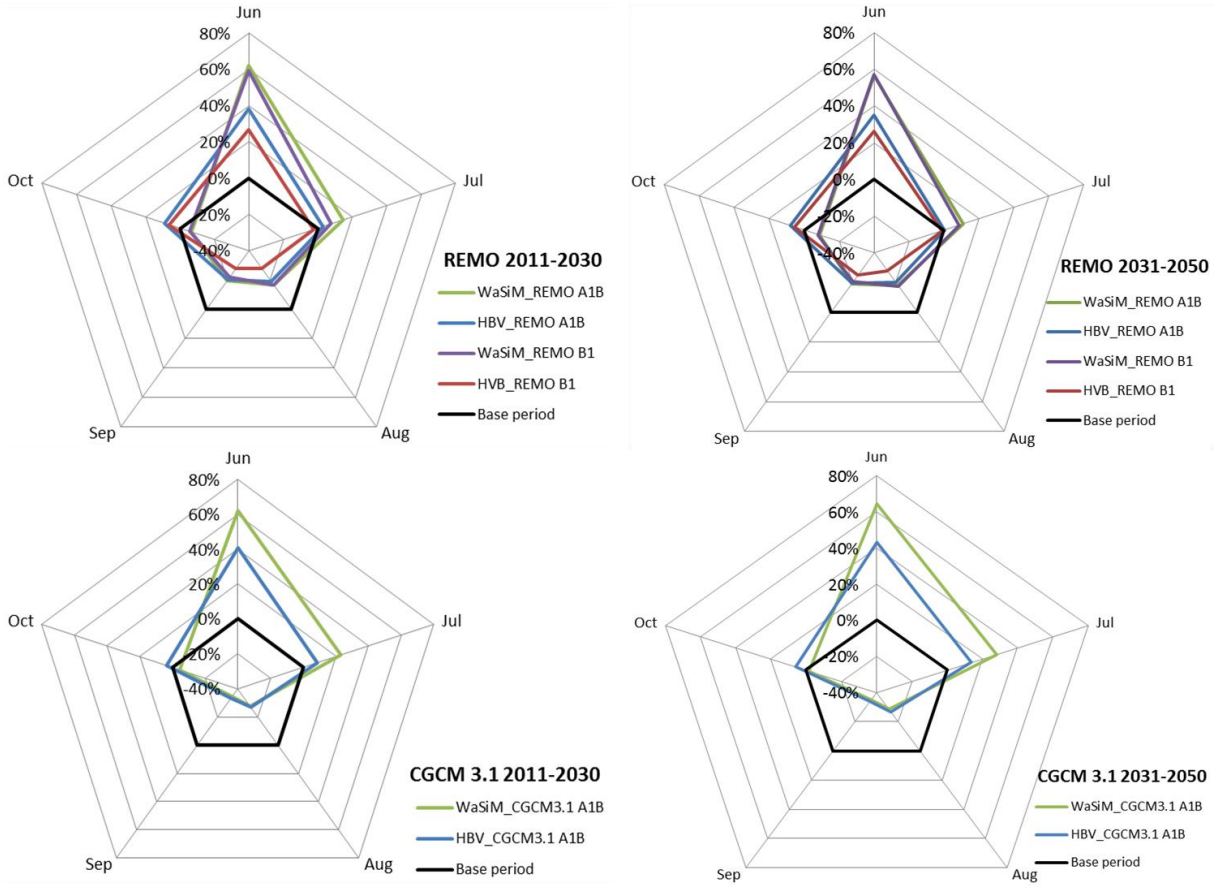

Figure 31: Sensitivity of average monthly discharge to climate change in the rainy season by comparing the WaSiM-ETH and HBV-Light scenarios (2011-2050) with the base period (1990-1992 and 1994-1997).

Figure 31 shows the simulated wet season (June to October) percentage discharge change (2011-2050) from the base period (1990-1992 and 1994-1997) for each hydrological model

using two climate models, each consisting of 20 statistical ensemble runs. Both hydrological models display a reduction in peak discharge (August and September), regardless of the magnitude, for all downscaled REMO and CGCM3.1 scenarios. The WaSim-ETH model indicates that discharge in June will increase up to +60%, whereas the HBV-Light model indicates increases up to +30 to +40% (Figure 31) for both climate models, and an early peak in July is observed (Figure 32) for both hydrological models using the CGCM3.1 A1B scenario compared with the base period peak in August and September. This is due to a slight decrease (-3%) in wet season rainfall and a 0.5° to 0.7°C increment of minimum temperature at the Mettu station.

When using the REMO, both hydrological models indicate a reduction of peak flow in August and September for both scenarios; however, the change is higher for the HBV-Light (-20% to -28%) than for the WaSiM-ETH (-17% to -22%) model (Figure 31). The low flow (October to December) present different directions (Figure 32), likely no change with the HBV-Light model and a decreasing trend with the WaSiM-ETH model. These results indicate that different hydrological models provide different stream flow results for a given input as a result of differences in model structures.

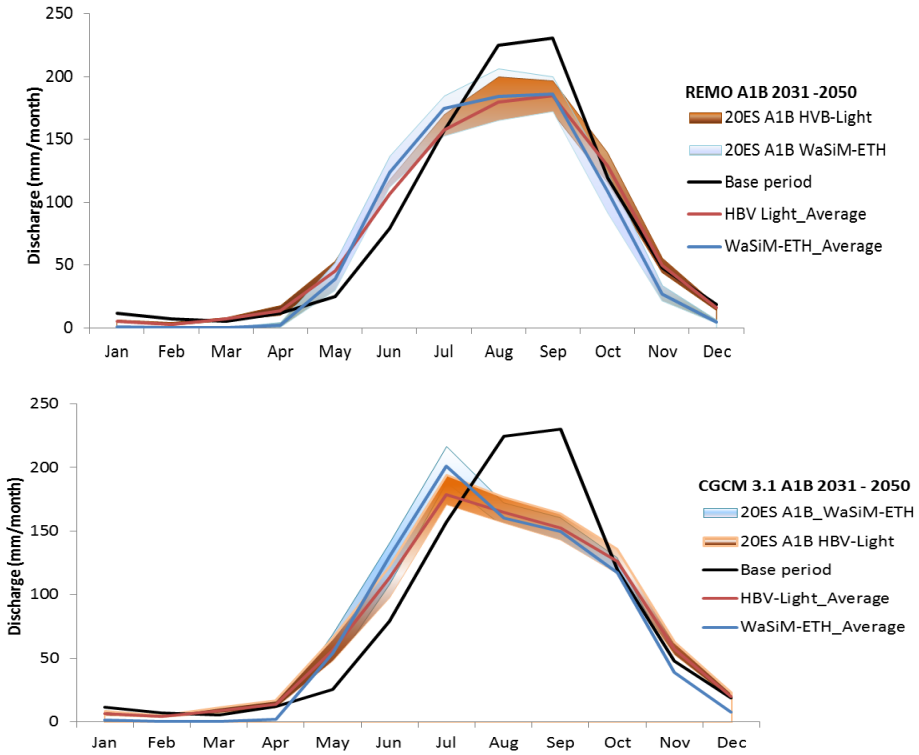

Figure 32: Comparison and uncertainty of WaSiM-ETH and HVB-Light models of monthly mean discharge using both REMO and CGCM3.1 models (base period and average ensembles).

As presented in Figure 32, both models generally indicate a shift in wet season discharge towards May to July. All simulations with the HBV-Light model indicate almost no change in the low flows of the dry season, particularly in the months of November to April. However, the WaSiM-ETH models indicate a slight decrease in November and December flows for all scenarios. Based on the simulations of the two models, we observed that wet season discharge is more sensitive than total annual discharge. Therefore, the likely increase in discharge from May to July compensates for the peak reduction in later seasons, which influences the total annual discharge minimum change, as shown in Table 10.

Regarding annual variability, Figure 33 shows the trends for rainfall and the total discharge as a mean per decade for the A1B scenario of the REMO and CGCM3.1 models. Table 10 also summarises the water balance for the base period (1990-1992, 1994-1996) and the four scenarios A1B and B1 decades with the REMO and CGCM3.1 models, as well as the relative percentage changes from the reference period. The results of the hydrological models reveal that the mean annual decadal discharge change (2011-2050) is not as extreme as the monthly or rainy season values because the discharge increase (May to July) is balanced by reduction from August to October. The mean decadal discharge change for both hydrological models (WaSim-ETH -7% to -0.5%; HBV-Light -2% to +2%) displays nearly the same direction in likely annual change (Table 10). Figure 34 displays the development of monthly discharge exceedance probabilities in the Sore watershed for the period 2021-2030 compared to the base period. The uncertainty range comprises 20 ensembles of two climate models, and it is clear that the two hydrological models indicate a similar direction of discharge change except for low flows.

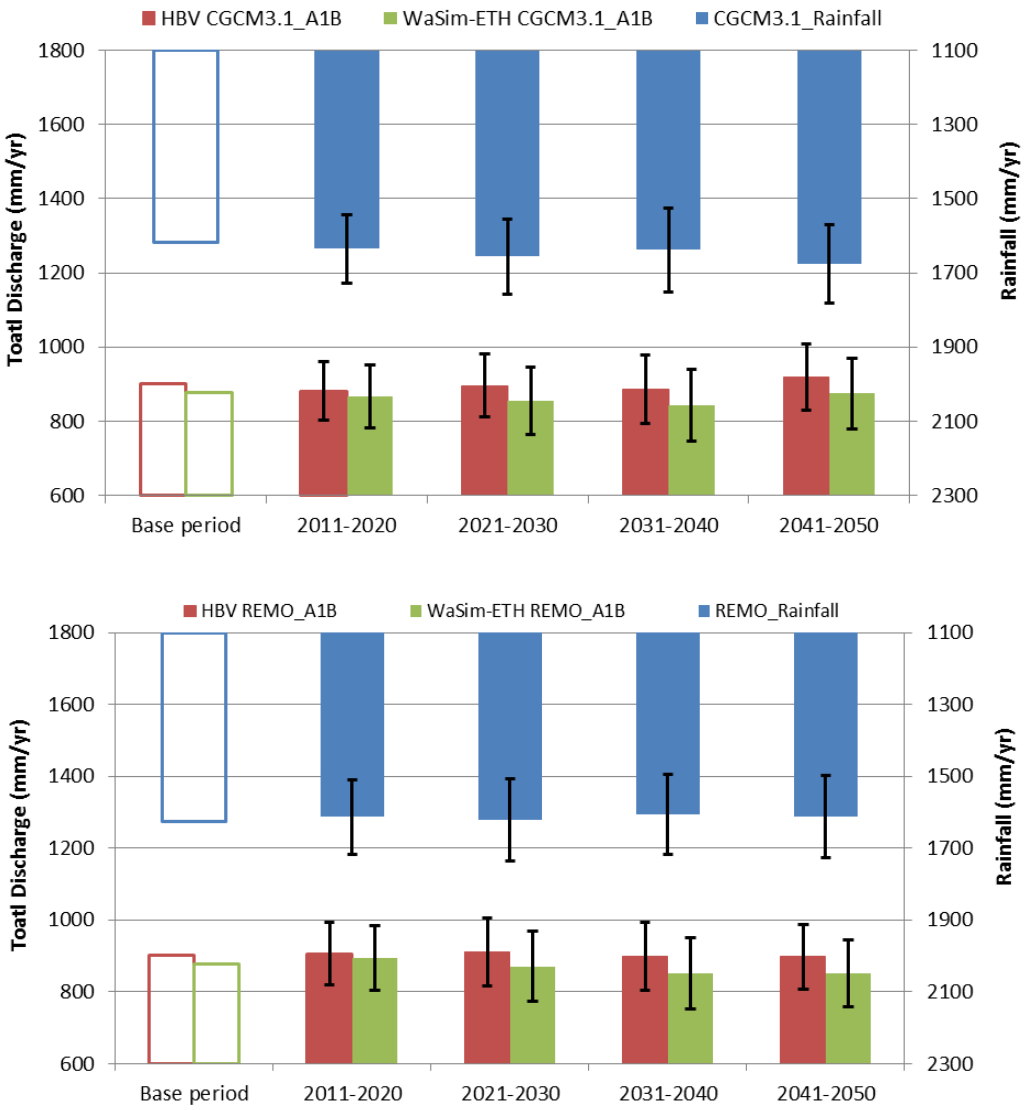

Figure 33: Total annual discharge and rainfall per decade of each model using the **CGCM3.1 A1B** and **REMO A1B** scenarios and the base period of the Sore watershed; filled bars, **WaSiM-ETH and HBV-Light** simulations (mean of 20 ensembles used); unfilled bars, model results using measured climate and rainfall data; error bars, standard deviation of the 20 ensemble runs for corresponding decade.

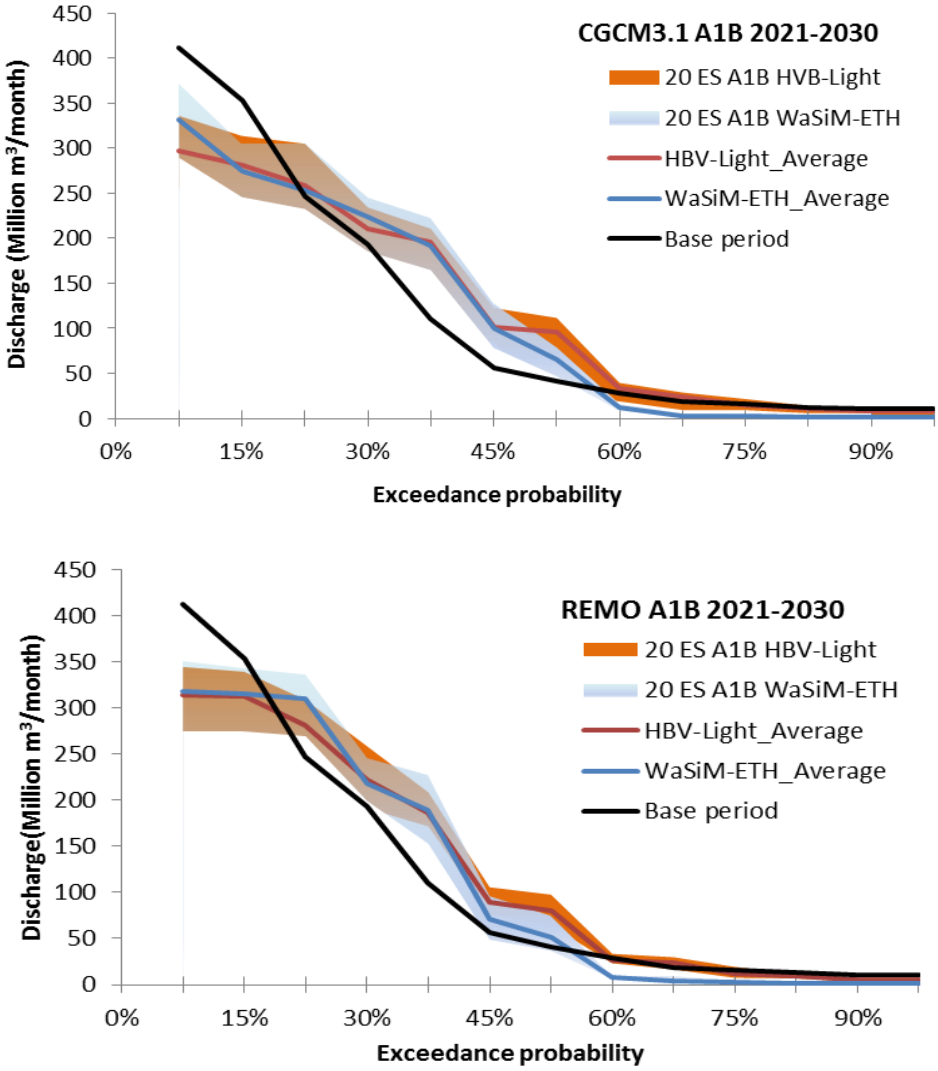

Figure 34: Development of monthly discharge exceedance probability in the Sore watershed under climate change scenario (simulated with the WaSiM-ETH and HBV-Light models).

Model and downscaling uncertainties

When estimating hydrologic climate change impacts, there are many sources of uncertainty. These sources are linked to scenarios, GCMs, statistical downscaling, and parameter uncertainties in hydrological models used in the impact assessment. Despite recent advances in GCM resolution, the resolution of climate models is still very coarse, even if regional climate models with a resolution of 0.5° are used. Therefore, downscaling to the local scale is required, which may introduce uncertainty in the input of the hydrological models. Moreover, different hydrological models compute different stream flows for the same input. As Xu et al. (2005) reports, the greatest uncertainties in the impact of climate on stream flow arise from uncertainties in climate change scenarios, as long as a conceptually sound hydrological model is used. In this study, the gap between GCMs and inputs required

by catchment-scale hydrological models was narrowed by applying statistical downscaling. The results reveal that the uncertainty band caused by statistical downscaling is wide for peak flows for both the examined climate models (Figure 32 and 34) and becomes smaller in the case of low flows. Generally, the exceedance probability uncertainty band (Figure 34) displayed the same pattern for the two hydrological models even though the models had different model structures. Therefore, as long as discharge simulation is being considered, the two models perform similarly for the study area, except for minor differences during low flow. Both climate models indicate a shift of the wet season to an earlier month (June to July), but the CGCM3.1 predicts lower flow for August and September compared to the REMO (Figure 32). This difference is caused by the climate models and not by the downscaling approach or the hydrological model used. In this study the uncertainty caused by using different climate models is larger than uncertainty caused by using different hydrological models. Even though the impact of hydrological models appears to be low in this study, other investigations have observed large impact differences between hydrological models (Cornelissen et al., 2013). Therefore, further investigations should be conducted using multiple GCMs and various hydrological models.

6.4. Conclusions

The objective of this study was to compare the uncertainty of two hydrological models in discharge modelling and their performance and catchment hydrological response to climate change. A hydrological modelling experiment was conducted using two hydrological models, HBV-Light and WaSiM-ETH. The rainfall, temperature and potential evapotranspiration data corresponding to the base period and climate change scenarios downscaled with the SDSM from REMO and CGCM3.1 were used as inputs for the hydrological models. In general, the hydrological impact analysis indicated an overall slight decreasing trend per decade (HBV-Light -2% to +1.4 % and WaSim-ETH -7% to -0.5%) in mean annual river discharge, corresponding to the input data downscaled with the SDSM for both the REMO and CGCM3.1 models. Furthermore, there is a likely seasonal shift, as indicated by the peak flow shift from August-September to June-July. It was also shown that the wet season discharge is highly sensitive to climate change. Abdo et al. (2009) also observed that wet season discharge is sensitive to climate change, and significant changes are likely in the seasonal

and monthly flows in other parts of the Nile, such as Lake Tana in the Blue Nile basin in Ethiopia. Sayed (2004) indicated similar results for the Blue Nile basin.

Table 10: Mean simulated annual water balance for the reference period and climate change scenarios A1B and B1 (REMO) and A1B CGCM3.1 in the Sore watershed. The results are the averages of the 20 ensemble runs for each climate scenario. Changes in % from the reference period are presented.

		RF* (mm/yr)	ETP* (mm/yr)	ETR* (mm/yr)	T-Dis* (mm/yr)	RF (Δ%)	ETP (Δ%)	ETR (Δ%)	T-Dis (Δ%)
	Observed (1990-1992, 1994-1996)	1618.5	1394.3	680	900	0	0	0	0
WaSiM-ETH	**REMO A1B**								
	2011-2020	1612	1342	670	895	-0.4	-3.8	-1.4	-0.5
	2021-2030	1622	1344	670	870	+0.2	-3.6	-1.4	-3.3
	2031-2040	1605	1349	670	851	-0.8	-3.3	-1.5	-5.4
	2041-2050	1613	1351	677	851	-0.3	-3.1	-0.5	-5.5
	REMO B1								
	2011-2020	1620	1363	687	887	+0.1	-2.3	+1.0	-1.4
	2021-2030	1602	1360	679	841	-1.0	-2.5	-0.1	-6.6
	2031-2040	1613	1365	683	845	-0.4	-2.1	+0.5	-6.1
	2041-2050	1622	1365	685	852	+0.2	-2.1	+0.7	-5.4
	CGCM3.1 A1B								
	2011-2020	1635	1390	722	868	+1.0	-0.3	+6.2	-3.6
	2021-2030	1656	1388	722	854	+2.3	-0.5	+6.1	-5.1
	2031-2040	1638	1383	715	843	+1.2	-0.8	+5.1	-6.4
	2041-2050	1675	1379	718	875	+3.5	-1.1	+5.6	-2.7
HBV-Light	**REMO A1B**								
	2011-2020	1612	1342	714	906	-0.4	-3.8	+5.0	+0.7
	2021-2030	1622	1344	710	912	+0.2	-3.6	+4.4	+1.4
	2031-2040	1605	1349	708	898	-0.8	-3.3	+4.1	-0.3
	2041-2050	1613	1351	715	898	-0.3	-3.1	+5.1	-0.3
	REMO B1								
	2011-2020	1620	1363	735	894	+0.1	-2.2	+8.1	-0.7
	2021-2030	1602	1360	723	879	-1.0	-2.5	+6.3	-2.3
	2031-2040	1613	1363	727	886	-0.4	-2.2	+6.9	-1.6
	2041-2050	1622	1365	728	893	+0.2	-2.1	+7.1	-0.8
	CGCM3.1 A1B								
	2011-2020	1635	1390	761	882	+1.0	-0.3	+11.9	-2.0
	2021-2030	1656	1388	759	896	+2.3	-0.5	+11.6	-0.4
	2031-2040	1638	1383	751	887	+1.2	-0.8	+10.4	-1.4
	2041-2050	1675	1379	757	918	+3.5	-1.1	+11.3	+2.0

*RF=rainfall, ETP=Potential evapotranspiration, ETR=Actual evapotranspiration, T-Dis=Total Discharge

In the present study, the hydrological models were consistent in the overall direction of change, regardless of the magnitude, and inconsistent in terms of direction of low flow change for both climate models scenarios until 2050. Both hydrological models simulated a decrease in wet season discharge and shift of the peak season (May to July) using the

CGCM3.1. Generally, both models evaluated in this study are suitable for simulations of annual discharge in climate scenarios because they produced comparable results. According to this study, the HBV-Light model is most suitable for discharge simulations in data-sparse regions such as the Baro-Akobo basin even if it is a conceptual model. However, if the interest is in assessing the impact of climate change on water balance components, distributed physically based models may be a good option to describe the impact on interflow conditions, as seen in our study. Abdo et al. (2009) used the HBV model to examine the Blue Nile basin and reported that the model performance was good. Taye et al. (2011) also used two lumped conceptual models (VHM and NAM) in Lake Tana, Blue Nile basin, and confirmed that both model performances were satisfying. The results of the catchment hydrological response to climate change are highly dependent on the input data and uncertainty of the models considered. Thus, further study in the Sore watershed and Baro-Akobo basin in general with updated data and a variety of models is required. In addition, possible adaptation options for the watershed impacts must be studied.

Chapter 7

7. Dry spell, onset, and cessation of the wet season rainfall in the Upper Baro-Akobo Basin, Ethiopia

Abstract

In this study the rainy season maximum dry spell length and number of dry spell periods were investigated to analyse the drought trend in the upper Baro-Akobo River basin which is a part of the Nile basin, Western Ethiopia. Daily rainfall records for the period 1972-2000 from 8 rain gauge stations were used in the analysis of the dry spells and tested for trends using the Mann-Kendall test of significance. Furthermore, the beginning and end of the trend development in the dry spell was also tested using the sequential version of Mann-Kendall test. Results shown that there is neither clear monotonic trend found in dry spell for the basin nor significant fluctuation in the onset, cession and duration of rainfall in the Baro-Akobo river basin. This sufficiently explains why rain-fed agriculture has suffered little in the western part of Ethiopia. The predictable nature of dry spell pattern may have allowed farmers to adjust to predictable rainfall variability in the basin. Unlike many parts of Ethiopia, the Baro-Akobo basin climate variability is not a limiting factor for rain-fed agriculture productivity which may contribute significantly to national food security.

KEY WORDS: Drought, Mann-Kendall test, dry spell, Baro-Akobo, rain-fed agriculture

7.1 Introduction

In countries like Ethiopia, where agriculture serves as a backbone of the economy as well as ensures the main source of food production and income for about 80 % of the labour force and 47.68 % of the gross domestic product (GDP) (Araya and Stroosnijder, 2011; World bank, 2011), the availability of water resource is quite essential. However the sector is mainly depending on rain-fed agriculture. For management of rainwater and agriculture as well as for the evaluation of drought risk the seasonal rainfall has to be evaluated concerning duration, onset and cessation of the rainy season and the dry spell lengths based on past records. In Ethiopia, the drought years of 1965, 1972-73, 1983-84, 1987-88, and 1997 resulted in low agricultural production and affected millions of rural poor farmers, pastoralists, domestic and wild animals, with serious degradation of the environment (Seleshi and Zanke, 2004). There have been reports of rainfall variability and occurrence of

drought in northern, eastern and south eastern part of Ethiopia (Araya and Stroosnijder, 2011; Tilahun, 2006; Tilahun, 1999).

Most of the dry spell studies carried out in various part of Africa pointed out the importance of a clear understanding of the length and number of dry spells, and their probabilities for assessing of recurring droughts and decreasing agricultural productivity (Muita et al., 2012; Sivakumar 1992). Many authors define a dry spell with different threshold values of rainfall at a dry day. In this study, rainfall amount of 1mm per day was used as the threshold, often 0.1mm used with respect to the common precision of rain gauges. Some studies employed a threshold of 1.0mm, on the assumption that rainfall less than this amount is evaporated off directly (Mathugama and Peiris, 2011). However, the definition of thresholds depends on the purpose of the study and methodology used.

Seleshi and Camberlin (2006) analysed dry spells based on the maximum number of consecutive days with rainfall less than 1mm all over Ethiopia using 11 stations. They found no trends in the annual maximum length of dry spells during the rainy season over Ethiopia. The main limitation of this work is the definition of the beginning and the end of rainy season were not computed per year but taken as constant depending on the location within Ethiopia. Besides, they indicated that their study was limited to the small number of stations as compared to the huge size of the investigated area. Such study at the whole county level which has different rainy season is not supportive for decision making at local administration level (zone scale). Nevertheless, Yemenu and Chemeda (2010) found higher probability of dry spell occurrences during the shorter rainy season but the occurrences of the same in the main rainy season (bi-modal rain) was very minimal using Markov Chain and Reddy model for central highlands of Ethiopia.

There is little or no work in the western part of Ethiopia to assess the onset and cessation of the rainy season and to examine dry and wet spells. Therefore, a detailed dry spell analysis is highly important for the agricultural water management in the highland of Baro-Akobo basin, western Ethiopia. This study focuses on the highlands of the Baro-Akobo basin which is characterized by dominantly rain-fed agriculture and having sufficient data for the analysis. The Oldeman and Van Velthuyzen (1991) and the FAO (1996) method adopted for determination of onset and cessation of rainfall, and the Mann-Kendall test were used for trend analysis.

This study analysed the rainy season with the objective to determine the onset and cessation of the rainy season over the period of 1972-2000, to analyse the trends of dry spells during the rainy season, and provide a summary of the rainfall data in a form that can easily be used in rain-fed agriculture in the upper Baro-Akobo basin, western Ethiopia. The introduction is followed by study area and data set, and methods were the statistical techniques used are briefly explained. Section 7.4 presents and discusses the results while section 7.5 provides the summary and the conclusion.

7.2 Study area and data set

The study area is located within the western part of Ethiopia as shown in Figure 35. The highland part of the basin (2200 – 1550 m.a.s.l) where this study focused on is one of the higher rainfall regimes of Ethiopia. The mean annual rainfall varies between 1086 mm at Dembi Dolo to 2201 mm at Masha stations based on (1980-2000 record). The monthly mean temperature varies between 17.5°C and to 21.5°C. The study area is dominantly dependent on rain fed agriculture and the rainfall variability and dry spell analysis are important planning tools in agricultural water management.

Daily rainfall data from 8 rainfall stations in the upper Baro-Akobo basin having longer records (22 to 29 years) were provided by the Ethiopian National Meteorological Agency, and used in this study to analyse the dry spell trends. These rain gauges stations have adequate rainfall records spanning from 1972-2000, which is considered to be appropriate as minimum record length for statistical validity of trend analysis (Karpouzos et al., 2010). Missing daily rainfall values were filled using multiple correlations of daily data with neighbouring stations. Partly outputs of the Statistical Downscaling Model (SDSM) as suggested by Wilby and Dawson (2012) are used to fill the data gaps. Four rainfall stations (Bure, Mettu, Gore and Chora) from the “Illu-Aba-Borra” zone, three stations (Gimbi, Yubdo and Dembi Dolo) from the “West Welega” administrative zone, and the third zone “Keficho Shekich” which has one station (Masha) (see Figure 35) were considered for the analysis.

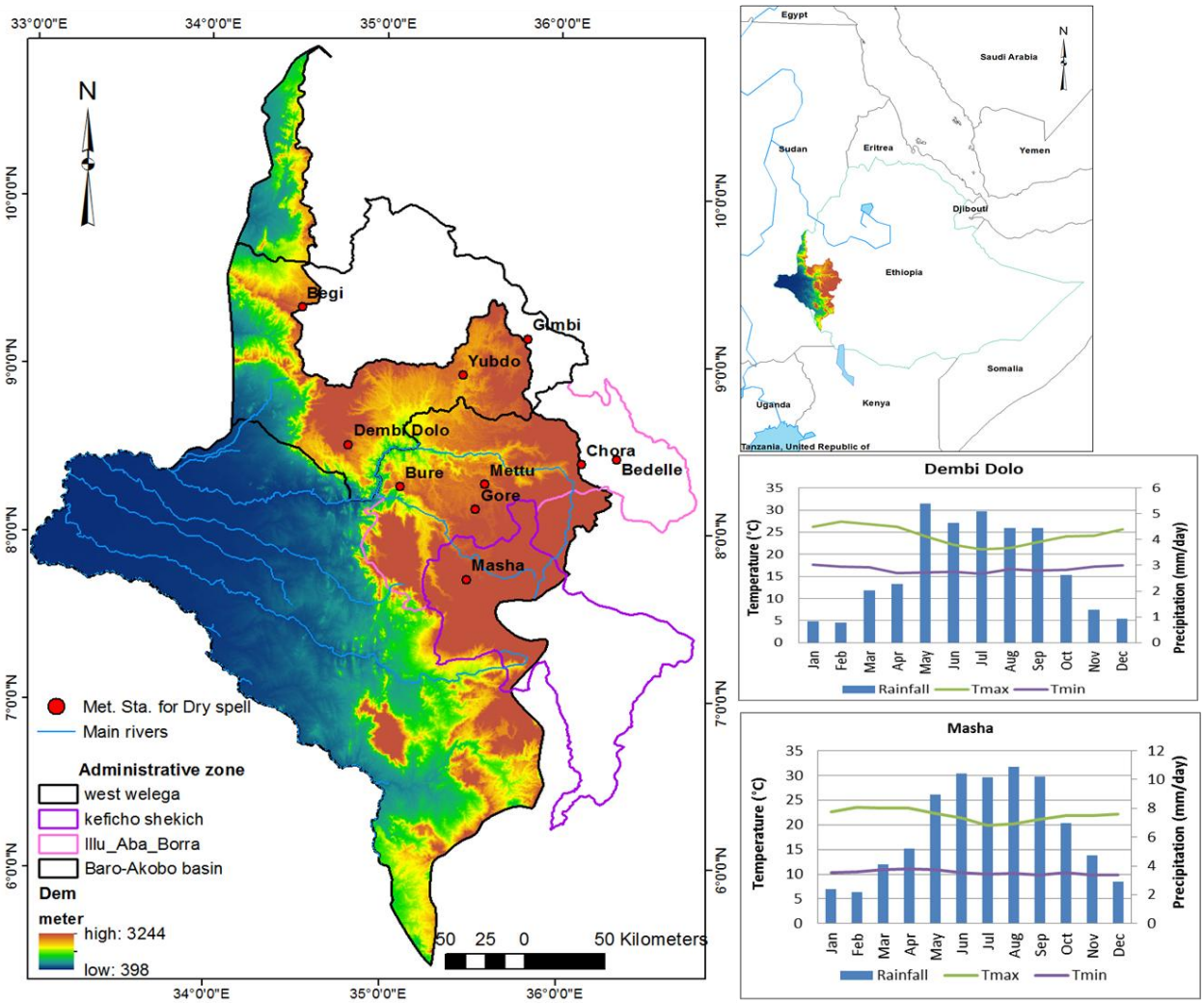

Figure 35: Study area: location of the Baro-Akobo basin, three administrative zones sharing the basin, monthly mean rainfall, Tmax, and Tmin for the Masha and Dembi Dolo stations and location of the rainfall stations.

7.3 Methods

Rainy season dry spell length and number of dry spells

From the rainfall data used in this study two parameters were derived namely ***R**ainy **S**eason **M**aximum **D**ry **S**pell length* (**RSMDS**) and ***R**ainy **S**eason **N**umber of **D**ry **S**pell periods (***RSNDS***)*. The first variable shows the maximum number of consecutive days without rainfall in each year rainy season, and the second variable is the number of periods without rainfall in each rainy season. These variables are important in controlling agricultural activities in the area by changing soil moisture content and ground water resources. We used the daily data of the rainy season for the analysis to compute the parameters RSMDS and RSNDS.

Rainfall onset and cessation

In studying dry spell trends it is important to determine as accurately as possible the beginning and the end of the rainy season because reliable estimates of starting and end of the rainy season could help optimized utilization of rainwater. After defining the onset and cessation of the rainy season for each station it is possible to estimate the trend of the dry spells. As Yemenu and Chemeda (2010) stated the assessment of beginning and end of rainy season is a key issue in countries which rely on rain-fed agriculture for better explanation of growing season of a given area and maximizing crop yield per unit of water. Accordingly, in this study the onset of rainy season is defined when decadal rainfall amount is greater than half of the evapotranspiration amount, and cessation of rainy season is when decadal rainfall is less than half of the evapotranspiration as used in other studies (e.g. Araya and Stroosnijder, 2011; Yemenu and Chemeda, 2010; FAO, 1996; Oldeman and Van Velthuyzen, 1991). A minimum daily rainfall threshold (greater than 1 mm per day) for defining a rainy day was the approach presented in Seleshi and Camberlin (2006), Seleshi and Zanke (2004). Yemenu and Chemeda (2010) also stated that 3mm rainfall depth per day is the minimum threshold value for crops to satisfy their crop water requirement during a growing season. Consequently, in this study an average of 30mm per decade of rainfall depth was taken as threshold value for evaluating each decade is in a dry or wet spell.

Test for homogeneity

Different methods are available for climatic variable time series homogeneity test. Detection of changes in daily rainfall characteristics requires the time-series to be homogenous (Seleshi and Camberlin, 2006). To test the homogeneity of the series, the non-parametric Thom's test (Run test) was performed in this study on the seasonal rainfall totals because it is recommended by many investigators as valid method (Nasri and Modarres, 2009; Lazaro et al., 2001; Rodrigo et al., 1999). As Rodrigo et al. (1999) explains the Run test is used for examining whether or not a set of observations constitutes a random sample from an infinite population. "In this test the number of uninterrupted runs, N, of values higher and lower than the median is counted, a code called "a" were assign for any value $X_j > X_{median}$ and a code "b" for any value $X_j < X_{median}$, each uninterrupted series of "a" and "b" codes is called a "run, R", the run test is based on the null hypothesis that the two elements "a" and "b" are

independently drawn from the same distribution, under the null hypothesis this statistic has an approximately normal distribution of mean (E) and variance (Var)" (Rodrigo et al. ,1999):

$$E(R) = \frac{N+2}{2} \ldots..11 \qquad Var(R) = \frac{N(N-2)}{4(N-1)} \ldots..12$$

The Z statistics is defined as: $Z = \frac{R-E(R)}{\sqrt{Var(R)}} \ldots..13$

For this study, if |Z|≤ 2.58, the null hypotheses of homogeneity is verified at 99% confidence interval.

Mann-Kendall (MK) test for trend

This method is a non-parametric rank based procedure that has been commonly used to assess if there is a trend in the time series of hydro-meteorological data (Karpouzos et al., 2010; Hamed, 2008; Nasri and Modrres, 2008; Su et al., 2006; Yue et al., 2002). The test compares the relative magnitudes of sample data rather than the data values. Each data value is compared to all subsequent data values. The use and computational procedures of the Mann-Kendall test statistics (Kendall's τ statistics) is described as indicated in many literatures (e.g. Hamed, 2008; Nasri and Modarres, 2008; Su et al., 2006; Yue et al., 2002).

Let X_1, X_2, … X_n represent n data points where X_j represents the data point at time j. Then the MK statistic (S) is given by

$$S = \sum_{k=1}^{n-1} \sum_{j=k+1}^{n} sign(X_j - X_k) \ldots..14$$

Where:

$$sign\,(X_j - X_k) = \begin{cases} 1 & if\ (X_j - X_k) > 0 \\ 0 & if (X_j - X_k) = 0 \\ -1 & (X_j - X_k) < 0 \end{cases}$$

A very high positive value of S is an indicator of an increasing trend, and a very low negative value indicates a decreasing trend. However it is necessary to compute the test statistic associated with S and the sample size, n, to statistically quantify the significance of the trend.

The mean E(S) and variance Var(S) of the statistic S is estimated as:

E(S) =0

$$Var(S) = \frac{n(n-1)(2n+5) - \sum_{p=1}^{q} t_p(t_p-1)(2t_p+5)}{18} \ldots\ldots 15$$

Where n is the number of data points, q is the number of tied groups (a tied group is a set of sample data having the same value), and t_p is the number of data points in the p^{th} group. The standardized test statistic (Z_{MK}) computed as follows:

$$Z_{MK} = \begin{cases} \frac{S-1}{\sqrt{Var(S)}} & if\ S > 0 \\ 0 & if\ S = 0 \\ \frac{S+1}{\sqrt{Var(S)}} & if\ S < 0 \end{cases} \quad \ldots\ldots 16$$

A positive Z_{MK} indicates an increasing trend, whereas a negative Z_{MK} indicate a decreasing trend. To test for either increasing or decreasing monotonic trend at p significant level, the null hypothesis should be accepted at the α significance level if the absolute value of $|Z_{MK}| \leq Z_{1-\alpha/2}$. In this study a significance level of α =0.05 are applied.

Sequential version of Mann-Kendall (SMK) test

The sequential version of Mann-Kendall test (Sneyers, 1990) is used to test an assumption about the beginning of the trend development within a sample. A brief description of the computational procedure is given here as described in Karpouzos et al. (2010), Nasri and Modarres (2009), and Gerstengarbe and Werner (1999):

1. The value of X_j of the two data time series (*rainy season maximum dry spell length* and *rainy season number of dry spell period*), (j=1, … , n) are compared with X_i, (i=1,…, j-1). At each comparison, the number of cases $X_j > X_i$ is counted and denoted by $n_j = \#\{X_i:(X_i<X_j, j=1,2,\ldots,j-1)\}$
2. The test statistic t is then calculated by equation

$$t_j = \sum_{1}^{j} n_j \quad \ldots 17$$

3. The mean and variance of the test statistic area

$$E(t) = \frac{n(n-1)}{4} \ldots 18$$

$$Var(t_j) = \frac{[j(j-1)(2j+5)]}{72} \ldots 19$$

4. The sequential values of the statistic u(t) are then calculated as

$$u(t) = \frac{t_j - E(t)}{\sqrt{var(t_j)}} \ldots .20$$

Similarly to the calculation of progressive rows of statistic u (t), the retrograde rows of statistic u' (t) are computed backwards starting from the end of series. In the absence of any trend, the graphical representation of the direct u (t) and the backward u' (t) series obtained with this method gives curves which overlap several times (Seleshi and Camberlin, 2006), i.e., no trend exists, the u (t) and u' (t) plots are expected to oscillate near and around the zero-line remaining within the ($-u_{crit}(\alpha)$, $u_{crit}(\alpha)$) interval. A significant trend for the whole period would be seen through the parallel monotonicity of the graph u (t) and u' (t), while the point of intersection of u (t) and u' (t) graph being below the $-u_{crit}(\alpha)$ or above the $u_{crit}(\alpha)$ line would suggest that the upward or downward trend is broken at that point, i.e., the change-point has been detected (Weglarczyk, 2009).

7.4 Results and discussion

7.4.1 *Dry spell statistics and test of trend*

This section presents the statistical analysis and results of the non-parametric Mann-Kendall (MK) test for the two dry spell parameters of RSMDS and RSNDS over the period of 1972-2000. The homogeneity tests of RSMDS and RSNDS series for all stations are shown in Table 11. From this table, it is clear that all RSMDS and RSNDS series are homogeneous because of the test statistics $|Z| \leq 2.58$ for all stations at 99% confidence level except station Gimbi for RSNDS parameter. Statistics of the maximum, average and standard deviation of the two dry spell parameters (RSMDS and RSNDS) generally indicate if there is significant spatial pattern. The RSMDS value increases from Northwest to South East of the basin. In the north western stations of Gimbi, Yubdo, Dembi Dolo, the maximum dry spell length varies between 10 to 5 days while in the south eastern stations of Chora, Masha, Gore stations, the variation is between 19 to 7 days as shown in Table 12. In terms of the maximum number of dry spells, there is no any pattern in terms of spatial variability.

Table 11 Homogeneity test statistics for dry spell length and number. RSMDS: Rainy Season Maximum Dry Spell length, RSNDS: Rainy Season Number of Dry Spell period.

Station name	Rainy Season Maximum Dry Spell Length (RSMDS)	Rainy Season Number Dry Spell Period (RSNDS)
	Z statistics	Z statistics
Masha	-0.40	-1.60
Gore	-1.43	-1.54
Gimbi	-1.04	-2.62
Chore	-1.38	-0.44
Bure	0.25	1.25
Mettu	-1.21	0.44
Yubdo	-0.75	-0.64
DembiDolo	-0.75	0.24

Table 12 Statistical characteristics of selected rainy season variable.

Station Name	Time Period	Elevation (meter)	Rainy season dry spell length (day)			Rainy season number of dry spell periods		
			Maximum	Mean	SD	Maximum	Mean	SD
Masha	1975-2000	2220	19	8.3	4.5	60	34.7	9.8
Gore	1972-2000	2024	18	6.9	4.5	49	30.4	7.4
Gimbi	1978-2000	1970	11	5.0	2.4	42	24.8	9.4
Chora	1975-2000	1930	19	6.8	4.0	48	31.0	8.6
Bure	1976-2000	1700	11	4.7	2.2	44	25.6	9.9
Mettu	1979-2000	1690	13	4.4	3.2	39	24.6	9.7
Yubdo	1976-2000	1560	10	5.0	2.0	50	26.4	9.3
Dembi Dolo	1979-2000	1550	10	5.0	2.1	41	26.2	10.9

Table 13 provides the test statistics and p-values derived for each station. As shown in the table there is no monotonic trend found in RSMDS length for all stations data sets at a 5% significant level over the period 1972-2000. Although visual indications exist on clear downward and upward trends in the station data (see Figures 36 and 37), it falls within the insignificant range of MK.

Table 13 MK test result for dry spell length and number of dry spell periods, RSMDS: Rainy Season Maximum Dry Spell length (RSMDS), RSNDS: Rainy Season Number of Dry Spell periods.

Station name	RSMDS Length			RSNDS Period		
	S statistic	Z_{MK}	p-value	S statistic	Z_{MK}	p-value
Masha	-76	-1.66	0.10	55	1.19	0.23
Gore	-36	-0.72	0.47	-7	-0.11	0.91
Gimbi	42	1.11	0.27	27	0.69	0.49
Chora	-27	-0.58	0.56	-78	-1.70	0.09
Bure	7	0.14	0.89	43	0.98	0.33
Mettu	16	0.45	0.65	67	1.87	0.06
Yubdo	21	0.48	0.63	-36	-0.82	0.41
Dembi Dolo	-54	-1.53	0.13	0	0.01	0.95

Generally based on the standardized test statistic (Z_{MK}) it is possible to conclude that MK test did not reveal a statistically significant trend in the study area for both parameters at the 5% level. For graphical illustration, the temporal change of maximum dry spell length and number of dry spell periods with trend lines are depicted in Figure 36 and 37. Linear regressions were used to estimate the temporal trend of the series. From the trend lines we have also seen that the change is not significant, for example RSMDS length for two stations (Masha and Dembi Dolo) decreases 2 and 1 day per ten years, whereas it increases 1 and 0.75 days per ten years at stations Gimbi and Yubdo respectively. The number of dry spells for two stations (Chora and Yubdo) decreases 4 and 9 dry spell periods per ten years, whereas it increases 3 and 7 dry spell periods per ten years at stations Masha and Mettu respectively. Therefore, the study generally indicates that the rainy season maximum dry spell (RSMDS) length and rainy season number of dry spell (RSNDS) period over upper Baro-Akobo basin show no trend over the study period.

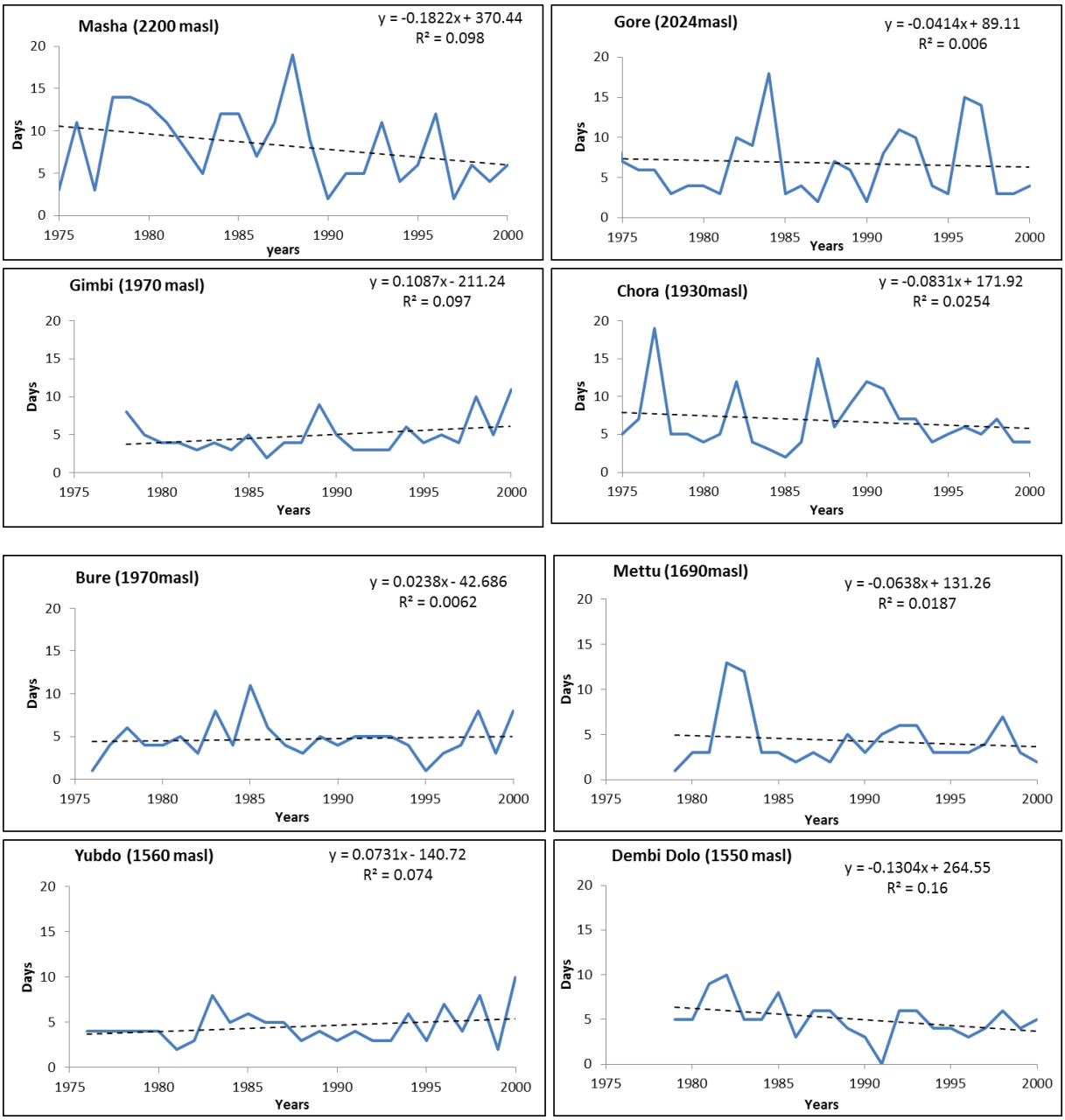

Figure 36: Time series of **RSMDS** (Rainy Season Maximum Dry Spell) length for Masha, Dembi Dolo, Yubdo and Gimbi stations. Dashed lines show the linear trends. The trend would be significant if $R^2 > 0.39$ (5 % significance level).

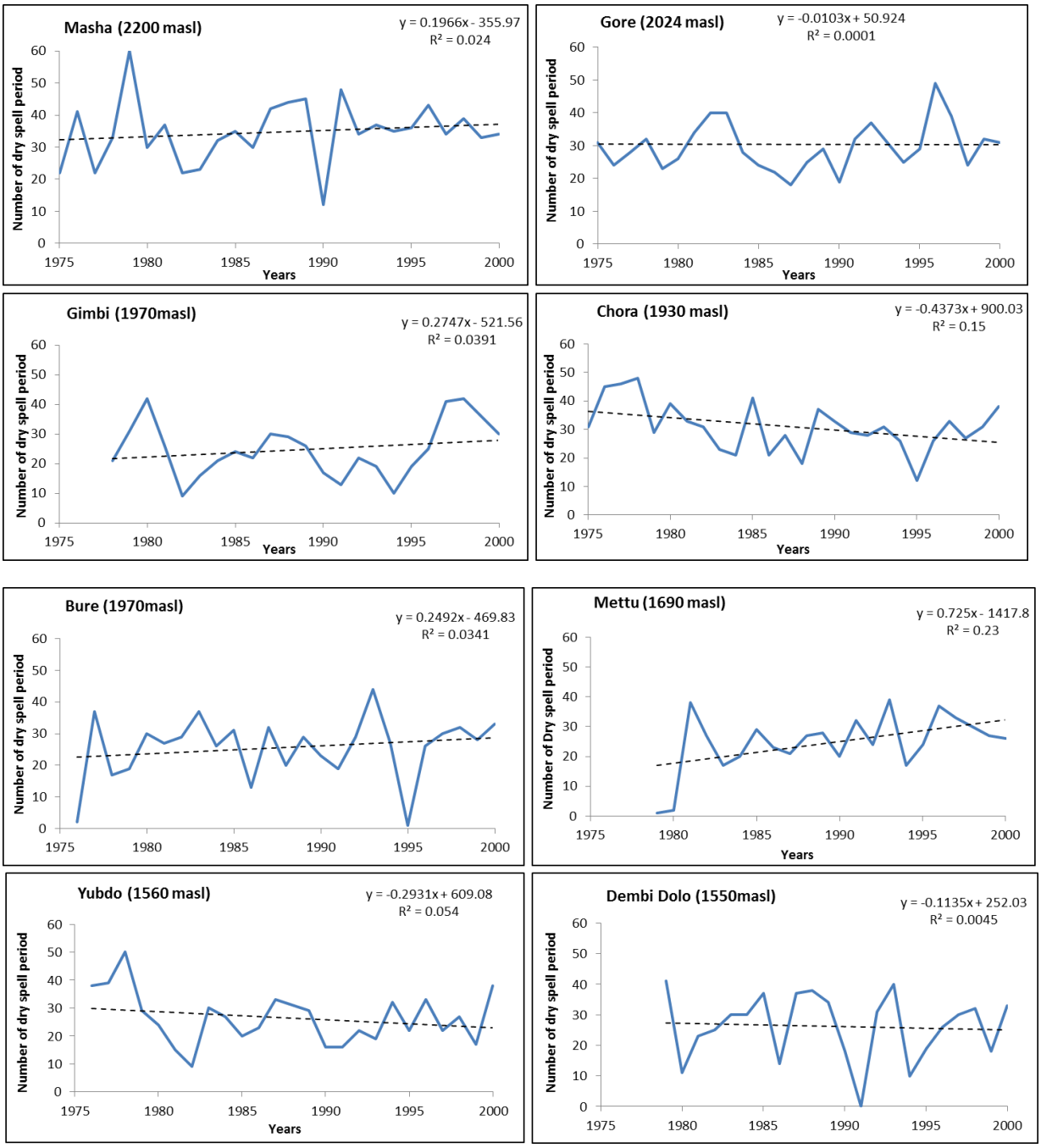

Figure 37: Time series of **RSNDS** (Rainy Season Number of Dry Spell) Period for Masha, Mettu, Chora and Yubdo stations. Dashed lines show linear trends. The trend would be significant if $R^2 > 0.39$ (5 % significance level).

7.4.2 Sequential version of Mann-Kendall (SMK) test result

The results of the sequential version of the Mann-Kendall (SMK) test are presented in Figure 38 and 39. The value of u(t) , u'(t) statistics and the confidence limit at 5% significant level are shown by solid lines, dashed lines and dashed box respectively. When we examine the

plot of u (t) of Gimbi station for **RSMDS** series (Figure 38), decreasing trends are detected from 1979-1984, and uneven changes observed from 1985 onwards that cuts u' (t) several times. This justify that there is no clear starting and ending of the trend. For all stations in the study area there is no substantial trend detected at 5% significance level, since the graphical representation of u (t) and u' (t) gives curves that overlap several times. The SMK tests for **RSNDS** period also justify this fact. Therefore, the sequential version of Mann-Kendall (SMK) consolidates the findings of the earlier Mann-Kendall test that rainy season maximum dry spell (RSMDS) length and rainy season number of dry spell (RSNDS) period over upper Baro-Akobo basin have no significantly changed over time.

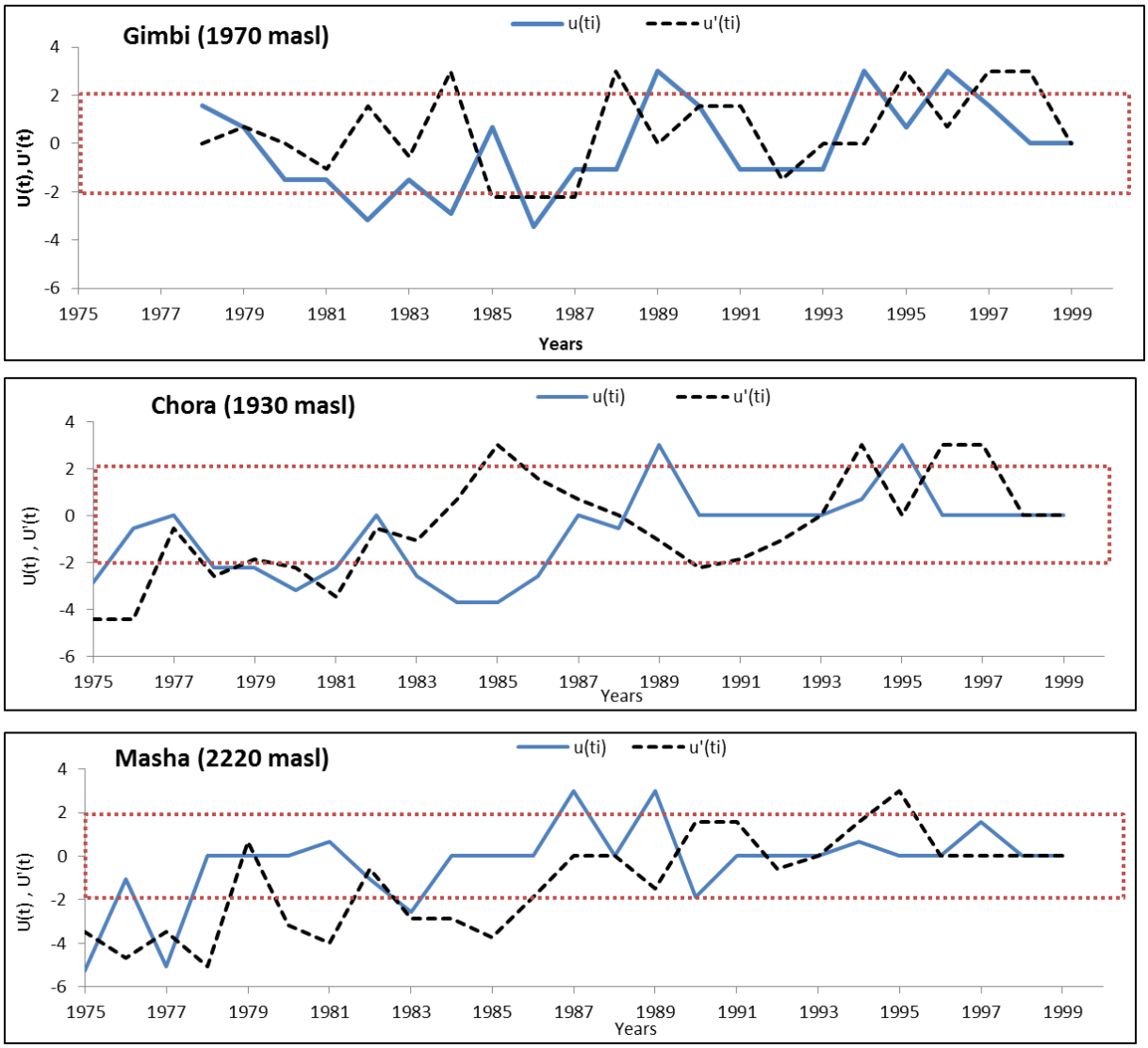

Figure 38: Sequential MK statistic values of u (t) "solid line", u' (t) "dashed line" and confidence limit at 5% "dashed box" for **RSMDS** (Rainy Season Maximum Dry Spell) length of station Gimbi, Chora, and Masha.

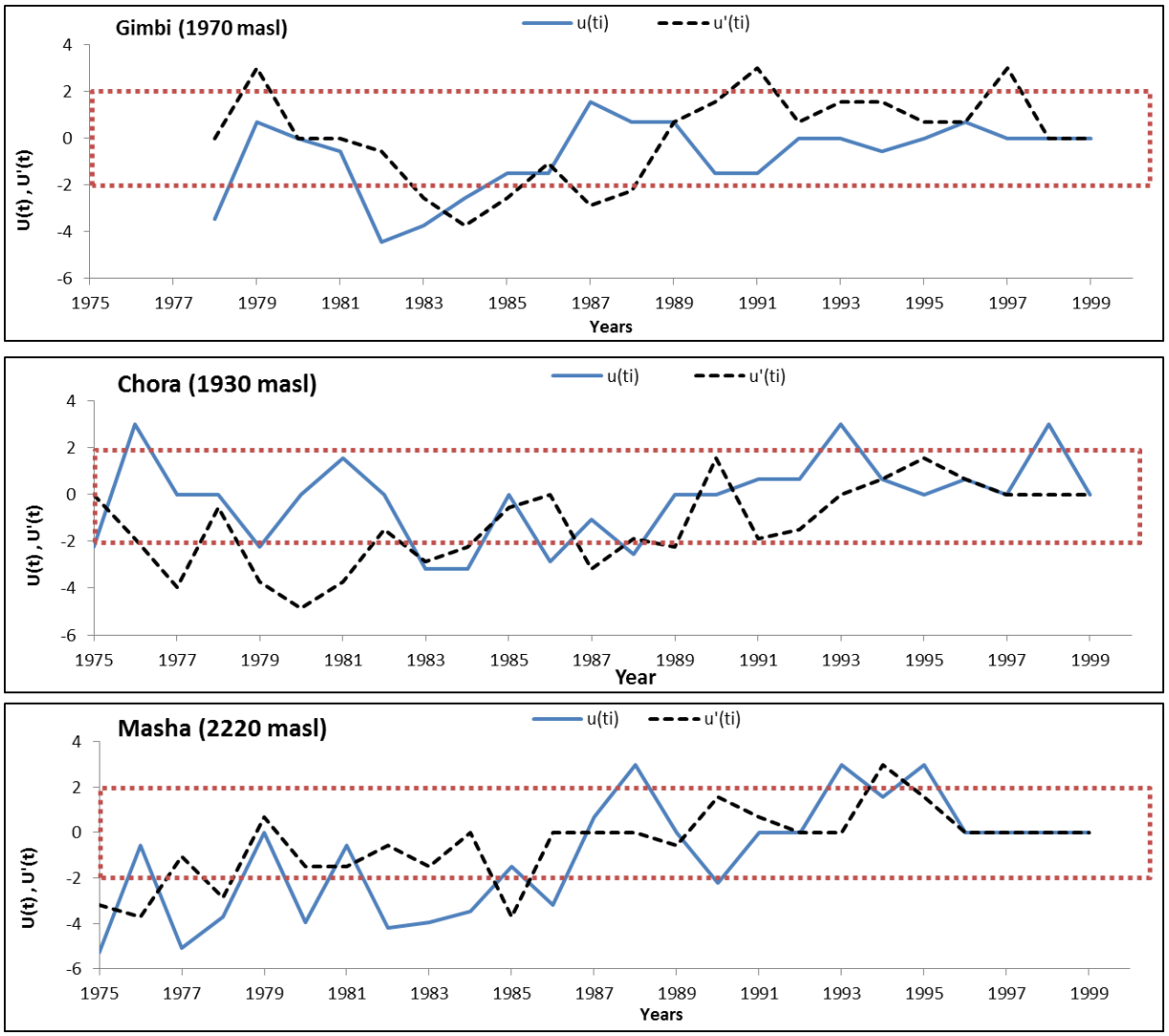

Figure 39: Sequential MK statistic values of u (t) "solid line", u' (t) "dashed line" and confidence limit at 5% "dashed box" for **RSNDS** (Rainy Season Number of Dry Spell) period of station Gimbi, Chora, and Masha.

7.4.3 Onset and cessation of rainy season

This section presents the analysis of the onset and the cessation of the rainy season (1972-2000) at the rainfall stations in the upper Baro-Akobo basin which is important for decision making purpose and planning agricultural water management. The analysis show that the mean onset of rainy season for stations Gimbi and Yubdo is during the third meteorological decade of May and ends during the third decade of September. Whereas Station Bure and Mettu have their onset during the second decade of May and the rainy season ends during

the second decade of September for Bure, and the first decade of October for Mettu (Figure 40 shows detail for all stations considered in the upper basin).

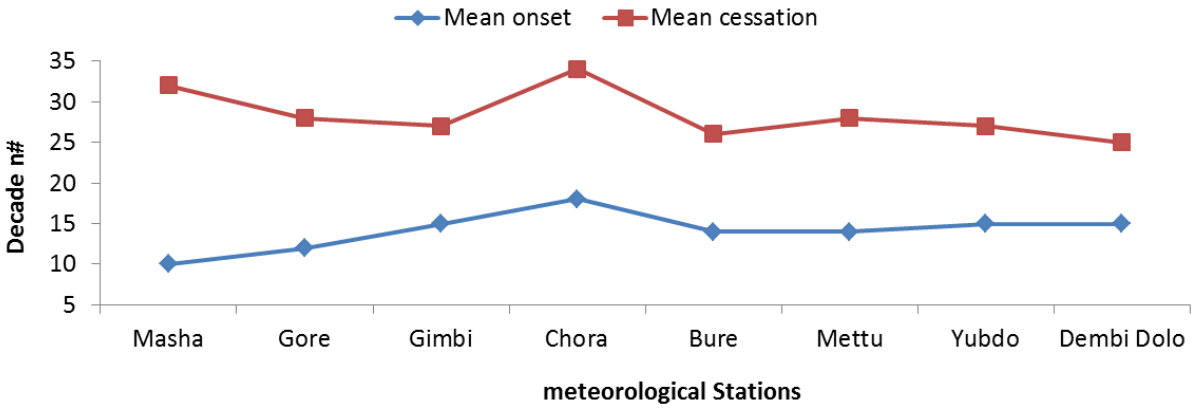

Figure 40: Mean onset and cessation of wet season rainfall for 8 stations.

The coefficient of variation (CV) for the end of the rainy season is less than 15% for all stations (Table 14) and it is less than 20% for all stations except Masha and Gore hence the consensus in the sample is strong (Labesse, 2008), which implies that decision making on planning of agricultural water management based on this analysis would be possible with low risk. Regarding the stations onset for the wet season rainfall, the coefficient of variation generally ranges from 0.12 to 0.42 across all stations. Wet season rainfall decrease early at Dembi Dolo station in the first decade of September as compared to others stations in the basin, while at station Chora it starts late (third decade of June) compared to other stations in the study area and ceases late (first decade of December) (Figure 40). The lowest variability of the onset of the wet season rainfall is observed at Gimbi station, which has a coefficient of variation of 0.12 decades, while the highest variability is at the stations Masha and Gore with a coefficient of variation of 0.42 and 0.3 respectively. The end of rainy season shows a very low variability with a coefficient of variation ranging from 0.10 to 0.05 across all stations.

Table 14 Summery of the onset and the end date of the rainy season for the period 1980-2000. (One meteorological decade=10days)

Stations	Mean onset Decade n#	SD_onset decade	CV_onset	Mean end Decade n#	SD_End decade	CV_End
Masha	10	4.3	0.42	31.8	2.6	0.08
Gore	12	3.7	0.30	28.5	1.7	0.06
Gimbi	15	1.7	0.12	27.5	1.7	0.06
Chora	18	3.1	0.17	33.7	1.7	0.05
Bure	14	2.2	0.16	26.5	2.9	0.11
Mettu	14	2.0	0.14	27.8	1.4	0.05
Yubdo	15	2.3	0.15	27.3	1.6	0.06
Dembi Dolo	15	3.2	0.21	25.1	2.9	0.12

General characteristics of the wet season rainfall onset and cessation are given in Table 15. The summary of the mean length of rainy season and its characteristics for each station is shown in Table 16, as indicated in the table the maximum length (224 days) is in Masha and the minimum is in Dembi Dolo station (109 days).

Table 15 Characteristics of the wet season rainfall at different rainfall stations (1980-2000).

	Stations							
Characteristics	**Masha**	**Gore**	**Gimbi**	**Chora**	**Bure**	**Mettu**	**Yubdo**	**Dembi Dolo**
	Decade n#							
Earliest onset	1	2	12	10	10	10	11	10
Delayed onset	21	16	18	26	18	18	20	22
Earliest cessation	27	25	24	30	18	25	24	19
Delayed cessation	36	33	30	36	30	30	30	30

Table 16 Summary of the length of the rainy season (days) for each station (1980-2000).

	Masha	Gore	Gimbi	Chora	Bure	Mettu	Yubdo	Dembi Dolo
Mean	224.3	174.3	137.1	163.8	134.8	149.0	135.2	109.5
SD	48.9	38.9	26.4	40.8	39.1	25.2	25.0	44.2
CV	0.2	0.2	0.2	0.2	0.3	0.2	0.2	0.4

7.5 Conclusions

The objective of this study was to determine the spatial and temporal variability of dry spell characteristics in Baro-Akobo basin focusing on the rainy season maximum dry spell length (RSMDS) and rainy season number of dry spell (RSNDS) over the period of 1972-2000. The rainfall onset and cessation was also investigated. From the MK test statistics we have seen that there is no monotonic trend (statistically significant trend) found in both parameters (RSMDS and RSNDS) for all stations. Though, the RSNDS period for two stations Chora and Yubdo decreases by 4 and 9 dry spell periods per decade, whereas it increases 3 and 7 dry spell period per decade at stations Masha and Mettu respectively. Seleshi and Camberlin (2006) also found that there is no general trend in the length of the wet season dry spell in Ethiopia which is in line with this study.

In terms of fluctuation of the onset and the cessation of rainfall, the variation is very low. The coefficient of variation for the onset of the rainy season reveals that planning of rain-fed agriculture in the study area involves low risk because of the stability of the onset dates. Therefore capitalize on rain-fed agriculture during rainy season in the study area is important, and such kind of study is supportive for decision making at local administrative scale. In general, for sustainable management of agricultural water (rain-fed agriculture) in the area and for reducing risk of droughts it is also recommended to investigate climate change impacts related to dry spell analysis.

Chapter 8

8. General conclusion and perspectives

In East African countries like Ethiopia, where agriculture serves as main sources of livelihood, the availability of water resources and its sustainable management is essential. Given that, there is a need to consider factors like impact of global change for sustainability of these resources. Here in this study, an assessment of temperature and precipitation projections, comparative study of hydrological models and the likely changes in water resources within the concept of climate change, and a dry spell trend analysis on the Baro-Akobo basin, Ethiopia, was addressed to provide supportive information on water resources management in the area. Therefore, the following steps were performed: (1) downscaling regional and global climate models for a reference and future scenario climate conditions, (2) applying physically-based distributed and conceptual models that were calibrated and validated under recent climate conditions, and driven by downscaled climate models for future scenarios of climate conditions, (3) investigating onset and cessation of the rainy season and the lengths of dry spells in the rainfall season using a statistical approach. In the first chapter four specific objectives were derived from recent literature where these topics should be addressed in this study. In brief what we have found in this study summarized by answering the specific objectives as follows:

- ✓ **Evaluate statistically downscaled climate variables from a regional climate model (REMO, 0.5° grid) and a global climate model (CGCM3.1, 3.75° grid) for the Baro-Akobo river basin.**

In this study climate variables from a regional (REMO) and a global climate model (CGCM3.1) were tested in the basin to give the first-hand information. It was shown that REMO is able to reproduce the observed precipitation and temperature (1972-2000) prior to downscaling over the basin than CGCM3.1. Therefore, it can be concluded that REMO can be one of the promising regional models for the basin. Regarding the future projections generally both climate models agree on the direction of change on the study area but having different magnitude. However, in order to recommend REMO for climate impact analysis in whole Ethiopia further evaluations on other parts of the country are required.

- ✓ **Assess future trend in precipitation and temperature compared to baseline and provide first-hand understanding of the direction of climate change in the basin**

For comprehensive climate change impact assessment studies, using climate models and downscaling methods is a necessary pre-requisite. In this study, large-scale atmospheric variables from CGCM3.1 global circulation model and the regional model REMO output are downscaled statistically to meteorological variables at the point scale and at daily time step to assess future climatic variables under climate changes. Statistical downscaling using SDSM smooth out the bias of REMO and CGCM3.1 and gives reasonable results for the Baro-Akobo basin as it is found that the downscaled variables captures baseline climate trend. Both REMO and CGCM3.1 outputs after downscaling capture the observed 20^{th} century trends of temperature and precipitation change over the basin. Here it was observed that the result of downscaled precipitation does not show a systematic increase or decrease in all future time horizons for both A1B and B1 scenarios. Both models show an increasing trend in annual maximum temperature for most of the stations compared to baseline. To conclude, different GCMs have different projections and the type of downscaling approach chosen also subject to uncertainty. Therefore, the uncertainty analysis of specific target variables must be carried out using additional climate models to properly assess future projections and to advise decision makers in a better ways.

- ✓ **Assess the performance of two different hydrological models to quantify the impact of climate change on water resources.**

The performance of the two hydrological models and their comparison for simulations of discharge of the SORE watershed (1711 km^2), Baro-Akobo basin, Ethiopia were shown by comparing model results at daily, weekly and monthly steps. The models are able to reproduce discharge with good performance (WaSiM-ETH R^2=0.79, NSE=0.78; and HBV-Light R^2=0.85, NSE=0.84) at daily scale. Difference between the two models was not strong for the SORE watershed even if they have different model structure. The two models were used to simulate future discharge (2011-2050) in the watershed using downscaled REMO and CGCM3.1 climate data. Both hydrological models show a reduction in peak discharge (August and September) for all downscaled REMO and CGCM3.1 scenarios. However, WaSiM-ETH

shows discharge in June likely to increase up to +60% while HBV-Light shows up to +30% to +40% for both climate models in future (2011-2050). The two hydrological models show similar directions of change except their differences in the magnitude and low flows. To conclude, the simulation of hydrological processes with WaSiM-ETH and HBV-Light in the SORE watershed was successful but further studies in the different part of the basin with updated data are required. It would be advisable to apply a range of hydrological models for additional comparative studies to quantify model based uncertainties. In addition, to understand the multiple sources of uncertainties in the complex climate and hydrological models the application of a comprehensive uncertainty analysis would be important.

- ✓ **Analyse and assess changes in the seasonal variability of rainfall (dry spell)**

In this study two time series measures namely "Rainy Season Maximum Dry Spell (RSMDS) length" and "Rainy Season Number of Dry Spells (RSNDS)" were computed for the upper Baro-Akobo basin, Ethiopia. The trends were investigated based on daily rainfall records taken from 8 rain gauge stations (1972-2000) using the Mann-Kendall test. Nonparametric statistic results show that both parameters have no trend over the study period. However, there is no monotonic trend found in dry spell. We also determine onset, cessation and duration of the rainy season at the meteorological stations scale, which is important for decision making purpose and for planning agricultural water management. The coefficient of variation for the onset of rainy season is within an acceptable limit (Labesse, 2008) this reveals that planning of rain-fed agriculture around the study area can be done with limited risk because of the stability of the onset dates of the season. However, for adaptation, mitigation and reducing drought risk it is recommended to investigate future climate change impacts.

References

Abdo, K. S., Fiseha B. M., Rientjes T. H. M., Gieske A. S. M. and Haile, A. T., (2009) Assessment of climate change impacts on the hydrology of Gilgel Abay catchment in Lake Tana basin, Ethiopia, HYDROLOGICAL PROCESSES 23, 3661-3669 (2009), John Wiley & Sons, Ltd

Anandhi, A., Srinivas, V.V., Nanjundiah, R.S., and Kumar, D.N., (2008) Downscaling precipitation to river basin in India for IPCC SRES scenarios using support vector machine. International Journal of Climatology.28:401-420

Araujo, M.B., and New, M., (2006) Ensemble forecasting of species distributions. TRENDS in Ecology and Evolution. Vol.22 No.1

Araya, A., Stroosnijder, Leo, (2011) Assessing drought risk and irrigation need in northern Ethiopia. Agricultural and Forest Meteorology, 151: 425-436 Available at http://www.mowr.gov.et/index.php?pagenum=3.3&pagehgt=1000px

Awulachew, S. B., Yilma, A. D., Loulseged, M., Loiskandl, W., Ayana, M., Alamirew, T., (2007) Water Resources and Irrigation Development in Ethiopia. Colombo, Sri Lanka: International Water Management Institute. 78p. (Working Paper 123). Available at http://www.iwmi.cgiar.org/publications/Working_Papers/working/WP123.pdf

Baede, A.P., Ahlonsou, M. E., Ding, Y., Schimel, D., (2001): The Climate System: an Overview. In: Climate Change 2001: The Scientific Basis. Contribution of Working Group I to the Third Assessment Report of the Intergovernmental Panel on Climate Change [Houghton, J.T.,Y. Ding, D.J. Griggs, M. Noguer, P.J. van der Linden, X. Dai, K. Maskell, and C.A. Johnson (eds.)]. Cambridge University Press, Cambridge, United Kingdom and New York, NY, USA, 881pp

Bardossy A., (2000) stochastic downscaling methods to assess the hydrological impacts of climate change on river basin hydrology. Beersma J, Agnew M, Viner D, Hulme M (eds). Climate Research Unit, UEA: Norwich, UK, KNMI: The Netherlands; 18-34

Beven, K.J., (2001) Rainfall-Runoff Modelling - the Primer, John Wiley & Sons, Ltd

Beyene, T., Lettenmaier, D.P., Kabat, P., (2010) Hydrological impact of climate change on the Nile River Basin; implication of the 2007 IPCC scenarios. Climate change 100:433-461

Booij MJ., (2005) Impact of climate change on river flooding assessed with different spatial model resolutions. Journal of Hydrology 303: 176-198

Bormann, H., and Elfert, S., (2010) Application of WaSiM-ETH model to North German lowland catchments: model performance in relation to catchment characteristics and sensitivity to land use change. Adv. Geosi., 27, 1-10

Busuioc, A., Chen, D., and Hellstrom, C., (2001) performance of Statistical downscaling Modeling Models in GCM validation and regional climate change estimates: application for Swedish precipitation. International Journal of Climatology

Cheung, W.H., Senay, G.B., and Singh, A., (2008) trends and spatial distribution of annual and seasonal rainfall in Ethiopia. Int. J climatol. DIO:10.1002/joc.1623

Collins, M., (2007) Ensembles and probabilities: a new era in the prediction of climate change. Phil.Trans.R.Soc. A2007 365, doil:10.1098/rsta. 2007.2068, Published online 15 August 2007

Conway, D., (2005) from headwater tributaries to international river basin: adaptation to climate variability and change in the River Nile basin. Global Environ. Change 15, 99–114

Conway, D., and Hulme, M., (1996) The Impact of Climate variability and Future Climate Change in the Nile Basin on Water Resources in Egypt. International Journal of Water Resources Development, 13(3):277-296

Cornelissen, Th., Diekkrüger, B., Giertz, S., (2013) A Scenario-Based Assessment of Climate and Land-Use Change Impact on the Discharge of a Tropical Catchment (Térou River, Benin, West Africa) using a Multi-Model Ensemble. Journal of Hydrology, 498:221-236. Doi:1016/j.jhydrol.2013.06.016

CSA (Central Statistical Agency) [Ethiopia] and ORC Macro (2006) Ethiopia Demographic and Health Survey 2005.Addis Ababa, Ethiopia and Calverton, Maryland, USA: Central Statistical Agency and ORC Macro

Cullmann, J., Mishra, V., Peters, R., (2006) Flow analysis with WaSiM-ETH – model parameter sensitivity at different scales. Adv. Geosci. 9 (73), 73-77

Di Baldassarre, G., Elshamy, M., van Griensven, A., Soliman, E., Kigobe, M., Ndomba, P., Mutemi, J., Mutua, F., Moges, S., Xuan, J. Q., Solomatine, D. & Uhlenbrook, S., (2011) Future hydrology and climate in the River Nile basin: a review. Hydrol. Sci. J. 56 (2), 199-211

DIA CGCM3 Predictors, (2008) "Set of Predictor Variables Derived from CGCM3 T47 and NCEP/NCAR Reanalysis", version 1.1, April 2008, Monterial, QC, Canada, 16 pp. Available at http://loki.qc.ec.gc.ca/DAI/predictors-e.html

Dibike, Y. B., and Coulibaly, P., (2005) Hydrological impact of climate change in Saguenay watershed: comparison of downscaling methods and hydrologic models. Journal of Hydrology, 307, 145-163

Dibike, Y.B., Gachon, P., St-Hilaire, A., Ouarda, T.B.M.J., and Nguyen, Van T.-V., (2008) Uncertainty analysis of statistically downscaled temperature and precipitation regimes in Northern Canada. Theoretical and Applied Climatology, 91,149-170

Duan, Q., Gupta, H. V., Sorooshian, S., Rousseau, A. N., and Turcotte, R., (Eds.) (2003), Calibration of Watershed Models, Water Sci. Appl., vol. 6, 345 pp., AGU, Washington, D. C., doi:10.1029/WS006

Elshamy, M. E., Seierstad, I. A., and Sorteberg, A., (2009) Impact of climate change on Blue Nile flows using bias-corrected GCM scenarios. Hydrol.Earth Syst.Sci., 13, 551-565

FAO (1996), Agro-Ecological Zoning Guidelines, FAO Soil Bulletin 76, Soil Resources, Management and Conservation Service, FAO Land and Water Development Division, Rome. Available at http://www.fao.org/docrep/W2962E/W2962E00.htm

Fowler, H.J., Blenkinsop, S., and Tebaldi, C., (2007) Linking climate change modelling to impacts studies: recent advances in downscaling techniques for hydrological modelling. Int. J. Climatol. 27:1547-1578. Dol: 10-1002 /joc.1556

Gelman, A., and Pardoe I., (2006) Bayesian measures of explained variance and pooling in multilevel (Hierarchical) models. American Statistical Association and the American Society for Quality. TECHNOMETRICS, Vol.48, No.2 Doi 10.1198/004017005000000517

Genuchten, M.TH. Van., (1980) A closed-form equation for predicting the hydraulic conductivity of unsaturated soils. Soil Science Society of American Journal, Vol 44, no 5

Gerstengarbe, F-W., and Werner P.C., (1999) Estimation of the beginning and end of recurrent events with a climate regime. Climate Research Vol.11:97-107

Gurtz,J. , Zappa, M., Jasper, K., Lang, H., Verbunt, M., Badoux, A., and Vitvar, T., (2003) A comparative study in modelling runoff and its components in two mountainous catchment. Hydrological Processes, 17, 297-311

Habte, A., Cullmann, J., and Horlacher, Hans-B., (2007) Application of Wasim Distributed Water Balance Simulation Model to the Abbay River Basin. Catchment and Lake Research LARS 2007. Available at http://www.uni-siegen.de/zew/publikationen/volume0607/habte.pdf

Hamed K.H., (2008) Trend detection in hydrologic data: The Mann-Kendall trend test under the scaling hypothesis. Journal of Hydrology, 349, 350-363

Hegerl, G.C., F. W. Zwiers, P. Braconnot, N.P. Gillett, Y. Luo, J.A. Marengo Orsini, N. Nicholls, J.E. Penner and P.A. Stott, (2007) Understanding and Attributing Climate Change. In: Climate Change 2007: The Physical Science Basis. Contribution of Working Group I to the Fourth Assessment Report of the Intergovernmental Panel on Climate Change [Solomon, S., D. Qin, M. Manning, Z. Chen, M. Marquis,K.B. Averyt, M. Tignor and H.L. Miller (eds.)]. Cambridge University Press, Cambridge, United Kingdom and New York, NY, USA

Houghton, J. T., Filho, L. G. M., Callander, B. A., Harris, N., Kattenberg, A., and Maskell, K., (1996) Climate Change 1995:The Science of Climate Change, Intergovernmental Panel on Climate Change, pp. 572, Cambridge University Press, Cambridge, GB.

Hulme, M., Doherty,R., Nagara,T., New,M. and Lister, D., (2001) African Climate change: 1900-2100. Climate Research, 17:145-168

IPCC, (2007) Summary for Policymakers. In: Climate Change 2007: The Physical Science Basis. Contribution of Working Group I to the Fourth Assessment Report of the Intergovernmental Panel on Climate Change [Solomon, S., D. Qin, M. Manning, Z. Chen, M. Marquis, K.B. Averyt, M.Tignor and H.L. Miller (eds.)]. Cambridge University Press, Cambridge, United Kingdom and New York, NY, USA.

Jacob, D., (2001) A note to the simulation of the annual and inter-annual variability of the water budget over the Baltic Sea drainage basin. Meteorology and Atmospheric Physics, Vol.77, Issue 1-4, 61-73

Jacob, D., Andrae, U., Elgered, G., Fortelius, C., Graham, L. P., Jackson, S. D., Karstens, U., Koepken, Chr., Lindau, R., Podzun, R., Rockel, B., Rubel, F., Sass, H.B., Smith, R.N.D., Van den Hurk, B.J.J.M., Yang, X., (2001) A Comprehensive Model Intercomparison Study Investigating the Water Budget during the BALTEX-PIDCAP Period. Meteorology and Atmospheric Physics, Vol.77, Issue 1-4, 19-43

Jasper, K., Calanca P., Gyalistras, D., **Fuhrer, J.,** (2004) Differential impacts of climate change on the hydrology of two alpine river basins. Climate Research, Vol. 26, No. 2, pp. 113-129. Details, doi: 10.3354/cr026113

Jung, G., (2006) Regional Climate Change and the Impact on Hydrology in the Volta Basin of West Africa. PhD Dissertation Garmisch-Partenkirchen, Germany

Karpouzos, D.K., Kavalieratou, S., and Babajimopoulos, C., (2010) Trend Analysis of Precipitation Data in Pieria Region (Greece). European water 30:31-40

Kasei, R., (2010): Modelling Impacts of Climate Change on Water Resources in the Volta Basin, West Africa. PhD Dissertation, University of Bonn, Germany. Available at http://hss.ulb.uni-bonn.de/2010/1977/1977.pdf

Kebede A., Diekkrüger B., Moges S.A., (2013) An Assessment of Temperature and Precipitation Change Projections using a Regional and a Global Climate Model for the Baro-Akobo Basin, Nile Basin, Ethiopia. J Earth Sci Climate Change 4: 133. doi:10.4172/2157-7617.1000133

Khan, M.S.,Coulibay, P., Dibike, Y., (2006) Uncertainty analysis of statistical downscaling methods. Journal of Hydrology. 316. 357-382

Khor, G.L., (2006) Estimation of Water Loss in the Baro River Basin, M.Sc. thesis, Arbaminch University, Ethiopia

Kim, U., Kaluarachchi, J. J., Smakhtin, V. U.,(2008) Climate change impacts on hydrology and water resources of the Upper Blue Nile River Basin, Ethiopia. International Water Management Institute (IWMI) Research Report 126, Colombo, Sri Lanka, 27p

Krause, P., Boyle, D.P., and Bäse, F., (2005) Comparison of different efficiency criteria for hydrological model assessment. Advances in Geosciences, 5, 89-97

Labesse, M.E., (2008) Terms of reference for training needs analysis. Institute National, pp 49 Quebec. Available at http://www.inspq.qc.ca/pdf/publications/884_Cadre_reference_ang.pdf

Lazaro, R., Rodrigo, F.S., Gutiervez, L., Domingo, F., and Puigdefabrefas, J., (2001) Analysis of a 3o-years rainfall record (1967-1997) in semi-arid SE Spain for implications on vegetation. Journal of Arid Environment 48:373-395

Leander, R., Buishand TA., (2007) Resampling of regional climate model output for the simulation of extreme river flows. Journal of Hydrology, 332, 487-496

Leemhuis, C., (2005) The Impact of El Niño Southern Oscillation Events on Water Resource Availability in Central Sulawesi, Indonesia: A hydrological modelling approach. PhD Dissertation, Universität zu Göttingen, Germany. Available at http://d-nb.info/97996864X/34

Legesse, D., Vallet-Coulomb, C., and Gasse, F., (2003) hydrological response of a catchment to climate and land use changes in Tropical Africa: case study South Central Ethiopia. Journal of Hydrology, 275, 67-85

Mathugama, S.C., and Peiris, T.S.G., (2011) Critical Evaluation of Dry Spell Research. International Journal of Basic & Applied Sciences IJBAS-IJENS Vol: 11 No: 06 153-160

McCornick P.G., Kamara A.B. and Girma T., (eds)., (2003) Integrated water and land management research and capacity building priorities for Ethiopia. Proceedings of a MoWR/EARO/IWMI/ILRI international workshop held at ILRI, Addis Ababa, Ethiopia, 2–4 December 2002. IWMI (International Water Management Institute), Colombo, Sri Lanka, and ILRI (International Livestock Research Institute), Nairobi, Kenya. 267 pp

McFarlane, N.A., J. F. Scinocca, M. Lazare, R. Harvey, D. Verseghy, and J. Li, (2005) The CCCma third generation atmospheric general circulation model. CCCma Internal Rep., 25 pp

McSweeney, C., New, M., Lizcano, G., (2010) The UNDP Climate Change Country Profiles: improving the accessibility of observed and projected climate information for studies of climate change in developing countries. Bulletin of the American Meteorological Society, 91, 157–166

Melesse, A.M., Loukas, A.G., Senay, G., Yitayew, M., (2009) Climate change, land-cover dynamics and eco-hydrology of the Nile River Basin. Hydrol Proc 23(26):3651–3652

Meselhe, E.A., and Habib, E.H., (2004) Performance Evaluation of Conceptual and Physically based Hydrologic models, Proceedings for the Army Science Conference (24th) Held on 29 November – 2 December 2005 in Orlando, Florida

MoFED, (Ministry of Finance and Economic Development) (2012) Federal Democratic Republic of Ethiopia, Growth and Transformation Plan (2012/2011-2014/2015) Annual Progress Report for F.Y.2010/2011 Addis Ababa

MoWR (Ministry of Water Resources), (1997) Baro-Akobo River Basin Integrated Development Master study, Volume II. Report, Addis Ababa

MoWR (Ministry of Water Resources), (2002) Water Sector Development Program. Report, Addis Ababa

MoWR (Ministry of Water Resources), (2011) Baro-Akobo Basin Integrated Development Master Plan. Available at http://www.mowr.gov.et/index.php?pagenum=3.1&pagehgt=5500px: Accessed on 2011,

Muita, R.R., van Ogtrop, F.F, and Vervoort, R.W., (2012) Dry spell trend analysis in Kenya and the Murray Darling Basin using daily rainfall. Geophysical Research Abstracts Vol. 14: EGU2012-6667

Nash, J. E. and Sutcliffe, J. V., (1970) River flow forecasting through conceptual models, Part I - A discussion of principles, Journal Hydrol., 10, 282–290

Nasri, M., and Modarres, R., (2009) Dry spell trend analysis of Isfahan Province, Iran. International Journal of Climatology. 29: 1430-1438

NMSA, (1996) Climate and agro climatic resources of Ethiopia. NMSA (National Meteorological Service Agency) Meteorological Research Report Series, Vol. 1, No.1, Addis Ababa

Oldeman, L.R. and Van Velthuyzen, H.T., (1991) Aspects and Criteria of the agro-ecological zoning approach of FAO. International soil reference and information centre and FAO

Paeth, H. and Thamm H., (2007) Regional modelling of future African climate north of 15°S including greenhouse warming and land degradation. Climatic Change, 83:401–427 DOI 10.1007/s10584-006-9235-y

Paeth, H., (2005) The climate of tropical and northern Africa – A statistical-dynamical analysis of the key factors in climate variability and the role of human activity in future climate change. St. Augustin: Asgard-Verlag, Hippe

Paeth, H., Born, K., Podzun, R., and Jacob, D., (2005) Regional dynamical downscaling over West Africa: model evaluation and comparison of wet and dry years. Meteorologische Zeitschrift, Vol. 14.No.3,349-367

Palmer, R. N., Clancy, E., Rheenen, N. T. Van, and Wiley, M. W., (2004) The Impacts of Climate Change on the Tualatin River Basin Water Supply: An Investigation into Projected Hydrologic and Management Impacts, Report. Department of Civil and Environmental Engineering, University of Washington

Palmer, T.N., Shutts, G.J., Hagedorn, R., Doblas-Reyes, F.J., Jung, T., and Leutbecher, M., (2005) Representing Model Uncertainity in Weather and Climate Prediction. Annu.Rev.Earth Planer.Sci.33:163-93

Parry M.L., Canziani, O.F., and Palutikof, J.P. (2007) IPCC 4AR Technical Summary. Climate Change 2007: Impacts, Adaptation and Vulnerability. Contribution of Working Group II to the Fourth Assessment Report of the Intergovernmental Panel on Climate Change, M.L. Parry, O.F. Canziani, J.P. Palutikof, P.J. van der Linden and C.E. Hanson, Eds., Cambridge University Press, Cambridge, UK, 23-78

Raper, S.C.B. and Cubasch, U., (1996) Emulation of the results from a coupled general circulation model using a simple climate model. Geophysical Research Letters, 23(10): 1107-1110

Rodrigo F.S., Esteban-Parra, M.J., Pozo-Vázquez, D., Castro-Diez, Y., (1999) A 500-year precipitation record in southern Spain. Int J Clim 19:1233–1253

Rößler Ole. , (2011) A climate change impact assessment study on mountain soil moisture with emphasis on epistemic uncertainties. PhD Dissertation, University of Bonn, Germany. Available at http://hss.ulb.uni-bonn.de/2011/2600/2600.htm

Rößler, O., and Löffler, J., (2010) Potentials and limitations of modelling spatio-temporal patterns of soil moisture in a high mountain catchment using WaSiM-ETH. Hydrological processes.24,2182-2196

Rößler, O., Diekkrüger, B., and Löffler J., (2012) Potential drought stress in a Swiss mountain catchment—Ensemble forecasting of high mountain soil moisture reveals a drastic decrease, despite major uncertainties, Water Resour. Res., 48, W04521, doi: 10.1029/2011WR011188

Sayed, M.A.A., (2004) Impacts of climate change on the Nile Flow, Ain Shams University, Cairo, Egypt

Schulla, J., Jasper, K., (2000**)** Model Description WaSiM-ETH. Institute for Atmospheric and Climate Science, Swiss Federal Institute of Technology, Zürich

Schulla, J., Jasper, K., (2007) Model description WaSiM-ETH (Water balance simulation model ETH). http://www.wasim.ch/downloads/doku/wasim/wasim 2000 en.pdf, Last updated 16 Oct 2007

Scinocca, J. F., McFarlane, N. A., Lazare, M., Li, J., and Plummer, **D.,** (2008) The CCCma third generation AGCM and its extension into the middle atmosphere. Atmos. Chem. and Phys., 8, 7055-7074

Seibert, J., (2005) HBV Light version 2 User's Manual. November 2005 Stockholm University, Department of Physical Geography and Quaternary Geology. Available at http://people.su.se/~jseib/HBV/HBV_manual_2005.pdf

Seleshi, Y., and Camberlin, P., (2006) Recent changes in dry spell and extreme rainfall event in Ethiopia. Theoretical and Applied Climatology, DOI 10.1007/s00704-005-0134-3

Seleshi, Y., and Zanke U., (2004) Recent changes in rainfall and rainy days in Ethiopia. Int. J. Climatol. 24:973-983

Setegn, S. G., Srinivasan, R., and Dargahi, B., (2009): Hydrological Modelling in the Lake Tana Basin, Ethiopia Using SWAT Model, Open Hydrol. J., 2, 49–62

Singh, V.P. and Frevert D., (2006), Watershed models. Boca Raton, Taylor & Francis

Singh, V.P. and Frevert, D.K. (eds.) (2002) Mathematical models of large watershed hydrology. Water Resources Publications, LLC

Singh, V.P. and Woolhiser D.A., (2002), Mathematical modelling of watershed hydrology, Journal of Hydrologic Engineering, 7(4), 270-292

Sivakumar, M.V.K., (1992) Empirical Analysis of Dry spells for Agricultural Applications in West Africa. Journal of Climate. Vol 5: 532-539

Sneyers, R. (1990) on the statistical analysis of series of observations. World Meteorological Organization Technical Note 143,192. Geneva

Soliman, E.S.A., Sayed, M.A.A, Jeuland M., (2009) Impact assessment of future climate change for the Blue Nile Basin, using a RCM Nested in a GCM. Nile Basin Water Engineering Scientific Magazine, Vol.2

Solomon S, Qin D, Manning M, Chen Z, Marquis M, et al. (2007) Summary for Policymakers. In: Climate Change 2007: The Physical Science Basis. Contribution of Working Group I to the Fourth Assessment Report of the Intergovernmental Panel on Climate Change. Cambridge University Press

Su, B.D., Jiang, T., and Jin, W.B., (2006) Recent trend in observed temperature and precipitation extreams in the Yangatze River basin, China. Theo.Appl.Climatol. 83: 139-151 DOI 10.1007/s00704-005-0139-y

Surfleet, C.G., Tullas, D., Change, H., Jung, I.W., (2012) Selection of hydrologic modelling approaches for climate change assessment: A comparison of model scale and structures. Journal of Hydrology, 464-465, 233-248

Tadege A., (ed.)., (2007) Climate Change National Adaptation Program of Action (NAPA) of Ethiopia. National Meteorological Agency, Addis Ababa, Ethiopia

Taye, M.T., Ntereka, V., Ogiramoi, N.P., and Willems, P., (2011) Assessment of climate change impact on hydrological extremes in two source regions of the Nile Basin. Hydrol. Earth Syst. Sci., 15,209-222

Thornton, P., Cramer, L., (editors), (2012) Impacts of climate change on the agricultural and aquatic systems and natural resources within the CGIAR's mandate. CCAFS Working Paper 23. CGIAR Research Program on Climate Change, Agriculture and Food Security (CCAFS). Copenhagen, Denmark. Available online at: www.ccafs.cgiar.org

Tilahun, K., (1999) Test of Homogeneity, frequency analysis of rainfall data and estimate of drought probabilities in Dire Dawa, Eastern Ethiopia. Ethiopian J. Nat. Resour. 1: 125-136

Tilahun, K., (2006) Analysis of rainfall climate and evapo-transpiration in arid and semi-arid regions of Ethiopia using data over the last half a century. J. Arid Environ. 64: 474-487

UNFPA (United Nation population Fund) Richard Kollodge (ed.)., (2011) The state of World Population 2011. People and possibilities in a world of 7 billion. UNFPA

Verbunt, M., Gurtz, J., Jasper, K., Lang, H., Warmerdam, P., and Zappa, M., (2003) The hydrological role of snow and glaciers in alpine river basins and the distributed modelling. Journal of Hydrology, 282, 36-55

Wagener, T. Wheater, H.S. and Gupta, H.V., (2004) Rainfall-Runoff Modelling in Gauged and Ungauged Catchments. Imperial College Press, 306pp

Wagner,S., Kunstmann, H., Bárdossy, A., Conrad ,C., Colditz, R.R., (2009) Water balance estimation of a poorly gauged catchment in West Africa using dynamically downscaled meteorological fields and remote sensing information. Physics and Chemistry of the Earth 34, 225–235

Weglarczyk, S., (2009) On the stationarity of extreme level of some Polish lakes. I. Preliminary results from statistical test. Limnological Review 9, 2-3: pp 129-138

Wilby, R. L. and Dawson C. W., (2007) SDSM 4.2 — A decision support tool for the assessment of regional climate change impacts, User Manual. Department of Geography, Lancaster University, UK. Available at http://co-public.lboro.ac.uk/cocwd/SDSM/SDSMManual.pdf

Wilby, R. L. and Dawson, C.W., (2012) The Statistical Downscaling Model: insights from one decade of application, International Journal of Climatology DOI: 10.1002/joc.3544

Wilby, R. L. and Wigley, T. M. L., (1997) Downscaling general circulation model output: a review of methods and limitations, Prog. Phys. Geogr., 21, 530–548

Wilby, R. L. and Wigley, T. M. L., (2000) Precipitation predictors for Downscaling: Observed and General Circulation model relationships, Int. J. Climatol. 20:641-661

Wilby, R. L., Dawson, C.W., and Barrow, E.M., (2002) SDSM-a decision support tool for the assessment of regional climate change impacts, Environmental Modelling & Software 17, 147-159

Wilby, R. L., Hay, L.E., and Leavesley, G.H., (1999) A comparison of downscaled and raw GCM output: implications for climate scenarios in the San Juan River Basin, Colorado, Journal of hydrology 225, 67-91

Wilby, R., Charles, S., Zorita, E., Timbal, B., Whetton, P., and Mearns, l., (2004) Guidelines for Use of Climatic Scenarios Developed from Statistical Downscaling Methods. Available at http://unfccc.int/resource/cd_roms/na1/v_and_a/Resoursce_materials/Climate/StatisticalDownscalingGuidance.pdf

Wing, H., Cheung, A., Gabriel, B.S. and Singh, A., (2008) Trends and spatial distribution of annual and seasonal rainfall in Ethiopia. Int. J. Climatol., 28(13), 1723-1734

World Bank, (2011) Ethiopia: Managing Water Resources to Maximize Sustainable Growth. The World Bank Agricultural and Rural Development, Report no. 36000-Et, Washington

Xu, C.Y, Widen, E., Halldin, S., (2005) Modelling Hydrological Consequence of Climate Change--Progress and Challenges. Advances in Atmospheric Sciences 22(6): 789-798

Xu, Chong-Yu., (1999) From CGCMs to river flow: a review of downscaling methods and hydrologic modelling approaches. Progress in physical geography 23, 2 PP. 229-249

Yemenu. A., and Chemeda, D., (2010) Climate resources analysis for use of planning in crop production and rainfall water management in the central highlands of Ethiopia, the case of Bishoftu district, Oromia region. Hydrology and Earth System Science Discussions, 7, 3733-3763

Yimer, G., Andreja J., van Griensven, A., (2009) Hydrological Response of a Catchment to Climate Change in the Upper Beles River Basin, Upper Blue Nile, Ethiopia, Nile Basin Water Engineering Scientific Magazine, Vol.2, 49-59

You, G. J.-Y., and Ringler, C., (2010) Hydro-Economic Modelling of climate change impacts in Ethiopia. IFPRI Discussion paper No. 960. (Washington, Dc: International Food Policy Research Institute, 2010)

Yu, Z., (2002) Hydrology: modelling and prediction. In Encyclopedia of Atmospheric Science. Academic Press, vol. 3, p. 980-986.

Yue, S., Pilon, P., and Cavadias, G., (2002) Power of the Mann-Kendall and Spearman' rho tests for detecting monotonic trends in hydrological series. Journal of Hydrology, 259, 254-271

Zeray, L., Roehrig, J., and Chekol, D.A., (2006) Climate change impact on Lake Ziway watershed water availability, Ethiopia. Tropentag 2006, Conference on International Agricultural Research for Development, University of Bonn, October 11-13, 2006. Available at http://www.tropentag.de/2006/abstracts/full/481.pdf